Title

Cardiac Parasympathetic Neural Remodeling and Electrophysiological Effects of Vagal Nerve Stimulation

Author

Vaseghi, Marmar

Publication Date

2016

Peer reviewed|Thesis/dissertation

UNIVERSITY OF CALIFORNIA

Los Angeles

Cardiac Parasympathetic Neural Remodeling and Electrophysiological Effects of Vagal Nerve Stimulation

A dissertation submitted in partial satisfaction of the requirements for the degree

Doctor of Philosophy in Molecular, Cellular, and Integrative Physiology

by

Marmar Vaseghi

2016

ABSTRACT OF THE DISSERTATION

Cardiac Parasympathetic Neural Remodeling

and Electrophysiological Effects of Vagal Nerve Stimulation

by

Marmar Vaseghi

Doctor of Philosophy in Molecular, Cellular, and Integrative Physiology

University of California, Los Angeles, 2016

Professor Kalyanam Shivkumar, Chair

The autonomic nervous system regulates cardiac excitability and genesis of ventricular tachyarrhythmias (VT/VF). Myocardial infarction leads to sympathetic activation and parasympathetic dysfunction, which act in concert to increase the risk of sudden cardiac death due to VT/VF. The mechanisms behind parasympathetic dysfunction and the electrophysiological effects of vagal nerve stimulation are poorly characterized.

The vago-symapthetic trunks carries both cardiac efferent and afferent fibers. To better delineate and compare their functional effects in normal porcine hearts *in vivo,* right and left vagal nerve stimulation (VNS) was performed and hemodynamic parameters and analysis of regional electrophysiological effects using activation recovery interval mapping (ARI) performed. ARI is a validated surrogate of local action potential duration. Subsequently, role of afferent fiber activation during VNS on efferent control of cardiac function was assessed by

transection of right and/or left, and ispilateral, contralateral, and/or bilateral trunks. Finally, the mechanism behind neural parasympathetic remodeling due to myocardial infarction and the anti-arrhythmic effects of VNS were assessed in a chronic porcine infarct model.

In normal porcine hearts, right and left VNS significantly decreased heart rate and dP/dt max and prolonged regional ARI. No anterior-posterior-lateral ventricular regional differences in regional ARI were found. However, endocardial ARI increased more than epicardial ARI, and apical ARI more than basal ARI, during right and left VNS. With regards to afferent fiber activation during VNS, an augmentation in hemodynamic and electrophysiological effects of right VNS after ipsilateral vagal nerve transection was observed. Similar changes were suggested by left VNS after left vagal nerve transection. However, contralateral vagal nerve transection did not modify the response to VNS. Finally, measurement of regional acetylcholine, the primary neurotransmitter of cardiac parasympathetic neurons, showed that this neurotransmitter is preserved in infarcted hearts. Direct neural recordings from intrinsic cardiac ganglia neurons demonstrated significant alterations in the basal activity of parasympathetic efferent neurons that receive input from the left vagal trunk, suggesting a decrease in central parasympathetic drive on that side. Augmentation of parasympathetic drive with VNS reduced ventricular tachy-arrhythmia inducibility by decreasing dispersion of repolarization in border zone regions of infarcted hearts.

In conclusion, both right and left vagi provided significant innervation to the ventricular myocardium, modulating both cardiac electrical and mechanical function.

VNS activated both afferent and efferent fibers in the ispilateral vagal trunk, and afferent fiber activation reduced efferent physiological effects. Myocardial infarction led to significant neural remodeling and alteration in the behavior of parasympathetic neurons in the cardiac ganglia, changes that were suggestive of decreased central parasympathetic drive. VNS restored this drive and electrically stabilized infarct border zones, acutely reducing ventricular arrhythmias.

The dissertation of Marmar Vaseghi is approved.

Jeffrey Laurence Ardell

Kristina Bostrom

Ronald Marven Harper

Yvette Taché

Kalyanam Shivkumar, Committee Chair

University of California, Los Angeles

2016

DEDICATION

This work is dedicated to the victims of sudden cardiac death, those whose lives were unpredictably taken and those who continue to suffer from defibrillator shocks.

It is equally dedicated to my family, George, Xander, and Arianna, who have given me perspective and a lens through which I view life, and to Julie Asfia, who continues to inspire me with her scientific mind.

TABLE OF CONTENTS

PREFACE

Chapter 1. A portion of this manuscript is published. William Huang and **Marmar Vaseghi**. Device-based autonomic modulation in arrhythmia patients: role of vagal nerve stimulation. Curr Treat Options Cardiovasc Med 2015;17:1-17.

Chapter 2. A version of this manuscript is published. Kentaro Yamakawa, Eileen L. So, Pradeep S. Rajendran, Jonathan D. Hoang, Nupur Makkar, Aman Mahajan, Kalyanam Shivkumar, and **Marmar Vaseghi**. Electrophysiological effects of right and left vagal nerve stimulation on ventricular myocardium. Am J Phys Heart Circ Phys 2014; 307:H722-31.

Chapter 3. A version of this manuscript is published. Kentaro Yamakawa, Pradeep S. Rajendran, Tatsuo Takamiya, Diago Yagishita, Eileen L. So, Aman Mahajan, Kalyanam Shivkumar, and **Marmar Vaseghi**. Vagal nerve stimulation activates vagal afferent fibers that reduce cardiac efferent parasympathetic effects. Am J Phys Heart Circ Phys 2015;309:H1579-90.

Chapter 4. A version of this manuscript has been submitted for publications. Parasympathetic dysfunction and anti-arrhythmic effect of vagal nerve stimulation following myocardial infarction. Marmar Vaseghi, Daigo Yagishita, Pradeep S. Rajendran, William R. Woodward, David Hamon, Kentaro Yamakawa, Tadanobu Irie, Beth A. Habecker, and Kalyanam Shivkumar.

This work was supported by an American Heart Association Fellow to Faculty Transition Award, 11FTF7550004 and National Institute of Health New Innovator Award 1DP2HL132356.

ACKNOWLEDGEMENTS

I am grateful for the eternal support of my family and friends in this journey, as words cannot convey how much they have helped me and how much I owe them. I would like to thank Dr. Kalyanam Shivkumar, who has not only been a dedicated mentor and friend over the past decade, but the very best source of intellectual inspiration and scholarship. I am thankful to Dr. Jeffrey Ardell for his advice and guidance, as well as his 30 years of dedication to the field of neurocardiology. I would like to extend a heart-felt thank you to Drs. Kristina Bostrom and Yvette Taché for their constant support and for being the very best role models. Finally, a special thank you to the American Heart Association for their research support and to Dr. Linda Demer and the Specialty Training and Advanced Research Program at the UCLA School of Medicine.

VITA

Clinical Training

University of California, Los Angeles. Internal Medicine, 7/2002-6/2005
University of California, Los Angeles. General Cardiology, 7/2005-6/2010
University of California, Los Angeles. Cardiac Electrophysiology, 7/2010-6/2011

Education

Northwestern University, B.S. Biomedical Engineering, 9/95 – 6/98

Stanford University School of Medicine, M.D. 9/98 – 6/02

UCLA Specialty Training and Advanced Research (STAR) Program Masters in Clinical Research – Department of Biomathematics. 6/05 – 1/11

Publications (16 of 60 listed)

1. **Vaseghi M**, Cesario DA, Valderrabano M, Boyle NG, Ratib O, Finn JP, Wiener I, Shivkumar K. Impedance monitoring during catheter ablation of atrial fibrillation. ***Heart Rhythm*** 2005; 2:914-20.
2. **Vaseghi M**, Cesario DA, Mahajan A, Wiener I, Boyle NG, Fishbein MC, Horowitz BN, Shivkumar K. Catheter ablation of right ventricular outflow tract tachycardia: value of defining coronary anatomy. ***J Cardiovasc Electrophysiol*** 2006;17:632-7.
3. **Vaseghi M**, Boyle NG, Kedia R, Patel J, Cesario DA, Wiener I, Kobashigawa J, Shivkumar K. Supraventricular tachycardia after orthotopic cardiac transplantation. ***J Am Coll Cardiol*** 2008;51:2241–9.
4. **Vaseghi M**, Shivkumar K. The role of the autonomic nervous system in sudden cardiac death. ***Prog Cardiovasc Dis*** 2008;50:404–419.
5. **Vaseghi M**, Lellouche N, Ritter H, Fonarow GC, Patel JK, Moriguchi J, Fishbein MC, Kobashigawa JA, Shivkumar K. Mode and mechanism of death following orthotopic heart transplantation. ***Heart Rhythm*** 2009;6:503-9.
6. Bourke T, **Vaseghi M**, Michowitz Y, Sankhla V, Shah M, Swapna N, Boyle NG Mahajan A, Narasimhan C, Lokhandwala Y, Shivkumar K. Neuraxial modulation for refractory ventricular arrhythmias: value of thoracic epidural anesthesia and surgical left cardiac sympathetic denervation. ***Circulation*** 2010;121:2255-62
7. Nakahara S*, **Vaseghi M***, Ramirez R, Fonseca C, Lai C, Finn P, Mahajan A, Boyle N, Shivkumar K. Characterization of Myocardial Scar. ***Heart Rhythm*** 2011;8:1060-1067.**Vaseghi M**, Lux R, Mahajan A, Shivkumar K. Sympathetic

stimulation increases dispersion of repolarization in humans with myocardial infarction. ***Am J Phys Heart Circ Physiol*** 2012;302:H1838-46

8. **Vaseghi M**, Zhou W, Shi J, Ajijola OA, Hadaya J, Shivkumar K, Mahajan A. Sympathetic innervation of the anterior left ventricular wall by the right and left stellate ganglia. ***Heart Rhythm*** 2012;9:1303-9.
9. **Vaseghi M**, Yamakawa K, Sinha A, So E, Zhou W, Ajijola OA, Lux RL, Laks MM, Shivkumar K, Mahajan A. Modulation of regional dispersion of repolarization and T-peak to T-end interval by the right and left stellate ganglia. ***Am J Physiol Heart Circ Physiol*** 2013;305:H1020-30.
10. **Vaseghi M**, Gima J, Kanaan C, Ajijola OA, Marmureanu A, Mahajan A, Shivkumar K. Cardiac sympathetic denervation in patients with refractory ventricular tachycardia or electrical storm: intermediate and long term follow up. ***Heart Rhythm*** 2014;11:360-6.
11. Yamakawa K, So E, Rajendran P, Hoang J, Makkar N, Mahajan A, Shivkumar K, **Vaseghi M.** Electrophysiological effects of right and left vagal nerve stimulation on the ventricular myocardium. ***Am J Physiol Heart Circ Physiol*** 2014;307:H722-31.
12. Yagishita D, Chui RW, Yamakawa K, Rajendran PS, Ajijola OA, Nakamura K, So EL, Mahajan A, Shivkumar K, **Vaseghi M**. Sympathetic nerve stimulation, not circulating norepinephrine, modulated T-peak to T-end interval by increasing global dispersion of repolarization. ***Circ Arrhythm Electrophysiol*** 2015;9:174-185.
13. Mao J, Moriarty J, Mandapati R, Shivkumar K, **Vaseghi M**. Catheter ablation of accessory pathways near the coronary sinus, value of defining coronary arterial anatomy. ***Heart Rhythm*** 2015;12:508-14
14. Huang WA, Shivkumar K, **Vaseghi M**. Device-based autonomic modulation in arrhythmia patients: the role of vagal nerves stimulation. ***Curr Treat Options Cardiovasc Med*** 2015;17:379.
15. **Vaseghi M***, Tung R*, Frankel DS, et al (IVTCC Investigators). Freedom from recurrent ventricular tachycardia after catheter ablation is associated with improved survival in patients with structural heart disease: An International VT Ablation Center Collaborative Group study. ***Heart Rhythm*** 2015;12:1997-2007
16. Yamakawa K, Rajendran PS, Takamiya T, Yagishita D, So EL, Mahajan A, Shivkumar K, **Vaseghi M**. Vagal nerve stimulation activates vagal afferent fibers that reduce cardiac efferent parasympathetic effects. ***Am J Phys Heart Circ Physiol*** 2015;309:H1579-90.

* indicates equal contribution

CHAPTER 1

VAGAL NERVE STIMULATION AND VENTRICULAR ARRHYTHMIAS: CURRENT PERSPECTIVES AND MECHANISMS

INTRODUCTION

Much of the attention on the role of the autonomic nervous system in genesis of arrhythmias has focused on the sympathetic branch. Current therapies involving blockade of the of the sympathetic nervous system, including beta-blockers, angiotensin converting enzyme inhibitors, and aldosterone antagonists have been the cornerstones for the treatment of arrhythmias and heart failure. However, there is growing attention and need for therapies targeting the parasympathetic nervous system to compliment and augment our current approach. Parasympathetic imbalance, as manifested by abnormal heart rate variability and decreased baroreceptor sensitivity, is a well-established manifestation of heart failure and increases the risk of sudden cardiac death (1-6). Furthermore, an increase in parasympathetic tone portends a greater likelihood of survival in the setting of ischemia.[7] Vagal nerve stimulation (VNS) represents a potential approach to increase parasympathetic efferent outflow and compensate for the parasympathetic dysfunction observed in the genesis of arrhythmias (8).

ANATOMY AND PHYSIOLOGY

The afferent fibers in the vago-sympathetic trunk synapse in the nucleus tractus solitaries, while efferent fibers originate in the nucleus ambiguus and dorsal motor nucleus of the brainstem (9), figure 1. Visceral efferent fibers synapse near target organs, whereas afferent fibers travelling through the vagus via the pseudo-unipolar neurons of the nodose ganglia (inferior vagal ganglion) carry information to the brainstem and higher centers. Within the vagosympathetic trunk, there is a predominance of parasympathetic

neural fibers, although sympathetic nerve fibers also exist (10, 11). The cardiomotor preganglionic parasympathetic nerve fibers converge and synapse within the intrinsic cardiac nervous system ganglia, lying on the dorsal and ventral fat pads on the basal aspect of the heart. The intrinsic cardiac nervous system forms a complex neural network that responds to and maintains beat-to-beat control of cardiac function (12, 13). The post-ganglionic parasympathetic fibers from the ganglia within these fat pads then innervate the sinoatrial and atrioventricular nodes as well as the atrial and the ventricular myocardium (14).

It is important to note that VNS can have different effects depending on the parameters and level of stimulation. High level stimulation, particularly at frequencies > 20 hz, has been shown to significantly reduce heart rate (> 60%) and increase AV nodal conduction time (15). At these high stimulation currents, VNS can induce asystole and complete heart block (16). With medium level stimulation, mild reductions in heart rate (10-50%) and prolongation in AV nodal conduction time are observed. Low level vagal nerve stimulation is defined as a combination of intensity and frequency which has no effect on heart rate or AV conduction. There is a threshold effect for voltage and pulse duration (17). Increasing frequencies up to 17Hz causes progressive sinus bradycardia while stimulation at 20-40 Hz (with voltage and pulse width held constant) can lead to prolonged pauses with junctional or ventricular escape beats. Therefore, there is an optimal range of frequencies and output to achieve the desired rhythm and degree of bradycardia (17).

VNS and VENTRICULAR ARRHYTHMIAS

VNS has multiple electrophysiological effects on the ventricular myocardium. VNS lengthens the ventricular effective refractory period (18-22) and attenuates the effects of stellate stimulation on refractory period as measured using VF intervals (23). The effects of VNS on ventricular arrhythmias have been studied primarily in the setting of myocardial ischemia, both in normal and previously infarcted hearts. In various animal models including rats, cats, rabbits, and canines, VNS has been shown to reduce the incidence of ischemia driven ventricular fibrillation (VF) and increase VF threshold (18, 24-37), whereas vagotomy decreases VFT (38). In a canine model of coronary artery ligation, high intensity VNS decreased the time to spontaneous VF in the setting of ischemia compared to controls without VNS (24). In rats 3 months after myocardial infarction, PVCs were significantly decreased with low to medium intensity VNS with decrease in heart rate of 10% or 20-30 beats per minute (39). VNS at an intensity to decrease heart rate to 60-100 bpm in a canine ischemia model was shown to improve survival and reduce the time to spontaneous VF (26). VNS has also been shown to reduce the restitution slope in normal hearts to < 1 (18, 34), thereby protecting against malignant arrhythmias (40).

Bradycardia is one mechanism behind the protection conferred by VNS. In the setting of acute cardiac ischemia, reducing heart rate can improve the supply-demand mismatch and thereby reduce electrical vulnerability to malignant arrhythmias. Pacing the atria (31) and ventricle (30,41) at fixed rates while performing VNS attenuates its protective effects in this setting. The traditional interpretation of this data was that the heart rate reduction itself is protective; however, there are new studies to suggest that

pacing itself can be pro-arrhythmic by increasing sympathetic tone (42, 43), and by altering the neural activation patterns in the intrinsic cardiac ganglia (44).

Another potential mechanism behind the anti-arrhythmic effects of VNS may involve preservation of electrotonic coupling and thereby electrical stabilization of the myocardium. Reduction of electrotonic coupling has been linked to arrhythmogenesis in ischemia (45). VNS preserves electrotonic coupling during ischemia along with reducing ST segment elevations and dispersion of repolarization (45). Interestingly, in the same study, pacing attenuated the protective effects of VNS whereas bilateral stellectomy did not, further supporting the notion that VNS mediates its effects by direct innervation of the heart rather than by causing reflex activation of afferent fibers in the central nervous system.

Gap junction down-regulation has been implicated in the genesis of arrhythmias with connexin-43 activity levels (regulated by phosphorylation) being closely linked to the pathogenesis of arrhythmias (46). In an ischemia induced VF rat model, connexin-43 phosphorylation is reduced with ischemia and preserved with VNS (33). Inhibition of connexin-43 with carbenoxelone negates both connexin-43 phosphorylation and the protection from VF by VNS (36). Furthermore, aging is associated with reduced connexin-43 expression and aged rats demonstrate a decrease in the protective effects of VNS on ischemia induced VF (36).

Finally, VNS can cause remodeling of the stellate ganglia neurons. In dogs subjected to low level left vagal stimulation for 1 week, left stellate ganglion neurons demonstrated increased expression of a small conductance calcium-activated potassium channel, SK2. SK channels are responsible for the slow afterhyperpolarization,

hyperpolarizing neurons and decreasing neuronal firing. This data suggests that VNS can lead to beneficial remodeling of the sympathetic nervous system (47).

Not all neurotransmitters released with VNS, however, are protective. When cholinergic effects on heart rate (HR) suppression are eliminated with atropine, VNS causes a surprising increase in HR, primarily through the release of vasoactive intestinal peptide (VIP) (35,45,48). Additionally, VIP does not seem to protect against ventricular arrhythmias, does not affect VF threshold or ventricular effective refractory period (35). Given that the vagal trunk contains a variety of nerve fibers and VNS releases a number of neurotransmitters, characterization of the neurotransmitters and their effects is important prior to its utilization for therapeutic purposes.

The anti-arrhythmic benefits of VNS appear to depend on stimulation parameters as well as whether continuous (which often leads to more bradycardia) or intermittent stimulation is utilized. Although VNS reduces ischemia induced VF and VT, stimulation of the vago-sympathetic trunk at high frequencies (> 20Hz) and at intensities that cause severe bradycardia or asystole can induce bigeminy (49-52) and monomorphic VT (15, 29, 49). With high intensity VNS in the setting of acute and chronic ischemia, monomorphic VT can be induced, which can degenerate into VF (21). The genesis of the PVCs induced by high intensity VNS has been attributed to sinus arrest and/or AV nodal blockade which unmasks the underlying ventricular automaticity (17). This phenomenon is eliminated when the ventricle is paced faster than underlying escape rate (53). The unmasking phenomenon of PVCs also carries over to VT (29,51,49). Scherf et al in 1962 showed that occurrence of ventricular couplets with VNS was more frequent when the sinus rhythm rate was lowered by more than 40% in a canine model (49). Therefore, the

pro-arrhythmic effects of VNS occur when high level stimulation unmasks underlying ventricular automaticity due to suppression of supraventricular pacemakers, and in addition, there exists either the simultaneous presence of the substrate for reentry, such as ischemia (53), concurrent sympathetic nerve stimulation (29), or local sodium chloride injections (49). Indeed, in a rabbit ischemia model where intermittent VNS led to a reduction in infarct size, continuous VNS for 10 minutes increased infarct size, while bilateral vagotomy or beta-blockers abolished this deleterious effect. Of note, continuous stimulation also led to significant bradycardia and an increase in loading conditions and atrial, which likely activated the reflex sympathetic nervous system (54). Although the majority of studies show protection against malignant ischemia driven ventricular arrhythmias at low to moderate levels of intermittent VNS, a case report of VNS implantation to treat electrical storm exacerbating ventricular arrhythmias in an ischemic cardiomyopathy patient has been reported (55). These studies demonstrate the importance of identifying the correct patient population and appropriate stimulation parameters of VNS for prevention of VT/VF. In addition, the utility of VNS in the setting of chronic myocardial infarction is currently unknown and needs to be further defined. Finally, there is limited literature examining the effects of low-to-medium intensity VNS on the mature post-infarct scars

HEART FAILURE AND VNS

In a variety of animal models of heart failure, VNS improves cardiac function and even survival. In a canine heart failure model, VNS combined with beta-blockers was superior to beta-blockers alone in improving left ventricular ejection fraction (LVEF) (56).

In a canine pacing induced heart failure model, chronic intermittent VNS with the goal of decreasing heart rate by 20 bpm improved left ventricular (LV) end diastolic and systolic volumes, LVEF, heart rate variability, and baroreflex sensitivity (57). Similar improvements in LVEF and LV end systolic volume were shown in an infarct heart failure canine model with low-level VNS (58). VNS attenuates much of the detrimental effects of ischemia. Low to medium level VNS reduces infarct size (59-61), lowers LVEDP, raises dp/dt, reduces biventricular weight, decreases LV dilation and wall thinning, and improves survival rate (62). Intermittent VNS compared to continuous VNS and initiating VNS during ischemia as opposed to after ischemia seem to increase these beneficial effects (60,61). It is important to understand, however, that variability in stimulation parameters and interspecies differences may lead to unexpected outcomes, particularly during continuous stimulation with significant bradycardia, which can lead to reflex sympathetic activation (54).

The mechanisms behind the beneficial effects of VNS on cardiac function are still under investigation. Calcium influx is reduced when VNS is performed in the setting of sympathetic stimulation, but not when VNS is performed alone (63). Modulation of sympathetic function via presynaptic inhibition of norepinephrine release has also been shown (64). The anti-inflammatory effects, described below, also play an important role in reducing infarct size and improving cardiac function. Finally, VNS causes vasodilation, an effect mediated by acetylcholine, nitric oxide, as well as VIP (65-67). VNS increases coronary blood flow in-situ in normal canine hearts, an effect that is reduced by infusion of a VIP receptor antagonist [(4Cl-D-Phe6Leu17)VIP]. VIP is released at 10-20hz stimulation frequencies in the coronary vasculature and throughout the myocardium (66)

and is a potent vasodilator (greater than adenosine or nitroprusside) (68). It interacts with VIP receptors (VPAC1 and VPAC2) and activates the adenylyl cyclase signaling cascade, leading to vasodilation and increase in inotropy and chronotropy. The vasodilatory effects could mediate the reduction in infarct size observed when applied simultaneously with ischemia due to coronary occlusion in a porcine model (60,61).

ANTI-INFLAMMATORY EFFECTS OF VNS

Low to medium intensity VNS has significant anti-inflammatory effects that may also explain much of its benefit. In a canine pacing induced heart failure model, the rise in plasma norepinephrine, angiotensin II, and CRP levels were attenuated with medium intensity VNS (57). In a post-infarct porcine model, low to medium intensity VNS reduced production of mitochondrial reactive oxygen species and release of cytochrome-c (60, 61). While continuous VNS increased inflammatory markers in a rabbit model of ischemia, potentially by activating the reflex sympathetic nervous system, intermittent VNS and decentralization of vagus eliminated these deleterious effects (54). Similar beneficial effects of intermittent VNS compared to continuous VNS have been observed in an ischemic porcine model where low level left VNS attenuated ventricular dysfunction through prevention of mitochondrial dysfunction (61). Oxidative stress is also modified by VNS. In a mouse chronic heart failure model 28 days post infarct, medium intensity VNS reduced the production of radical oxygen species (69, 70).

The effects of VNS on TNF-alpha are controversial and may be species dependent. TNF-alpha has historically been considered a harmful inflammatory mediator. Its levels are variably affected by VNS depending on the species. Studies in rats (71, 72)

and rabbits (59) with medium level VNS have shown TNF-alpha levels increase with ischemia, an effect that is attenuated with VNS. TNF-alpha is also reduced by low VNS in a canine microembolization heart failure model (58), in endotoxin exposed rats (73), and in heatstroke exposed rats (74). These anti-inflammatory effects are in alignment with the known anti-inflammatory effects of acetylcholine, which inhibits the synthesis of TNF-alpha in the liver and spleen as well as the heart (75). On the other hand, TNF-alpha has pleiotropic effects and can function as a protective inflammatory molecule mediating ischemic preconditioning and prevention of heart failure in mice (76). In a mice model of acute ischemia, an increase in TNF-alpha levels was observed, in contrast to other studies, though VNS in this study was still protective (76). These differences may be explained by the effects of VNS on TNF receptors, rather than TNF levels. VNS in this study simultaneously increased protective TNFR2 and down-regulated the destructive TNFR1, which imparted an overall protective effect to TNF-alpha, and attenuated infarct size (76).

VNS also affects levels of interleukins (IL). Pro-inflammatory IL-6 is reduced with low level VNS in canine heart failure model (58), medium level VNS in rat ischemia model (71), medium level VNS in dog ischemia model (77), and in a rat heatstroke model (74). Pro-inflammatory IL-1 and lipopolysaccharide-inducible CXC chemokine (LIX, IL-8 analogue in rats) were attenuated in the presence of medium intensity VNS in ischemic rat models (71,72,78). Anti-inflammatory IL-4 is increased in a post-infarct porcine model with low to medium intensity VNS (60).

Other inflammatory markers are generally reduced across various studies. A decrease in neutrophil count, MMP-8, and MMP-9 is observed with medium level VNS in

rabbits undergoing coronary occlusion (59). MCP-1 (monocyte chemoattractant protein) is increased with ischemia, and the increase is attenuated in the presence of medium intensity VNS in an ischemic rat model (78).

In summary, VNS has shown promise in reducing malignant ventricular arrhythmias, particularly in the setting of ischemia. The improvement in heart failure and the anti-inflammatory and vasodilatory properties of VNS provide additional anti-arrhythmic benefit. Given the complexity of the cardiac autonomic nervous system, including the presence of both afferent and efferent as well as parasympathetic and dopaminergic fibers in the vago-sympathetic trunk, it is critical to carefully elucidate the mechanisms of VNS and the parameters of stimulation to ensure that vagal nerve stimulators achieve the desired therapeutic effect. Furthermore, the role of VNS in a chronic remodeled infarct needs to be further defined. Lastly, the role of afferent fiber activation within the vagal trunk on efferent parasympathetic effects needs further clarification. This dissertation focuses on addressing these objectives.

Figure 1. The vagus nerve contains afferent fibers that transmit information from the heart via the pseudo-unipolar neurons of the nodose ganglion to the nucleus tractus solitarius (NTS) in the brainstem. The NTS provides connections to the dorsal motor nucleus (DMN) of the vagus and nucleus ambiguus (NA), dashed red line, where the efferent vagal preganglionic fibers to the heart originate. These fibers synapse in the intrinsic cardiac ganglia. Post-ganglionic parasympathetic fibers originate from these ganglia and innervate the myocardium. AP = area postrema.

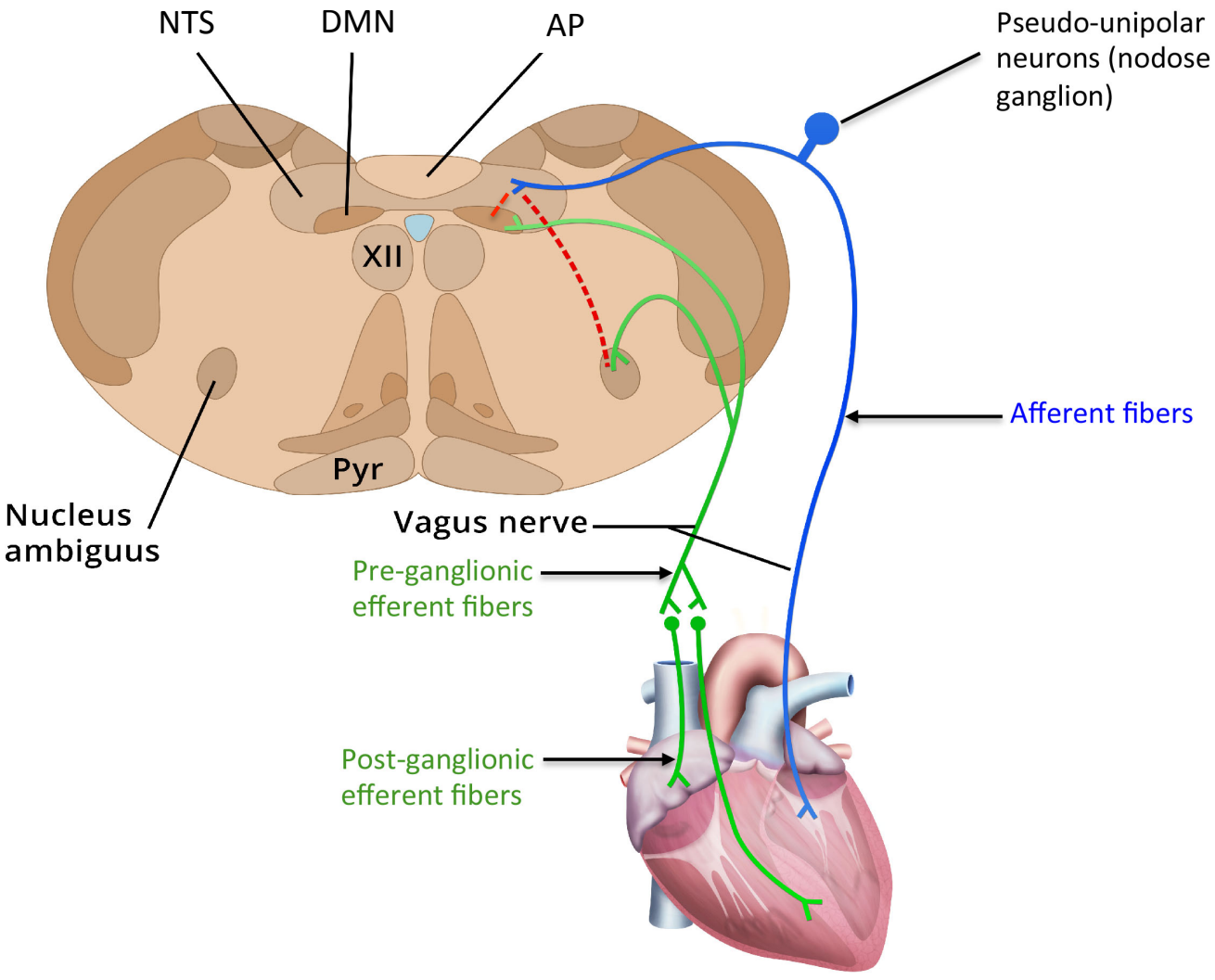

REFERENCES

1. Farrell TG, Bashir Y, Cripps T, et al. Risk stratification for arrhythmic events in postinfarction patients based on heart rate variability, ambulatory electrocardiographic variables and the signal-averaged electrocardiogram. *J Am Coll Cardiol.* 1991;18:687-697.
2. Farrell TG, Paul V, Cripps TR, et al. Baroreflex sensitivity and electrophysiological correlates in patients after acute myocardial infarction. *Circulation.* 1991;83:945-952.
3. Hull SS, Jr., Evans AR, Vanoli E, et al. Heart rate variability before and after myocardial infarction in conscious dogs at high and low risk of sudden death. *J Am Coll Cardiol.* 1990;16:978-985.
4. Kleiger RE, Miller JP, Bigger JT, Jr., Moss AJ. Decreased heart rate variability and its association with increased mortality after acute myocardial infarction. *Am J Cardiol.* 1987;59:256-262.
5. La Rovere MT, Bigger JT, Jr., Marcus FI, Mortara A, Schwartz PJ. Baroreflex sensitivity and heart-rate variability in prediction of total cardiac mortality after myocardial infarction. ATRAMI (Autonomic Tone and Reflexes After Myocardial Infarction) Investigators. *Lancet.* 1998;351:478-484.
6. Vanoli E, Schwartz PJ. Sympathetic--parasympathetic interaction and sudden death. *Bas Res Cardiol.* 1990;85 Suppl 1:305-321.
7. Schwartz PJ, Billman GE, Stone HL. Autonomic mechanisms in ventricular fibrillation induced by myocardial ischemia during exercise in dogs with healed

myocardial infarction. An experimental preparation for sudden cardiac death. *Circulation.* 1984;69:790-800.

8. Bonaz B, Picq C, Sinniger V, Mayol JF, Clarencon D. Vagus nerve stimulation: from epilepsy to the cholinergic anti-inflammatory pathway. *Neurogastroenterol Motil.* 2013;25:208-221.
9. Waxman SG. *Clinical Neuroanatomy.* 27e ed: Mc-Graw Hill Medical; 2013.
10. Randall WC, Priola DV, Pace JB. Responses of individucal cardiac chambers to stimulation of the cervical vagosympathetic trunk in atropinized dogs. *Circ Res.* 1967;20:534-544.
11. Seki A, Green HR, Lee TD, et al. Sympathetic nerve fibers in human cervical and thoracic vagus nerves. *Heart Rhythm.* 2014;11:1411-1417.
12. Armour JA. Potential clinical relevance of the "little brain" on the mammailian heart. *Exp Physiol*. 2008;93:165-76.
13. Armour JA, Murphy DA, Yuan BX, Macdonald S, Hopkins DA. Gross and microscopic anatomy of the human intrinsic cardiac nervous system. *Anat Rec.* 1997;247:289-298.
14. Shen MJ, Zipes DP. Role of the autonomic nervous system in modulating cardiac arrhythmias. *Circ Res.* 2014;114:1004-1021.
15. Takahashi N, Zipes DP. Vagal modulation of adrenergic effects on canine sinus and atrioventricular nodes. *Am J Physiol.* 1983;244:H775-781.
16. Naggar I, Nakase K, Lazar J, Salciccioli L, Selesnick I, Stewart M. Vagal control of cardiac electrical activity and wall motion during ventricular fibrillation in large animals. *Auton Neurosci.* 2014;183:12-22.

17. Peiss CN, Spurgeon HA. Origin of initial escape beat during graded vagal stimulation.*J Electrocardiol.* 1975;8:25-29.

18. Brack KE, Patel VH, Coote JH, Ng GA. Nitric oxide mediates the vagal protective effect on ventricular fibrillation via effects on action potential duration restitution in the rabbit heart. *J Physiol.* 2007;583:695-704.

19. Martins JB, Zipes DP. Effects of sympathetic and vagal nerves on recovery properties of the endocardium and epicardium of the canine left ventricle. *Circ Res.* 1980;46:100-110.

20. Martins JB, Zipes DP, Lund DD. Distribution of local repolarization changes produced by efferent vagal stimulation in the canine ventricles. *J Am Coll Cardiol.* 1983;2:1191-1199.

21. Scherlag BJ, Kabell G, Harrison L, Lazzara R. Mechanisms of bradycardia-induced ventricular arrhythmias in myocardial ischemia and infarction. *Circulation.* 1982;65:1429-1434.

22. Yamakawa K, So EL, Rajendran PS, et al. Electrophysiological effects of right and left vagal nerve stimulation on the ventricular myocardium. *Am J Physiol Heart Circ Physiol.* 2014;307:H722-731.

23. Opthof T, Dekker LR, Coronel R, Vermeulen JT, van Capelle FJ, Janse MJ. Interaction of sympathetic and parasympathetic nervous system on ventricular refractoriness assessed by local fibrillation intervals in the canine heart. *Cardiovasc Res.* 1993;27:753-759.

24. Scherlag BJ, Helfant RH, Haft JI, Damato AN. Electrophysiology underlying ventricular arrhythmias due to coronary ligation. *Am J Physiol.* 1970;219:1665-1671.

25. Kent KM, Smith ER, Redwood DR, Epstein SE. Electrical Stability of Acutely Ischemic Myocardium: Influences of Heart Rate and Vagal Stimulation. *Circulation.* 1973;47:291-298.

26. Myers RW, Pearlman AS, Hyman RM, et al. Beneficial Effects of Vagal Stimulation and Bradycardia During Experimental Acute Myocardial Ischemia. *Circulation.* 1974;49:943-947.

27. Kolman BS, Verrier RL, Lown B. The effect of vagus nerve stimulation upon vulnerability of the canine ventricle: role of sympathetic-parasympathetic interactions. *Circulation.* 1975;52:578-585.

28. Yoon MS, Han J, Tse WW, Rogers R. Effects of vagal stimulation, atropine, and propranolol on fibrillation threshold of normal and ischemic ventricles. *Am Heart J.* 1977;93:60-65.

29. Takahashi N, Ito M, Iwao T, et al. Vagal modulation of ventricular tachyarrhythmias induced by left ansae subclaviae stimulation in rabbits. *Jap Heart J.* 1998;39:503-511.

30. Zuanetti G, De Ferrari GM, Priori SG, Schwartz PJ. Protective effect of vagal stimulation on reperfusion arrhythmias in cats. *Circ Res.* 1987;61:429-435.

31. Vanoli E, De Ferrari GM, Stramba-Badiale M, Hull SS, Foreman RD, Schwartz PJ. Vagal stimulation and prevention of sudden death in conscious dogs with a healed myocardial infarction. *Circ Res.* 1991;68:1471-1481.

32. Rosenshtraukh L, Danilo P, Anyukhovsky EP, et al. Mechanisms for vagal modulation of ventricular repolarization and of coronary occlusion-induced lethal arrhythmias in cats. *Circ Res.* 1994;75:722-732.

33. Ando M, Katare RG, Kakinuma Y, et al. Efferent vagal nerve stimulation protects heart against ischemia-induced arrhythmias by preserving connexin43 protein. *Circulation.* 2005;112:164-170.

34. Ng GA, Brack KE, Patel VH, Coote JH. Autonomic modulation of electrical restitution, alternans and ventricular fibrillation initiation in the isolated heart. *Cardiovasc Res.* 2007;73:750-760.

35. Brack KE, Coote JH, Ng GA. Vagus nerve stimulation protects against ventricular fibrillation independent of muscarinic receptor activation. *Cardiovasc Res.* 2011;91:437-446.

36. Wu W, Lu Z. Loss of anti-arrhythmic effect of vagal nerve stimulation on ischemia-induced ventricular tachyarrhythmia in aged rats. *Tohoku J Exp Med.* 2011;223:27-33.

37. Matta RJ, Verrier RL, Lown B. Repetitive extrasystole as an index of vulnerability to ventricular fibrillation. *Am J Physiol.* 1976;230:1469-1473.

38. Brooks WW, Verrier RL, Lown B. Influence of vagal tone on stellectomy-induced changes in ventricular electrical stability. *Am J Physiol.* 1978;234:H503-507.

39. Zheng C, Li M, Inagaki M, Kawada T, Sunagawa K, Sugimachi M. Vagal stimulation markedly suppresses arrhythmias in conscious rats with chronic heart failure after myocardial infarction. *Conference proceedings : ... Annual International Conference of the IEEE Engineering in Medicine and Biology Society.*

IEEE Engineering in Medicine and Biology Society. Annual Conference. 2005;7:7072-7075.

40. Weiss JN, Karma A, Shiferaw Y, Chen PS, Garfinkel A, Qu Z. From pulsus to pulseless: the saga of cardiac alternans. *Circ Res.* 2006;98:1244-1253.
41. James R, Arnold J, Allen JD, Pantridge JF, Shanks RG. The effects of heart rate, myocardial ischemia and vagal stimulation on the threshold for ventricular fibrillation. *Circulation.* 1977;55:311-317.
42. Herre JM, Thames MD. Responses of sympathetic nerves to programmed ventricular stimulation. *J Am Coll Cardiol.* 1987;9:147-153.
43. Smith ML, Hamdan MH, Wasmund SL, Kneip CF, Joglar JA, Page RL. High-frequency ventricular ectopy can increase sympathetic neural activity in humans. *Heart Rhythm.* 2010;7:497-503.
44. Rajendran PS, Vaseghi M, Armour JA, Ardell JL, Shivkumar K. Abstract 12655: Cardiac Pacing Alters Neural Information Processing in the Intrinsic Cardiac Nervous System. *Circulation.* 2014;130:A12655.
45. Del Rio CL, Dawson TA, Clymer BD, Paterson DJ, Billman GE. Effects of acute vagal nerve stimulation on the early passive electrical changes induced by myocardial ischaemia in dogs: heart rate-mediated attenuation. *Exp Physiol.* 2008;93:931-944.
46. Remo BF, Giovannone S, Fishman GI. Connexin43 cardiac gap junction remodeling: lessons from genetically engineered murine models. *J Membr Biol.* 2012;245:275-281.

47. Shen MJ, Hao-Che C, Park HW, et al. Low-level vagus nerve stimulation upregulates small conductance calcium-activated potassium channels in the stellate ganglion. *Heart Rhythm.* 2013;10:910-915.

48. Hill MR, Wallick DW, Mongeon LR, Martin PJ, Levy MN. Vasoactive intestinal polypeptide antagonists attenuate vagally induced tachycardia in the anesthetized dog. *Am J Physiol.* 1995;269:H1467-1472.

49. Scherf D, Blumenfeld S, Yildiz M. Experimental study on ventricular extrasystoles provoked by vagal stimulation. *Am Heart J.* 1961;62:670-675.

50. Takato T, Ashida T, Seko Y, Fujii J, Kawai S. Ventricular tachyarrhythmia-related basal cardiomyopathy in rabbits with vagal stimulation--a novel experimental model for inverted Takotsubo-like cardiomyopathy. *J Cardiol.* 2010;56:85-90.

51. Manning J.W. CMD. Mechanism of Cardiac Arrhythmias induced by diencephalic stimulation. *Am J Physiol.* 1962;203:1120-1124.

52. Ashida T, Ono C, Sugiyama T, Fujii J. Mitral valve hemorrhage and mitral annulus shrinkage in rabbits with transient ventricular bigeminies induced by vagal stimulation. *J Heart Valve Dis.* 2004;13:779-783.

53. Kerzner J, Wolf M, Kosowsky BD, Lown B. Ventricular Ectopic Rhythms following Vagal Stimulation in Dogs with Acute Myocardial Infarction. *Circulation.* 1973;47:44-50.

54. Buchholz B, Donato M, Perez V, et al. Changes in the loading conditions induced by vagal stimulation modify the myocardial infarct size through sympathetic-parasympathetic interactions. *Pflugers Arch.* 2014;467:1509-22

55. Katsouras G, Sakabe M, Comtois P, et al. Differences in atrial fibrillation properties under vagal nerve stimulation versus atrial tachycardia remodeling. *Heart Rhythm.* 2009;6:1465-1472.

56. Sabbah HN. Electrical vagus nerve stimulation for the treatment of chronic heart failure. *Cleve Clin J Med.* 2011;78 Suppl 1:S24-29.

57. Zhang Y, Popovic ZB, Bibevski S, et al. Chronic vagus nerve stimulation improves autonomic control and attenuates systemic inflammation and heart failure progression in a canine high-rate pacing model. *Circ Heart fail.* 2009;2:692-699.

58. Hamann JJ, Ruble SB, Stolen C, et al. Vagus nerve stimulation improves left ventricular function in a canine model of chronic heart failure. *Eur J Heart Fail.* 2013;15:1319-1326.

59. Uemura K, Zheng C, Li M, Kawada T, Sugimachi M. Early short-term vagal nerve stimulation attenuates cardiac remodeling after reperfused myocardial infarction. *J Card Fail.* 2010;16:689-699.

60. Shinlapawittayatorn K, Chinda K, Palee S, et al. Vagus nerve stimulation initiated late during ischemia, but not reperfusion, exerts cardioprotection via amelioration of cardiac mitochondrial dysfunction. *Heart Rhythm.* 2014;11:2278-87.

61. Shinlapawittayatorn K, Chinda K, Palee S, et al. Low-amplitude, left vagus nerve stimulation significantly attenuates ventricular dysfunction and infarct size through prevention of mitochondrial dysfunction during acute ischemia-reperfusion injury. *Heart Rhythm.* 2013;10:1700-1707.

62. Li M, Zheng C, Sato T, Kawada T, Sugimachi M, Sunagawa K. Vagal nerve stimulation markedly improves long-term survival after chronic heart failure in rats. *Circulation.* 2004;109:120-124.

63. Brack KE, Coote JH, Ng GA. Vagus nerve stimulation inhibits the increase in Ca2+ transient and left ventricular force caused by sympathetic nerve stimulation but has no direct effects alone--epicardial Ca2+ fluorescence studies using fura-2 AM in the isolated innervated beating rabbit heart. *Exp Physiol.* 2010;95:80-92.

64. Muscholl E. Peripheral muscarinic control of norepinephrine release in the cardiovascular system. *Am J Physiol.* 1980;239:H713-720.

65. Feigl EO. Parasympathetic control of coronary blood flow in dogs. *Circ Res.* 1969;25:509-519.

66. Henning RJ, Sawmiller DR. Vasoactive intestinal peptide: cardiovascular effects. *Cardiovasc Res.* 2001;49:27-37.

67. Zhao G, Shen W, Xu X, Ochoa M, Bernstein R, Hintze TH. Selective impairment of vagally mediated, nitric oxide-dependent coronary vasodilation in conscious dogs after pacing-induced heart failure. *Circulation.* 1995;91:2655-2663.

68. Sawmiller DR, Henning RJ, Cuevas J, Dehaven WI, Vesely DL. Coronary vascular effects of vasoactive intestinal peptide in the isolated perfused rat heart. *Neuropeptides.* 2004;38:289-297.

69. Tsutsumi T, Ide T, Yamato M, et al. Modulation of the myocardial redox state by vagal nerve stimulation after experimental myocardial infarction. *Cardiovasc Res.* 2008;77:713-721.

70. Kong SS, Liu JJ, Yu XJ, Lu Y, Zang WJ. Protection against ischemia-induced oxidative stress conferred by vagal stimulation in the rat heart: involvement of the AMPK-PKC pathway. *Int J Mol Sci.* 2012;13:14311-14325.

71. Wang Q, Cheng Y, Xue FS, et al. Postconditioning with vagal stimulation attenuates local and systemic inflammatory responses to myocardial ischemia reperfusion injury in rats. *Inflamm Res.* 2012;61:1273-1282.

72. Zhao M, He X, Bi XY, Yu XJ, Gil Wier W, Zang WJ. Vagal stimulation triggers peripheral vascular protection through the cholinergic anti-inflammatory pathway in a rat model of myocardial ischemia/reperfusion. *Bas Res Cardiol.* 2013;108:345.

73. Borovikova LV, Ivanova S, Zhang M, et al. Vagus nerve stimulation attenuates the systemic inflammatory response to endotoxin. *Nature.* 2000;405:458-462.

74. Yamakawa K, Matsumoto N, Imamura Y, et al. Electrical vagus nerve stimulation attenuates systemic inflammation and improves survival in a rat heatstroke model. *PloS one.* 2013;8:e56728.

75. Tracey KJ. The inflammatory reflex. *Nature.* 2002;420:853-859.

76. Katare RG, Ando M, Kakinuma Y, Arikawa M, Yamasaki F, Sato T. Differential regulation of TNF receptors by vagal nerve stimulation protects heart against acute ischemic injury. *J Moll Cell Cardiol.* 2010;49:234-244.

77. Zhang R, Wugeti N, Sun J, et al. Effects of vagus nerve stimulation via cholinergic anti-inflammatory pathway activation on myocardial ischemia/reperfusion injury in canine. *Int J Clin Exp Med.* 2014;7:2615-2623.

78. Calvillo L, Vanoli E, Andreoli E, et al. Vagal stimulation, through its nicotinic action, limits infarct size and the inflammatory response to myocardial ischemia and reperfusion. *J Cardiovasc Pharm.* 2011;58:500-507.

CHAPTER 2

ELECTROPHYSIOLOGICAL EFFECTS OF RIGHT AND LEFT VAGAL NERVE STIMULATION ON THE VENTRICULAR MYOCARDIUM

INTRODUCTION

The autonomic nervous system plays a significant role in the genesis and persistence of ventricular arrhythmias (55, 60). Sympathetic activation is pro-arrhythmic (16, 33, 54), whereas parasympathetic activation is thought to be cardioprotective (17, 31). The vagal nerve trunk provides important cardio-motor efferent fibers to the heart and also carries afferent signals from the heart. Vagal nerve stimulation (VNS) has been shown to decrease infarct size (49), reduce ventricular fibrillation threshold (40), and decrease incidence of ventricular arrhythmias and mortality during ischemia (13, 27, 39, 53). Further, a preserved parasympathetic reflex has been reported to be protective during myocardial infarction (47). Right vagal nerve (RVN) stimulation has shown benefit in a series of patients with cardiomyopathy and is undergoing evaluation in clinical trials (20, 48). The mechanisms of the anti-arrhythmic effects of VNS are less clear and are thought to be multifactorial, with a decrease in heart rate (HR) (15), release of nitric oxide (9), and antagonism of the sympathetic nervous system all thought to play a role (8, 30, 50).

Modulation of repolarization by sympathetic nerve stimulation has been well characterized (1, 25, 42, 56, 59). However, effects of parasympathetic regulation of ventricular repolarization have not been extensively studied. Indeed, parasympathetic innervation of the ventricular myocardium was considered minimal for many years. Histological studies have now confirmed evidence of abundant ventricular parasympathetic innervation (24, 26, 52), but the distribution of right vs. left cardiac vagal cardiomotor fibers is unclear. Prior studies of ventricular repolarization during VNS were limited in using small number of electrodes (36), extra-stimulus pacing (34),

or VF intervals (42): techniques that can alter autonomic tone (23) and do not provide detailed spatial data. Furthermore, differences between RVN and LVN on regional repolarization remain unclear and may be important given presence of disease processes that can affect certain areas of the heart to different degrees. For unilateral stimulation, lack of laterality would also be significant in allowing similar effects of VNS from either side.

The aim of this study was to assess the effects of right and left VNS on cardiac function and global and regional ventricular repolarization of the endocardium and epicardium.

METHODS

Animal Protocol

All animal experiments were performed in accordance with the National Institutes of Health *Guide for the Care and Use of Laboratory Animals* and approved by the UCLA Institutional Chancellor's Animal Research Committee.

Yorkshire pigs (n = 12, 20-50 kg) were sedated (telazol 8-10 mg/kg intramuscular), intubated, and ventilated. General anesthesia was maintained with isoflurane (1-1.5%) and intravenous boluses of fentanyl (2-4 μg/kg). A median sternotomy was performed to expose the heart and cervical right and left vago-sympathetic trunks were isolated. Following completion of surgery, anesthesia was switched to α-chloralose (10 mg/kg/hr intravenous infusion). HR was monitored via electrocardiogram recordings. Right femoral artery was catheterized for monitoring of systemic blood pressure (SBP). Hourly arterial blood gases were obtained, and tidal volume adjusted and/or infusions of sodium bicarbonate given to maintain acid-base homeostasis.

Hemodynamic Assessment

Pressure-volume loops, left ventricular end-systolic pressure (LVESP), left ventricular end-diastolic pressure (LVEDP), dP/dt max and min, and Tau were obtained using a 12-pole conductance pressure catheter in the left ventricle (LV), n=8, connected to a Pressure Volume Loop System (Millar Instruments, Houston, TX). Tau was calculated using the Weiss method(57) from the pressure-volume loop as a parameter describing the time course of the exponential decay in LV pressure during isovolumic relaxation. The following equation was used to calculate Tau: $P(t) = A \exp(-t/Tau)$.

Vagal Nerve Stimulation

Right and left vagal nerves were stimulated separately using bipolar electrodes (Cyberonics, Houston, TX) connected to a Grass S88 Stimulator (Grass Technologies, Warwick, RI). Square stimulation pulses were delivered at 0.5-1.0 ms in duration and 10-20 Hz in frequency. To determine the threshold current, the current was increased starting from 0.2 mA by 0.2 mA intervals until either 10-20% drop in HR (the percentage of 10 versus 20% was selected based on the animals' baseline HR so that severe bradycardia or significant drop in blood pressure was avoided) for both right and left VNS. After reaching the threshold current, the stimulation current was decreased by 0.1 mA to confirm that the threshold was accurate. If a stimulation frequency of 20 Hz led to complete heart block or asystole with right VNS, left VNS, or both, 10 Hz was use as the stimulation frequency for both right and left VNS. Right and left VNS was performed at 1.2 times threshold current for 15 seconds followed by a 15- minute stabilization period to allow for ARI and hemodynamic parameters to return to baseline. In order to account for any HR effects on ARI, atrial pacing at the baseline HR was performed in 4 animals

during right and left VNS. In addition, sub-threshold VNS at a level just below HR response was performed in 1 animal and the ARI was analyzed.

Activation Recovery Interval Recordings

A 56-electrode nylon sock was placed around the heart (n = 12) and a 64-electrode basket catheter (n = 9) was placed into LV via the left carotid artery. Unipolar electrograms (EGMs) were obtained using a Prucka CardioLab System (GE Healthcare, Fairfield, CT) and a custom-made, 128-channel multiplexor. EGMs were band-pass filtered between 0.05-500 Hz. A minimum of 10 EGMs was analyzed from each electrode prior to and during stimulation. An electrofield electroanatomic mapping system (NavX, St. Jude Medical, St. Paul, MN) was used to assess basket catheter position. At the end of the experiment, direct incision of the LV was performed to confirm endocardial electrode locations. ARIs were measured and calculated using customized software, ScalDyn (University of Utah, Salt Lake City, UT) as previously described (56). ARI has been shown to correlate well with APD and allows for multiple simultaneous measurements. Further, changes in ARI at a given site during an intervention correlate well with changes in APD measured from micro-electrodes (21, 38). This method allows for measurement of local APD without extra-stimulus delivery, or induction of VF, methods that can alter autonomic tone. Global dispersion of repolarization (DOR) was calculated using the variance of all mean ARIs recorded in a specific region. EGMs with flattened T waves, fractionation, or noise were excluded.

Regional ARI Analysis

For purposes of this manuscript, anterior refers to the ventral aspect and posterior refers to the dorsal aspect of the animal. Mean ARI in the following regions was

analyzed: LV anterior, lateral and posterior, RV anterior, lateral, and posterior, RVOT, LV base and apex. The median number of electrodes in each region was 4 (range of 3-7). For assessment of trans-mural (endocardial vs. epicardial) differences in ARI, electrodes directly across from each other on the anterior, lateral, and posterior aspects of the mid LV were used.

Three-dimensional sock ARI data were projected on to two-dimensional polar maps using publicly available software Map3D (University of Utah, http://www.sci.utah.edu/cibc/software/107-map3d.html).

Statistical Analysis

For comparison of continuous variables, Wilcoxon rank sum test or Wilcoxon signed rank test was used. For regional analysis, means and variances in ARI were compared using a parametric repeated measure analysis of variance (ANOVA). The *p* value for a particular pairwise, mean, standardized ARI comparison was considered significant only if the corresponding overall F statistic was significant. Dispersion in ARI was defined as the variance in the mean ARI recorded from all the electrodes over a given region. To account for baseline differences, percentage change in ARI was also compared. Given the range of values for DOR, the log mean difference was used for statistical analysis of regional differences. Data are presented as mean ± SE. SAS 9.1 was used for statistical analysis. $p < 0.05$ was considered statistically significant. Correlation between hemodynamics parameters and ARI changes were performed using the Pearson correlation test.

RESULTS

The right vagal nerve stimulation current was 4.0 ± 0.8 mA and left vagal nerve stimulation current was 4.2 ± 0.8 mA, p = 0.6 for right vs. left stimulation current. Three animals developed complete heart block with right and four animals developed complete heart block with left VNS.

Hemodynamic Response to Stimulation

The effects of right and left VNSstimulation on hemodynamic parameters are shown in table 1. Both right and left VNS decreased dP/dt max and LVESP, increased dP/dt min and Tau. There were no statistically significant differences between right and left VNS on hemodynamic parameters, and therefore, no laterality on the hemodynamic effects of right vs. left VNS, table 1. The increase in dP/dt min and Tau by both right and left VNS suggested a worsening of diastolic function by VNS. The PR interval increased right VNS (from 114±4 ms to 137±5 ms) and left VNS (from 112 ± 4 ms to 140 ± 4 ms). There was no difference in PR interval prolongation between right vs. left VNS (p = 0.4).

Effects of Right and Left VNS on Epicardial ARI and DOR

Right and left VNS prolonged global epicardial ARI from 327 ± 18 to 350 ± 23 ms (7 ± 2%, p < 0.05 vs. baseline), and from 327 ± 16 to 347 ± 21 ms (6 ± 2 %, p < 0.05 vs. baseline), respectively, with no significant differences between right or left, (p = 0.4). Epicardial dispersion of ARI (DOR) was increased by both right and left VNS from 354 ± 53 to 512 ±121 ms^2 and from 338 ± 57 to 476 ± 110 ms^2, respectively (p < 0.05 vs. baseline for both conditions), figure 1. With respect to anterior, posterior, and lateral changes on the RV and LV, each region demonstrated ARI prolongation (p < 0.05) as compared to baseline (figure 2) without statistically significant differences in prolongation between these regions. The regional changes in DOR at baseline and

during right and left VNS are shown in table 2. These changes from baseline were not statistically significant. With regards to regional comparisons, no significant anterior, lateral, or posterior differences in DOR during right or left VNS were observed on the epicardium, figure 3. Detailed regional DOR comparisons are provided in table 3 and 4.

When comparing apico-basal differences, the apex showed a slightly greater prolongation of ARI than the base with both right and left VNS from 339 ±19 to 366 ± 25 ms and from 339 ± 18 to 363 ± 23 ms, respectively ($p < 0.05$ vs. baseline for both right and left VNS), figure 4. ARI at the base increased from 322 ± 17 ms to 342 ± 21 ms with RVN and from 323 ± 16 ms to 341 ± 20 ms with LVN stimulation. The direction of repolarization, however, was maintained during stimulation as the base of heart had a shorter ARI as compared to the apex at baseline prior to both right and left VNS ($p < 0.05$ for baseline apex vs. base mean ARI), figure 4.

Amongst hemodynamic parameters, effects of VNS on HR, dP/dt max, and LVESP had the highest correlation with the increase in ventricular ARI (R^2= -0.58 for HR, $p = 0.002$, R^2 = -0.52, $p = 0.04$ for LVESP, and $R^2 = 0.81$, $p < 0.0001$ for dP/dt max). Of note, the parameter that correlated most strongly with ARI effects was dP/dt max, figure 5.

Effects of Right and Left VNS on Endocardial ARI and DOR

On the endocardium, right and left VNS prolonged ARI from 281 ± 16 to 298 ± 17 ms ($p < 0.001$) and from 276 ± 18 to 297 ± 19 ms ($p = 0.04$) vs. baseline, respectively. DOR of the LV endocardium changed from 84 ± 22 ms^2 to 127 ± 28 ms^2 with right and from 115 ± 35 ms^2 to 139 ± 49 ms^2 with left VNS, although these differences from baseline were not statistically significant ($p = 0.2$ for right and $p = 0.4$ for left). Similar to the epicardium, no regional differences in the increase in endocardial ARI across the

anterior, lateral, and posterior regions of the LV were found during right or left VNS or between right and left VNS, figure 6. Similar to the epicardium, no significant anterior, lateral, or posterior differences in DOR during right or left VNS were observed on the endocardium, figure 7. Regional DOR comparisons are provided in tables 3 and 4.

Transmural Differences in ARI

During right VNS, mean LV endocardial ARI increased from 281 ± 16 to 298 ± 17 ms (6 ± 2 %, $p = 0.04$). LV epicardial ARI increased from 313 ± 11 to 324 ± 13 ms (4 ± 1 %, $p < 0.01$). During left VNS, LV endocardial ARI prolonged from 276 ± 18 to 297 ± 19 ms (8 ± 2 %, $p < 0.01$). LV epicardial ARI prolonged from 312 ± 12 to 325 ± 12 ms (4 ± 1 %, $p < 0.01$). Therefore, the endocardium showed a greater prolongation of ARI than the epicardium during both right and left VNS ($p < 0.01$ both conditions, figure 8).

Effect of Heart Rate on Ventricular ARI by VNS

Atrial pacing was performed during VNS at the same HR as baseline in 4 animals. Global ARI prolonged from 362 ± 30 to 389 ± 32 ms by right VNS alone. During pacing, ARI still prolonged to 370 ± 30 ms (mean ± SE). left VNS also demonstrated prolongation of ARI from 357 ± 23 to 379 ± 30 ms, and remained prolonged during atrial pacing 367 ± 24 ms.

The PR interval prior to right VNS was 123 ± 4 ms and increased to 133 ± 8 ms during VNS and was further increased to 194 ± 10 ms (mean ± E), likely due faster pacing during VNS leading to greater decremental conduction in the AV node. Prior to left VNS, the PR interval in was 128 ± 8 ms, which increased to 142 ± 13 ms during VNS and further increased to 198 ± 10 ms (mean ± SE) with atrial pacing during VNS

Sub-threshold VNS in 1 animal showed that despite a lack of change in HR, right VNS prolonged ARI from 423 ± 4 to 444 ± 5 ms, and left VNS prolonged ARI from 424 ± 4 to 431 ± 4 ms.

DISCUSSION

Major Findings

This study in a porcine model shows that both right and left VNS increased ventricular ARI. This increase was strongly correlated with dP/dt max. HR and LVESP showed moderate correlations. Parameters of diastolic function were not improved with VNS. Furthermore, during both right and left VNS, the epicardial ARI at the apex prolonged more than the ARI at the base of the heart. VNS prolonged ARI to a similar degree on the anterior, posterior, and lateral walls of the LV and RV. The endocardium showed greater prolongation in ARI as compared to epicardium. These effects were similar between right and left VNS. Finally, there were no differences *between* right and left VNS on hemodynamic response or regional repolarization of the epicardium or endocardium. Therefore, no significant laterality to functional innervation of these nerves was observed.

Global and Regional Increase in ARI due to Right and Left VNS

Histological studies have shown that there may be small differences in the parasympathetic innervation of the RV and LV in guinea pigs (14), however, few studies have analyzed functional regional differences in detail. Martin et al. demonstrated that LVN stimulation showed a slightly greater prolongation of the LV epicardial posterior wall (mean difference of 1.2 ms) as compared to RVN stimulation in a canine model. Further,

they found that VNS did not prolong APD on the anterior epicardial RV (36). In our study, no significant regional differences between right and left VNS on ARI of the LV or RV across anterior, posterior, and lateral regions were noted. A clear increase in endocardial ARI as compared to epicardial ARI was observed with both RVN and LVN stimulation, and both increased ARI at the apex more than the base. Further, a significant prolongation in ARI from baseline with both right and left VNS on the anterior RV epicardium was seen. The difference in the results of this study may be due to a more detailed assessment of repolarization, with multiple electrodes in each region, the fact that ARI may be a more accurate surrogate of APD, and inter-species differences in innervation between the canine and porcine model.

From a physiological and anatomical perspective, the lack of anterior, lateral, and posterior regional differences and laterality of the effects of right and left VNS on repolarization may be due to the type of nerve fibers (pre-ganglionic rather than post-ganglionic) in the vago-sympathetic trunk and their obligatory synapse within the ganglia of the intrinsic cardiac nervous system (3, 45). Post-ganglionic fibers to the myocardium arise from these intrinsic cardiac ganglia (44). The intrinsic cardiac nervous system is known to regulate hemodynamic effects of VNS via a complex, integrated neural network. Therefore, elimination of a single ganglion may reduce but does not eliminate chronotropic or dromotropic response (44). The fact that both right and left VNS have similar effects suggests that the neurons of the intrinsic cardiac ganglia mitigate and “smooth out” any electrophysiological laterality between the two sides, distributing the post-ganglionic effects to all regions in a more homogenous manner. These results are further confirmed by microdialysis studies demonstrating that the level of LV epicardial

acetylcholine release is similar with right versus left VNS (2). This is unlike the sympathetic ganglia, where the left stellate ganglion's post-ganglionic fibers provide greater functional innervation to the posterior walls of the ventricles, and the right stellate ganglion provides greater innervation to the anterior walls of the ventricles (29, 56, 59). These results support the value of unilateral VNS for cardiac therapeutic purposes as the net effects are likely to be distributed uniformly to the ventricles.

Apico-basal Differences in ARI

In this study, significant apico-basal differences in response to VNS were noted, with the apex demonstrating a greater prolongation of ARI than the base. Right or left VNS, however, did not lead to a reversal in the direction of repolarization as the base had a shorter ARI at baseline. Mantravadi et al., using optical mapping studies in a decentralized Langendorff model, showed that bilateral VNS prolonged APD more at the apex than the base, consistent with this study. Mantravadi and colleagues, however, reported that the repolarization at the apex was shorter than the base at baseline (32). This difference with our study may be due to the type of ex-vivo preparation versus the location of the optical mapping performed, as certain regions of the anterior base of the LV have been reported to have a longer APD than the apex or the posterior base of the heart (6, 51). Analysis of our data shows that base of heart had a shorter ARI at baseline, consistent with rabbit myocyte, canine, porcine, and human mapping studies showing a shorter APD, functional refractory period, and ARI at the base under control conditions (10, 11, 41, 43, 56). The shorter ARI at baseline in vivo could be due to the distribution of potassium channels, such as greater concentration of IKs channels at the base as well as a greater concentration of sympathetic fibers in this region (11, 26). The

apico-basal differences during VNS were surprising, and cannot be attributed to HR alone, as bradycardia would have affected all regions. Furthermore, they can not be solely attributed release of other co-transmitters that may prolong APD, such as VIP, as this would have led to a greater prolongation of ARI at the base rather than the apex, similar to differences observed on the endocardium vs. epicardium. Therefore, the apico-basal differences may be due to reflex sympathetic activation (via activation of IKs which is more prominent at the base, leading to shorter APD) or the distribution of IKAch channels, which maybe more densely distributed at the base, leading to a greater shortening of ARI at the base as compared to the apex.

Transmural Differences in ARI

Overall, both right and left VNS caused small increases in DOR on the epicardium. This may be due to the bradycardia caused by VNS (28), or to the more sparse density of parasympathetic nerve fibers on the epicardium (52). In fact, functional parasympathetic innervation of the endocardium was greater than the epicardium, consistent with histological studies showing that endocardium has greater density of parasympathetic fibers (52). Furthermore, parasympathetic fibers are thought to run from the endocardium to the epicardium, as supported by the observation that denervation of the epicardium does not reduce the endocardial ventricular response to VNS (35).

Hemodynamic Correlates of VNS

Cervical VNS has been shown to result in a negative chronotropic and inotropic response (4, 18, 22, 37, 58), although specific branches of the thoracic vagus nerve

intermingle with sympathetic fibers and can have varied localized chronotropic and inotropic effects (5). Previous studies had suggested that the right vagal nerve may provide greater innervation to the SA node while the left vagal nerve may provide greater innervation to the AV node in decentralized hearts.(12, 19) However, Armour et al. showed that both right and left VNS affect the sinoatrial node in a canine model with intact VNS (46). In this study, we aimed to keep a similar sinus rate between right and left VNS, in order to eliminate differences between right and left VNS that maybe due to heart rate alone. However, we did not observe a difference on PR interval, and therefore, AV node conduction between right vs. left VNS. With regards to LV pressure, both right and left cervical VNS decrease LV pressure to a similar degree in a decentralized rabbit Langendorff model (7). Analogously, our study showed a significant decrease in LVESP, and dP/dt max. However, dP/dt max showed the strongest correlation with repolarization effects. This finding is potentially significant in that when assessing ventricular effects of stimulation, particularly in clinical trials, HR may not be the best marker of the appropriate level of VNS.

Effects of VNS on lusitropy and diastolic function are more controversial. Xenopolous et al. demonstrated no changes in LVESP or the time constant of isovolumic relaxation (Tau) (58), while Henning et al. showed that VNS decreased ESP and increased Tau in a canine model. In this porcine model, both right and left VNS decreased LVESP without affecting LVEDP, increased dP/dt min, and increased Tau, suggesting that VNS does not improve, and may worsen diastolic function.

Limitations

General anesthetics can suppress nerve activity, however, we were able to reliably record a cardio-motor response during VNS with isoflurane. In addition the drug concentrations were maintained at a constant level in this study. Further, to reduce effects of inhaled anesthetics, α-chloralose infusion was used during ARI recording and VNS. For global and regional analysis, ARIs were not corrected for HR, as any HR effects on DOR are physiologically important. Atrial and ventricular pacing was not performed in all animals given the effect of pacing on altering autonomic tone. Finally, HR would not affect comparison of regional differences within right and left VNS, and we were able to achieve a similar mean HR response during both right and left VNS. Beta-blockers were not given during these experiments. Therefore, the effects of VNS in the setting sympathetic blockade cannot be assessed from these studies. Lastly, VNS is currently being performed in various clinical trials in different ways without a clear standard, therefore, the results of this study may not completely duplicate what may be seen in clinical studies.

CONCLUSIONS

In this study, detailed assessment of regional ARI and hemodynamic parameters showed a lack of laterality between the effects of right vs. left VNS. In addition, the functional effects of VNS were greater at the apex than the base, and greater on the endocardium than the epicardium, likely reflecting the functional distribution of parasympathetic innervation. The ventricular electrophysiological effects of VNS correlate best with the decrease in ventricular inotropy, and specifically, dP/dt max. Our

results have significant implications given the advent of neuromodulation therapies using unilateral VNS for ventricular arrhythmias and cardiomyopathy.

REFERENCES

1. Ajijola OA, Vaseghi M, Zhou W, Yamakawa K, Benharash P, Hadaya J, Lux RL, Mahajan A, and Shivkumar K. Functional differences between junctional and extrajunctional adrenergic receptor activation in mammalian ventricle. *Am J Physiol Heart Circ Physiol. 2013* 304: H579-588.
2. Akiyama T and Yamazaki T. Effects of right and left vagal stimulation on left ventricular acetylcholine levels in the cat. *Acta Physiol Scand.* 2001 172: 11-16.
3. Ardell JL. Intrathoracic neuronal regulation of cardiac function. In: *Basic and Clinical Neurocardiology*, edited by Armour JA and Ardell JL. New York, NY: Oxford University Press, 2004, p. 118-152.
4. Armour JA and Randall WC. Rebound cardiovascular responses following stimulation of canine vagosympathetic complexes or cardiopulmonary nerves. *Can J Physiol Pharmacol.* 1985;63: 1122-1132.
5. Armour JA, Randall WC, and Sinha S. Localized myocardial responses to stimulation of small cardiac branches of the vagus. *Am J Physiol* 228: 141-148, 1975.
6. Autenrieth G, Surawicz B, and Kuo CS. Sequence of repolarization on the ventricular surface in the dog. *Am Heart J.* 1975;89:463-469, 1975.
7. Brack KE, Coote JH, and Ng GA. The effect of direct autonomic nerve stimulation on left ventricular force in the isolated innervated Langendorff perfused rabbit heart. *Auton Neurosci.* 2006;124: 69-80.
8. Brack KE, Coote JH, and Ng GA. Vagus nerve stimulation inhibits the increase in Ca2+ transient and left ventricular force caused by sympathetic nerve stimulation

but has no direct effects alone--epicardial Ca2+ fluorescence studies using fura-2 AM in the isolated innervated beating rabbit heart. *Exp Physiol*. 2010;95:80-92.

9. Brack KE, Patel VH, Coote JH, and Ng GA. Nitric oxide mediates the vagal protective effect on ventricular fibrillation via effects on action potential duration restitution in the rabbit heart. *J Physiol.* 2007;583:695-704.

10. Burgess MJ, Green LS, Millar K, Wyatt R, and Abildskov JA. The sequence of normal ventricular recovery. *Am Heart J.*1972*;*84:660-669.

11. Cheng J, Kamiya K, Liu W, Tsuji Y, Toyama J, and Kodama I. Heterogeneous distribution of the two components of delayed rectifier K+ current: a potential mechanism of the proarrhythmic effects of methanesulfonanilideclass III agents. *Cardiovasc Res*. 1999;43:135-147.

12. Cohn AE and Lewis T. The Predominant Influence of the Left Vagus Nerve Upon Conduction between the Auricles and Ventricles in the Dog. *J Exp Med.* 1913;18:739-747.

13. Corr PB and Gillis RA. Role of the vagus nerves in the cardiovascular changes induced by coronary occlusion. *Circulation.* 1974;49:86-97.

14. Crick SJ, Anderson RH, Ho SY, and Sheppard MN. Localisation and quantitation of autonomic innervation in the porcine heart II: endocardium, myocardium and epicardium. *J Anat*. 1999;195:359-373.

15. Du XJ, Cox HS, Dart AM, and Esler MD. Depression of efferent parasympathetic control of heart rate in rats with myocardial infarction: effect of losartan. *J Cardiovasc Pharmacol*. 1998;31:937-944.

16. Euler DE, Nattel S, Spear JF, Moore EN, and Scanlon PJ. Effect of sympathetic tone on ventricular arrhythmias during circumflex coronary occlusion. *Am J Physiol*. 1985;249:H1045-1050.

17. Facchini M, De Ferrari GM, Bonazzi O, Weiss T, and Schwartz PJ. Effect of reflex vagal activation on frequency of ventricular premature complexes. *Am J Cardiol*. 1991;68:349-354.

18. Hageman GR, Randall WC, and Armour JA. Direct and reflex cardiac bradydysrhythmias from small vagal nerve stiumaltions. *Am Heart J* 89: 338-348, 1975.

19. Hamlin RL and Smith CR. Effects of vagal stimulation on S-A and A-V nodes. *Am J Physiol*.1968;215:560-568.

20. Hauptman PJ, Schwartz PJ, Gold MR, Borggrefe M, Van Veldhuisen DJ, Starling RC, and Mann DL. Rationale and study design of the increase of vagal tone in heart failure study: INOVATE-HF. *Am Heart J*. 2012;163:954-962 e951.

21. Haws CW and Lux RL. Correlation between in vivo transmembrane action potential durations and activation-recovery intervals from electrograms. Effects of interventions that alter repolarization time. *Circulation*. 1990;81:281-288.

22. Henning RJ and Levy MN. Effects of autonomic nerve stimulation, asynchrony, and load on dP/dtmax and on dP/dtmin. *Am J Physiol.* 1991;260:H1290-1298.

23. Herre JM and Thames MD. Responses of sympathetic nerves to programmed ventricular stimulation. *J Am Coll Cardiol*. 1987;9:147-153.

24. Hoover DB, Ganote CE, Ferguson SM, Blakely RD, and Parsons RL. Localization of cholinergic innervation in guinea pig heart by

immunohistochemistry for high-affinity choline transporters. *Cardiovasc Res*. 20014;62:112-121.

25. Janse MJ, Schwartz PJ, Wilms-Schopman F, Peters RJ, and Durrer D. Effects of unilateral stellate ganglion stimulation and ablation on electrophysiologic changes induced by acute myocardial ischemia in dogs. *Circulation*.1985;72:585-595.

26. Kawano H, Okada R, and Yano K. Histological study on the distribution of autonomic nerves in the human heart. *Heart Vessels*. 2003;18:32-39.

27. Kent KM, Smith ER, Redwood DR, and Epstein SE. Electrical stability of acutely ischemic myocardium. Influences of heart rate and vagal stimulation. *Circulation*. 1973;47:291-298.

28. Kim JJ, Nemec J, Papp R, Strongin R, Abramson JJ, and Salama G. Bradycardia alters Ca(2+) dynamics enhancing dispersion of repolarization and arrhythmia risk. *Am J Physiol Heart Circ Physiol*. 2013;304:H848-860.

29. Kralios FA, Martin L, Burgess MJ, and Millar K. Local ventricular repolarization changes due to sympathetic nerve-branch stimulation. *Am J Physiol.* 1975;228:1621-1626.

30. Levy MN and Blattberg B. Effect of vagal stimulation on the overflow of norepinephrine into the coronary sinus during cardiac sympathetic nerve stimulation in the dog. *Circ Res.* 1976;38:81-84.

31. Li M, Zheng C, Sato T, Kawada T, Sugimachi M, and Sunagawa K. Vagal nerve stimulation markedly improves long-term survival after chronic heart failure in rats. *Circulation*. 2004;109:120-124.

32. Mantravadi R, Gabris B, Liu T, Choi BR, de Groat WC, Ng GA, and Salama G. Autonomic nerve stimulation reverses ventricular repolarization sequence in rabbit hearts. *Circ Res*. 2007;100: e72-80.

33. Martins JB. Autonomic control of ventricular tachycardia: sympathetic neural influence on spontaneous tachycardia 24 hours after coronary occlusion. *Circulation.* 1985*;* 72:933-942.

34. Martins JB and Zipes DP. Effects of sympathetic and vagal nerves on recovery properties of the endocardium and epicardium of the canine left ventricle. *Circ Res*. 1980;46:100-110.

35. Martins JB and Zipes DP. Epicardial phenol interrupts refractory period responses to sympathetic but not vagal stimulation in canine left ventricular epicardium and endocardium. *Circ Res*. 1980;47:33-40.

36. Martins JB, Zipes DP, and Lund DD. Distribution of local repolarization changes produced by efferent vagal stimulation in the canine ventricles. *J Am Coll Cardiol*. 1983;2:1191-1199.

37. Massari VJ, Dickerson LW, Gray AL, Lauenstein JM, Blinder KJ, Newsome JT, Rodak DJ, Fleming TJ, Gatti PJ, and Gillis RA. Neural control of left ventricular contractility in the dog heart: synaptic interactions of negative inotropic vagal preganglionic neurons in the nucleus ambiguus with tyrosine hydroxylase immunoreactive terminals. *Brain Res*. 1998;802:205-220.

38. Millar CK, Kralios FA, and Lux RL. Correlation between refractory periods and activation-recovery intervals from electrograms: effects of rate and adrenergic interventions. *Circulation*. 19875; 72: 372-1379.

39. Myers RW, Pearlman AS, Hyman RM, Goldstein RA, Kent KM, Goldstein RE, and Epstein SE. Beneficial effects of vagal stimulation and bradycardia during experimental acute myocardial ischemia. *Circulation*/ 1974;49: 943-947.

40. Ng GA, Brack KE, Patel VH, and Coote JH. Autonomic modulation of electrical restitution, alternans and ventricular fibrillation initiation in the isolated heart. *Cardiovasc Res*. 2007;73: 750-760.

41. Opthof T, Coronel R, Wilms-Schopman FJ, Plotnikov AN, Shlapakova IN, Danilo P, Jr., Rosen MR, and Janse MJ. Dispersion of repolarization in canine ventricle and the electrocardiographic T wave: Tp-e interval does not reflect transmural dispersion. *Heart Rhythm*. 2007;4:341-348.

42. Opthof T, Dekker LR, Coronel R, Vermeulen JT, van Capelle FJ, and Janse MJ. Interaction of sympathetic and parasympathetic nervous system on ventricular refractoriness assessed by local fibrillation intervals in the canine heart. *Cardiovasc Res*. 1993;27:753-759.

43. Ramanathan C, Jia P, Ghanem R, Ryu K, and Rudy Y. Activation and repolarization of the normal human heart under complete physiological conditions. *Proc Natl Acad Sci U S A*. 2006;103:6309-6314.

44. Randall DC, Brown DR, McGuirt AS, Thompson GW, Armour JA, and Ardell JL. Interactions within the intrinsic cardiac nervous system contribute to chronotropic regulation. *Am J Physiol Regul Integr Comp Physiol*. 2003;285:R1066-1075.

45. Randall WC, Ardell JL, Wurster RD, and Milosavljevic M. Vagal postganglionic innervation of the canine sinoatrial node. *J Auton Nerv Syst*. 1987;20:13-23.

46. Randall WC and Armour JA. Regional vagosympathetic control of the heart. *Am J Physiol*. 1974;227: 444-452.

47. Schwartz PJ, Billman GE, and Stone HL. Autonomic mechanisms in ventricular fibrillation induced by myocardial ischemia during exercise in dogs with healed myocardial infarction. An experimental preparation for sudden cardiac death. *Circulation*. 1984;69:790-800.

48. Schwartz PJ, De Ferrari GM, Sanzo A, Landolina M, Rordorf R, Raineri C, Campana C, Revera M, Ajmone-Marsan N, Tavazzi L, and Odero A. Long term vagal stimulation in patients with advanced heart failure: first experience in man. *Eur J Heart Fail*. 2008;10:884-891.

49. Shinlapawittayatorn K, Chinda K, Palee S, Surinkaew S, Thunsiri K, Weerateerangkul P, Chattipakorn S, KenKnight BH, and Chattipakorn N. Low-amplitude, left vagus nerve stimulation significantly attenuates ventricular dysfunction and infarct size through prevention of mitochondrial dysfunction during acute ischemia-reperfusion injury. *Heart Rhythm*. 2013;10:1700-1707.

50. Stramba-Badiale M, Vanoli E, De Ferrari GM, Cerati D, Foreman RD, and Schwartz PJ. Sympathetic-parasympathetic interaction and accentuated antagonism in conscious dogs. *Am J Physiol*. 1991;260:H335-340.

51. Toyoshima H, Lux RL, Wyatt RF, Burgess M, and Abildskov JA. Sequences of early and late phases of repolarization on dog ventricular epicardium. *J Electrocardiol*. 1981;14:143-152.

52. Ulphani JS, Cain JH, Inderyas F, Gordon D, Gikas PV, Shade G, Mayor D, Arora R, Kadish AH, and Goldberger JJ. Quantitative analysis of parasympathetic innervation of the porcine heart. *Heart Rhythm*. 2010;7:1113-1119.

53. Vanoli E, De Ferrari GM, Stramba-Badiale M, Hull SS, Jr., Foreman RD, and Schwartz PJ. Vagal stimulation and prevention of sudden death in conscious dogs with a healed myocardial infarction. *Circ Res*. 1991;68:1471-1481.

54. Vaseghi M and Shivkumar K. Neuraxial modulation for ventricular arrhythmias: a new hope. *Heart Rhythm.* 2012;9:1888-1889.

55. Vaseghi M and Shivkumar K. The role of the autonomic nervous system in sudden cardiac death. *Prog Cardiovasc Dis*. 2008;50:404-419.

56. Vaseghi M, Yamakawa K, Sinha A, So EL, Zhou W, Ajijola OA, Lux RL, Laks M, Shivkumar K, and Mahajan A. Modulation of regional dispersion of repolarization and T-peak to T-end interval by the right and left stellate ganglia. *Am J Physiol Heart Circ Physiol.* 2013;305:H1020-1030.

57. Weiss JL, Frederiksen JW, and Weisfeldt ML. Hemodynamic determinants of the time-course of fall in canine left ventricular pressure. *J Clin Invest*. 1976;58:751-760.

58. Xenopoulos NP and Applegate RJ. The effect of vagal stimulation on left ventricular systolic and diastolic performance. *Am J Physiol*. 1994;266:H2167-2173.

59. Yanowitz F, Preston JB, and Abildskov JA. Functional distribution of right and left stellate innervation to the ventricles. Production of neurogenic

electrocardiographic changes by unilateral alteration of sympathetic tone. *Circ Res*. 1966;18:416-428.

60. Zipes DP and Rubart M. Neural modulation of cardiac arrhythmias and sudden cardiac death. *Heart Rhythm*. 2006;3:108-113.

Figure 1. Global epicardial ARI response to right and left vagal nerve stimulation. Upper panel: isolation of the vagal nerves, bipolar electrodes used for stimulation, and the sock electrode on the heart are shown. Locations of electrodes are marked to create ARI polar maps. Lower Panel: mean epicardial ARI and DOR show a significant difference during stimulation when compared to baseline, but no significant difference between right and left vagal nerve stimulation is observed. BL = baseline, Stim = during stimulation, RVN = right vagal nerve, LVN = left vagal nerve, LAD = left anterior descending artery. *p < 0.01 vs. baseline. Bar graphs represent mean ± SE (n = 12).

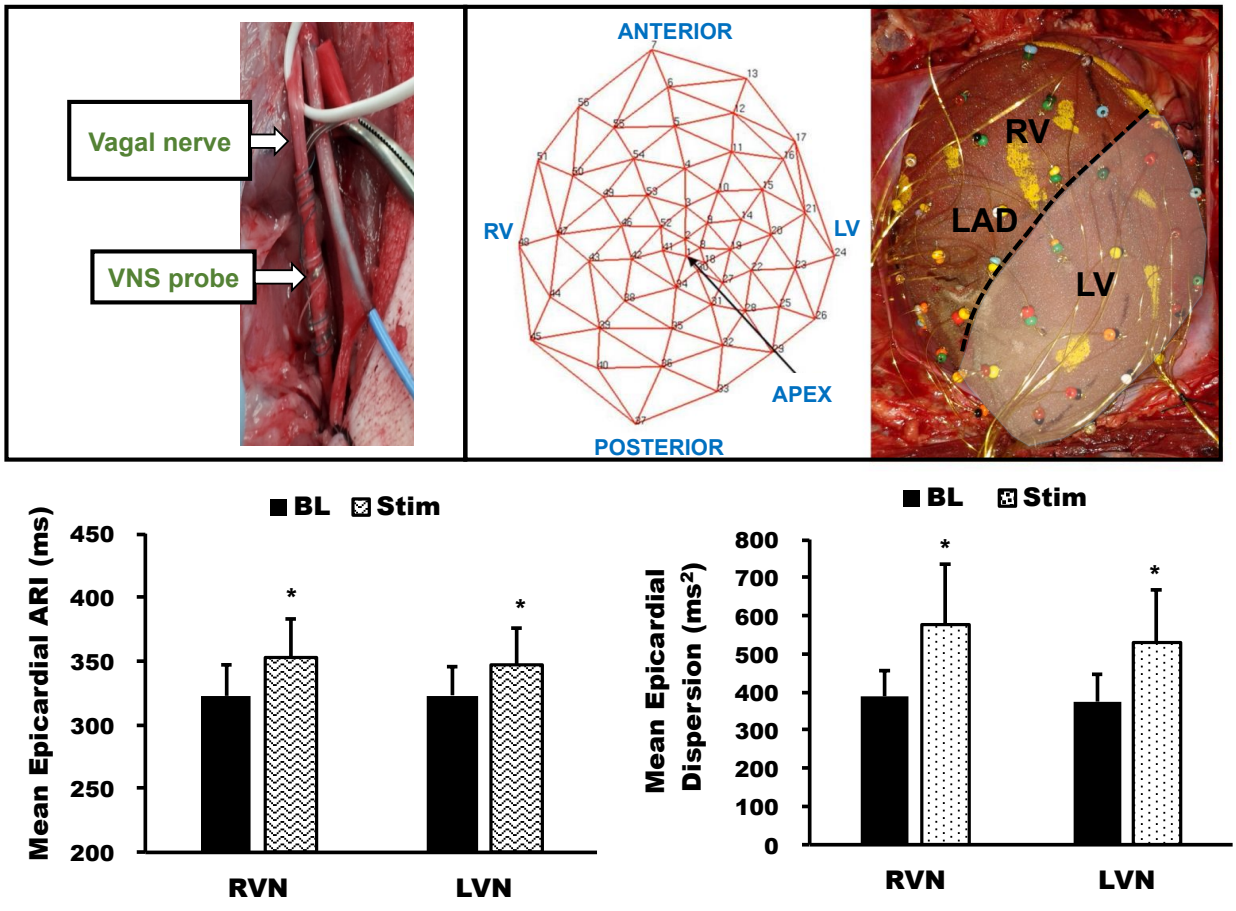

Figure 2. Regional epicardial ARI response to right and left vagal nerve stimulation. Upper panel: polar maps obtained from one animal at baseline and during RVN and LVN stimulation. No significant anterior, lateral, or posterior regional differences in response are noted. Lower panel: quantified data for all the animals is shown. BL = baseline. RVNS = right vagal nerve stimulation. LVNS = left vagal nerve stimulation. *p < 0.01 vs. baseline. Bar graphs represent mean ± SE (n =12).

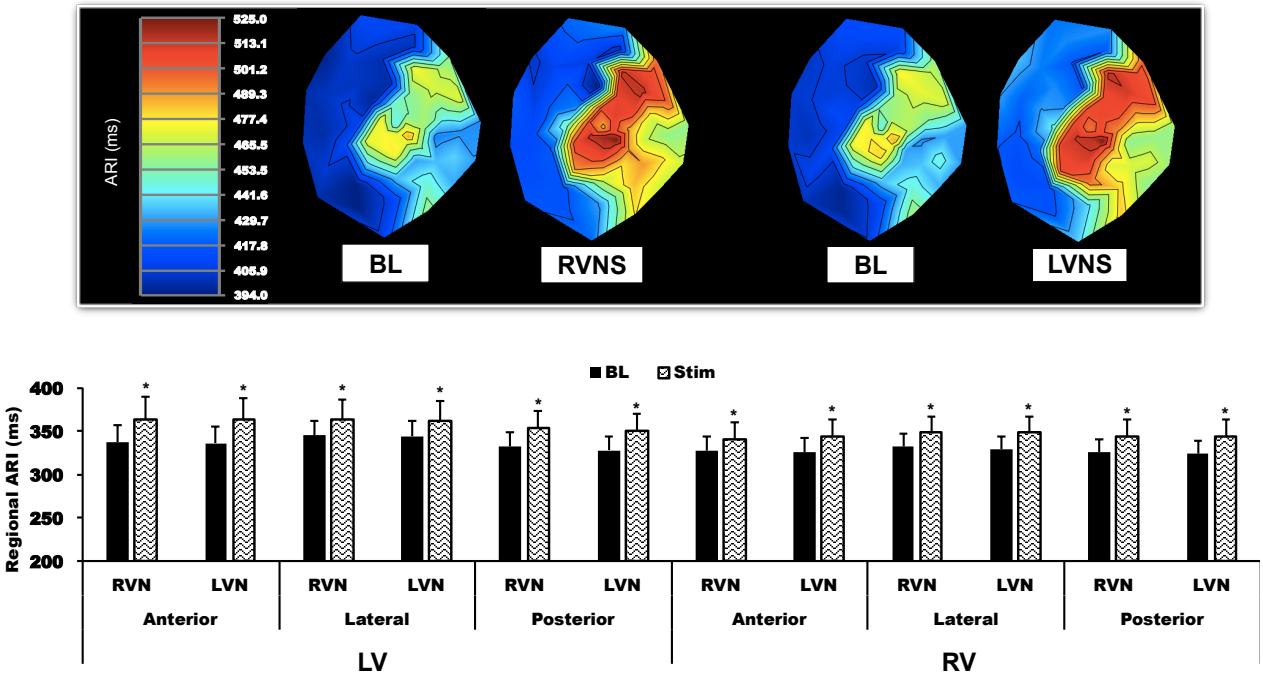

<u>Figure 3.</u> Epicardial differences in the change in DOR from baseline for anterior, lateral, posterior regions of the left ventricle and right ventricle for RVN and LVN stimulation. Note that no regional differences in DOR are noted. LV = left ventricle, RV = right ventricle, RVN = right vagal nerve, LVN = left vagal nerve. Bar graphs represent mean ± SE, (n = 12).

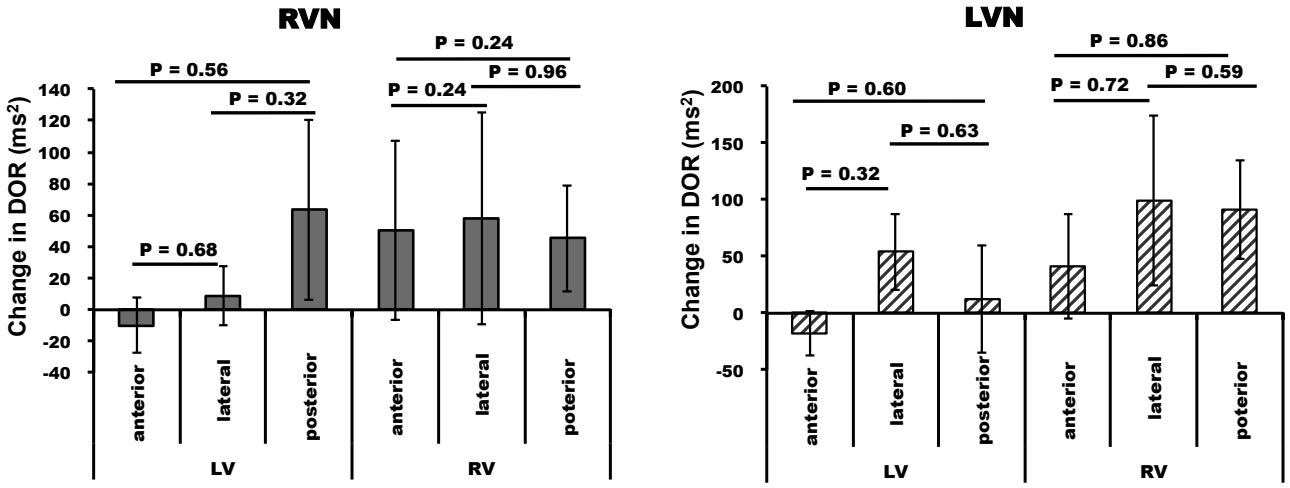

Figure 4. Apico-basal differences in response to right and left vagal nerve stimulation. Right and left vagal nerve stimulation have greater effects on the apex than the base without changing the direction of repolarization, as the base of the heart has a shorter ARI at baseline. Effects of right and left vagal nerve stimulation on apex and base are similar, again showing no laterality in response. Bar graphs represent mean ± SE, (n = 12). RVN = right vagal nerve, LVN = left vagal nerve.

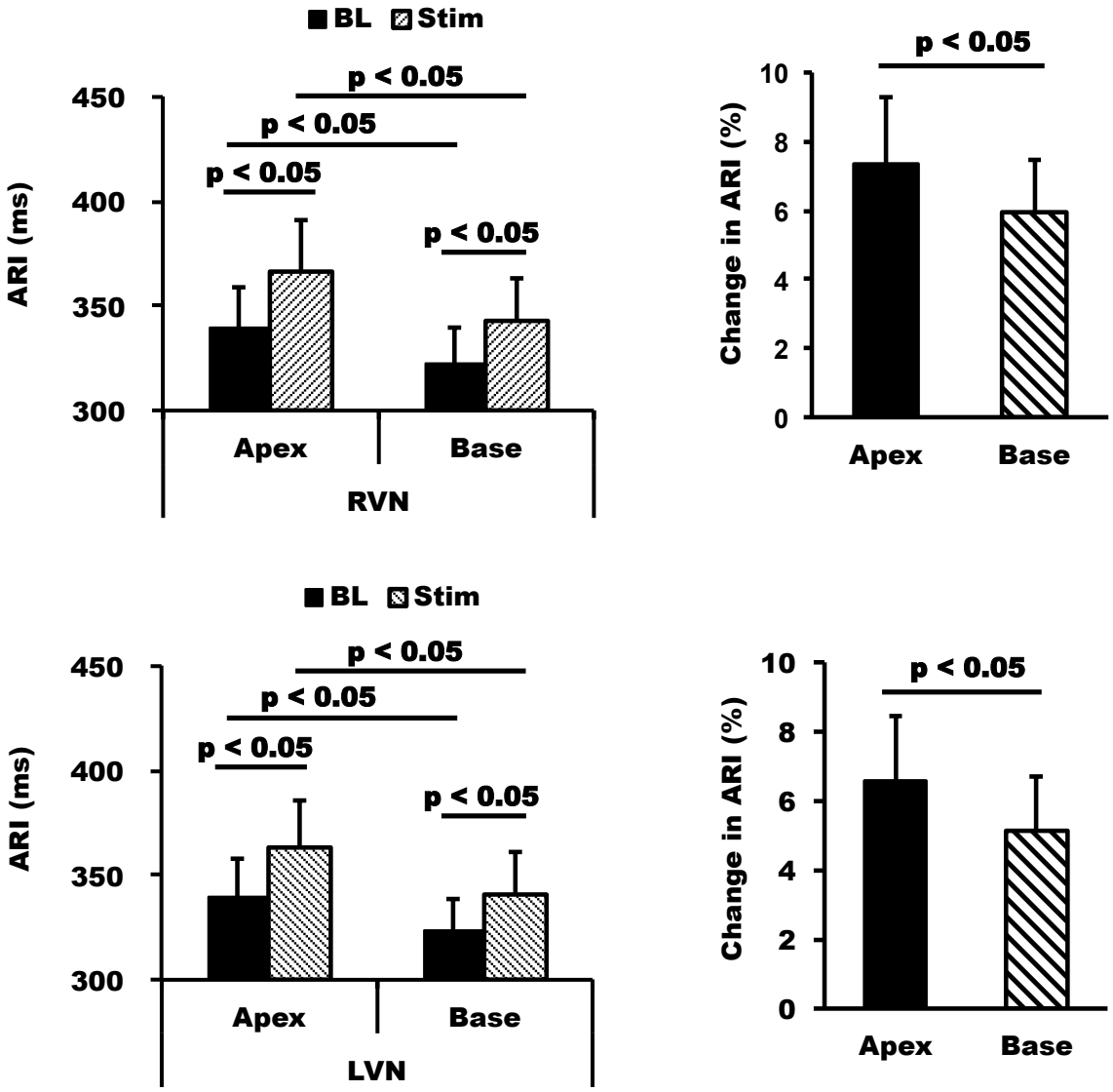

Figure 5. Correlation between effects of vagal nerve stimulation on ARI and hemodynamic parameters. The decrease in dP/dt max, and not HR or LVESP, had the highest correlation with the increase in ARI, also further illustrating ventricular myocardial effects of vagal nerve stimulation. The plots show combined right and left stimulation data.

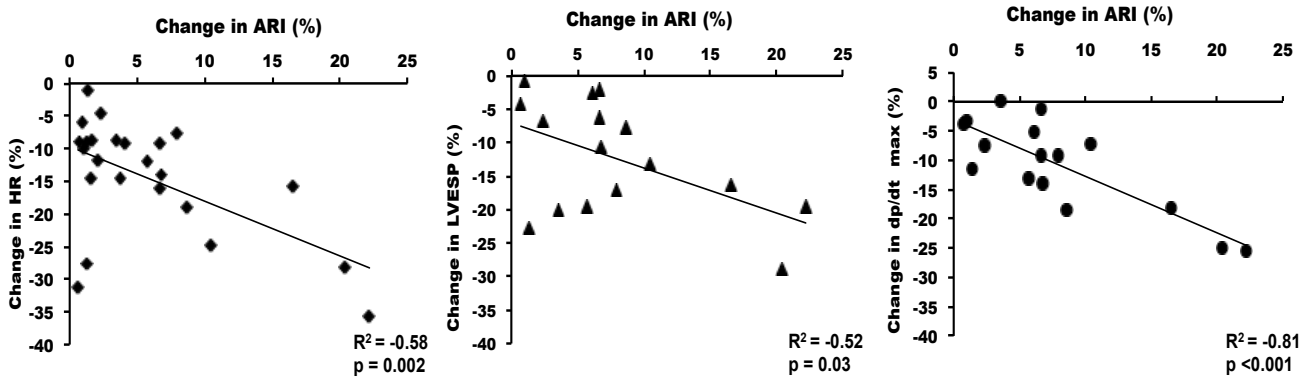

<u>Figure 6.</u> Global and regional mean endocardial ARIs in response to right and left vagal nerve stimulation. Note that all endocardial regions (anterior, lateral, posterior, and septal LV) demonstrate a similar increase in ARI with no significant differences in the magnitude of response for each region. No differences between right vs. left vagal nerve stimulation are seen. *p < 0.01 vs. baseline. Bar graphs represent mean ± SE, (n =12). RVN = right vagal nerve, LVN = left vagal nerve.

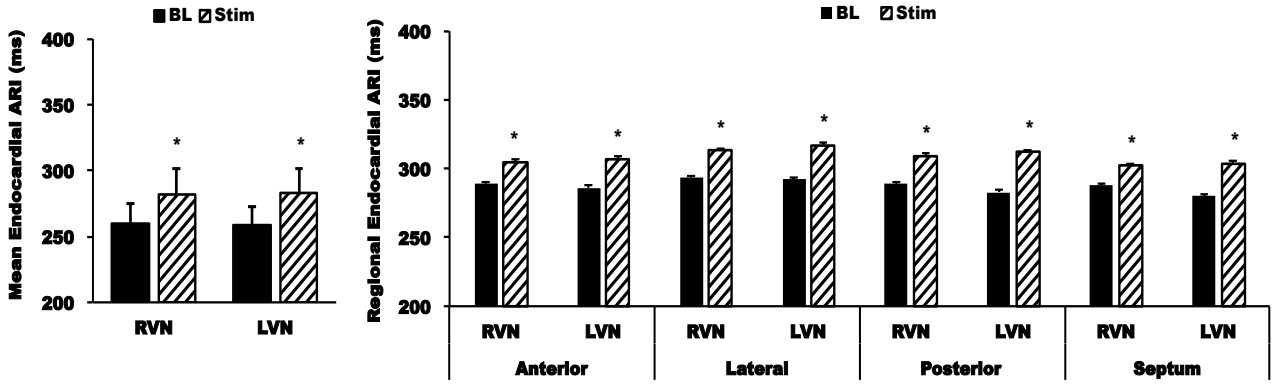

Figure 7. Endocardial comparisons in the change in DOR from baseline for anterior/lateral/posterior regions of the LV and RV for right and left vagal nerve stimulation. Note that no statistically significant regional differences in change DOR from baseline are noted. Bar graphs represent mean ± SE, (n = 12). RVN = right vagal nerve, LVN = left vagal nerve.

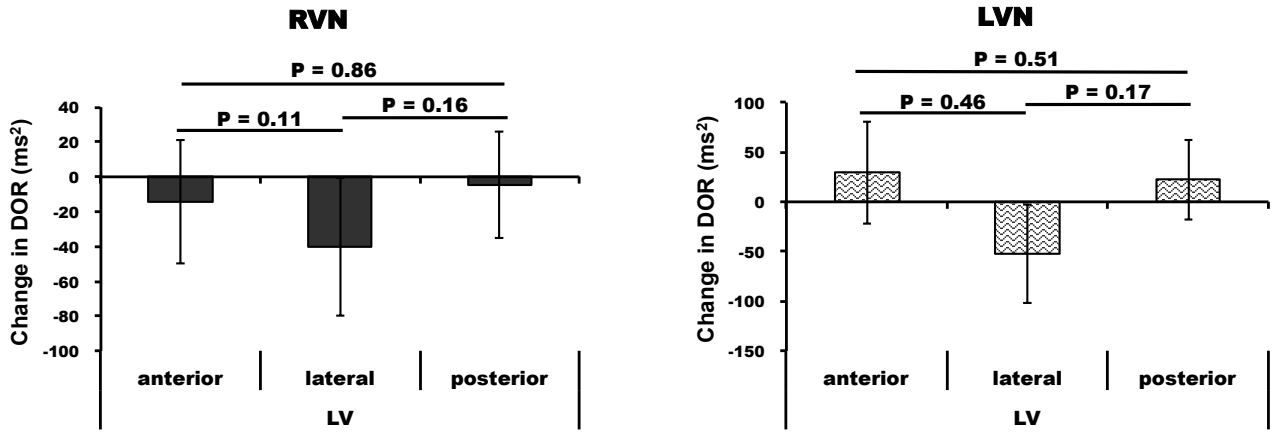

Figure 8. Epicardial and endocardial differences in ARI during right and left vagal nerve stimulation. Both right and left vagal nerve stimulation increased endocardial ARI more than epicardial ARI. BL = baseline, Stim = stimulation, RVN = right vagal nerve, LVN = left vagal nerve. *p < 0.01 vs. baseline. #p < 0.05 vs. epicardium.

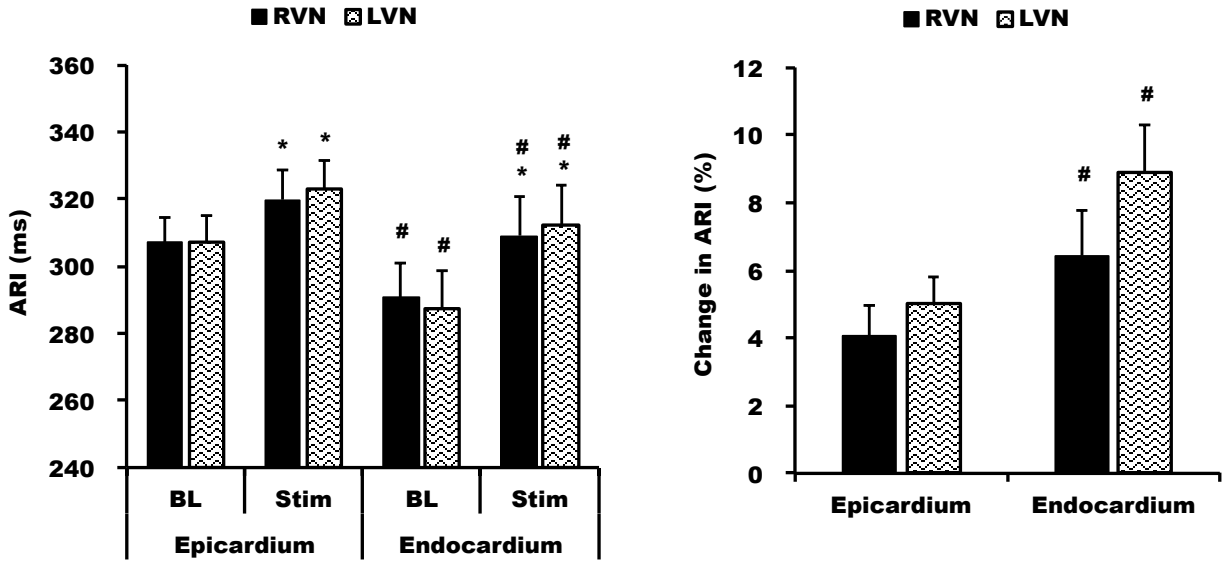

TABLE 1. RESPONSE TO RIGHT AND LEFT VAGAL NERVE STIMULATION

	RVN		LVN	
	BL	**Stim**	**BL**	**Stim**
HR (bpm)	84 ± 5	71 ± 5*	84 ± 4	73 ± 5*
SBP (mmHg)	120 ± 7	110 ± 8*	119 ± 8	111 ± 8*
DBP (mmHg)	83 ± 8	73 ± 8*	83 ± 9	74 ± 9*
ESP (mmHg)	89 ± 9	77 ± 9*	91 ± 9	83 ± 9*
EDP (mmHg)	4 ± 1	6 ± 1	6 ± 2	6 ± 2
dp/dt max (mmHg/s)	1660 ± 154	1490 ± 160*	1595 ± 155	1416 ± 135*
dp/dt min (mmHg/s)	-1511 ± 211	-1090 ± 208*	-1520 ± 213	-1161 ± 231*
tau (ms)	41 ± 4	50 ± 7*	41 ± 3	50 ± 5*
PR interval (ms)	114 ± 4	137 ± 5*	112 ± 4	140 ± 4*

RVN = right vagal nerve, LVN = left vagal nerve

TABLE 2. REGIONAL DISPERSION OF REPOLARIZATION IN RESPONSE TO RIGHT AND LEFT VAGAL NERVE STIMLUATION

		RVN			LVN		
		BL (ms^2)	Stim (ms^2)	*p* value	BL (ms^2)	Stim (ms^2)	*p* value
Epicardial Regional DOR							
LV	**Anterior**	158 ± 38	148 ± 35	0.82	131 ± 39	113 ± 42	0.50
	Lateral	131 ± 44	143 ± 52	0.72	122 ± 42	176 ± 52	0.45
	Posterior	111 ± 49	173 ± 79	0.30	94 ± 44	109 ± 69	0.90
RV	**Anterior**	110 ± 31	160 ± 68	0.10	104 ± 35	145 ± 41	0.14
	Lateral	125 ± 51	183 ± 94	0.90	120 ± 56	220 ± 107	0.05
	Posterior	156 ± 67	206 ± 87	0.92	143 ± 57	227 ± 96	0.22
Endocardial Regional DOR							
LV	**Anterior**	52 ± 32	41 ± 13	0.56	37 ± 20	66 ± 46	0.60
	Lateral	88 ± 42	33 ± 17	0.10	103 ± 52	50 ± 20	0.60
	Posterior	84 ± 40	88 ± 41	0.74	34 ± 16	60 ± 34	0.20

RVN = right vagal nerve, LVN = left vagal nerve, LV = left ventricle, RV = right ventricle

TABLE 3. COMPARISON OF REGIONAL DISPERSION OF REPOLARIZATION DURING RIGHT VAGAL NERVE STIMULATION

Ventricular Region	Region	vs. Region	Log Mean Difference	SE of Difference	P Value
LV Endocardium	Anterior	Lateral	0.98	0.61	0.11
LV Endocardium	Anterior	Posterior	0.11	0.61	0.86
LV Endocardium	Anterior	Septum	0.34	0.61	0.58
LV Endocardium	Lateral	Posterior	-0.87	0.61	0.16
LV Endocardium	Lateral	Septum	-0.64	0.61	0.30
LV Endocardium	Posterior	Septum	0.23	0.61	0.70
LV Epicardium	Anterior	Lateral	0.20	0.49	0.68
LV Epicardium	Anterior	Posterior	-0.28	0.49	0.56
LV Epicardium	Lateral	Posterior	-0.49	0.49	0.32
RV Epicardium	Anterior	Lateral	0.58	0.49	0.24
RV Epicardium	Anterior	Posterior	0.61	0.49	0.24
RV Epicardium	Anterior	RVOT	-0.02	0.50	0.98
RV Epicardium	Lateral	Posterior	0.03	0.49	0.96
RV Epicardium	Lateral	RVOT	-0.60	0.50	0.24
RV Epicardium	Posterior	RVOT	-0.63	0.50	0.22

LV = Left ventricle, RV = right ventricle, RVOT = right ventricular outflow tract

TABLE 4. COMPARISON OF EPICARDIAL AND ENDOCARDIAL DISPERSION OF REPOLARIZATION DURING RIGHT VAGAL NEREV STIMULATION

Region	vs. Region	Log Mean Difference	SE of Difference	P Value
Endo LV anterior	Epi LV anterior	0.17	0.56	0.76
Endo LV anterior	Epi RV anterior	-0.32	0.56	0.56
Epi LV anterior	Epi RV anterior	-0.50	0.49	0.31
Endo LV lateral	Epi LV lateral	-0.60	0.56	0.28
Endo LV lateral	Epi RV lateral	-0.72	0.56	0.20
Epi LV lateral	Endo RV lateral	-0.11	0.49	0.82
Endo LV posterior	Epi LV posterior	-0.22	0.56	0.69
Endo LV posterior	Epi RV posterior	0.18	0.56	0.76
Epi LV posterior	Epi RV posterior	0.40	0.49	0.42

LV = left ventricle, RV = right ventricle, Epi = epicardial, Endo = endocardial

TABLE 5. COMPARISON OF REGIONAL DISPERSION OF REPOLARIZATION DURING LEFT VAGAL NERVE STIMULATION

Ventricular Region	Region	vs. Region	Log Mean Difference	SE of Difference	P Value
LV Endocardium	Anterior	Lateral	0.43	0.58	0.46
LV Endocardium	Anterior	Posterior	-0.40	0.60	0.51
LV Endocardium	Anterior	Septum	0.61	0.58	0.30
LV Endocardium	Lateral	Posterior	-0.83	0.60	0.17
LV Endocardium	Lateral	Septum	0.18	0.58	0.76
LV Endocardium	Posterior	Septum	1.00	0.60	0.099
LV Epicardium	Anterior	Lateral	-0.46	0.46	0.32
LV Epicardium	Anterior	Posterior	-0.24	0.46	0.60
LV Epicardium	Lateral	Posterior	0.22	0.46	0.63
RV Epicardium	Anterior	Lateral	-0.17	0.46	0.72
RV Epicardium	Anterior	Posterior	0.08	0.46	0.86
RV Epicardium	Anterior	RVOT	0.00	0.49	0.99
RV Epicardium	Lateral	Posterior	0.25	0.46	0.59
RV Epicardium	Lateral	RVOT	0.17	0.49	0.73
RV Epicardium	Posterior	RVOT	-0.08	0.49	0.86

LV = Left ventricle, RV = right ventricle, RVOT = right ventricular outflow tract

TABLE 6. COMPARISON OF EPICARDIAL AND ENDOCARDIAL DISPERSION OF REPOLARIZATION DURING LEFT VAGAL NERVE STIMULATION

Region	vs. Region	Log Mean Difference	SE of Difference	P Value
Endo LV anterior	Epi LV anterior	0.43	0.52	0.41
Endo LV anterior	Epi RV anterior	-0.26	0.52	0.61
Epi LV anterior	Epi RV anterior	-0.69	0.46	0.14
Endo LV lateral	Epi LV lateral	-0.46	0.52	0.38
Endo LV lateral	Epi RV lateral	-0.86	0.52	0.10
Epi LV lateral	Endo RV lateral	-0.40	0.46	0.39
Endo LV posterior	Epi LV posterior	0.59	0.55	0.29
Endo LV posterior	Epi RV posterior	0.21	0.55	0.70
Epi LV posterior	Epi RV posterior	-0.37	0.46	0.42

LV = left ventricle, RV = right ventricle, Epi = epicardial, Endo = endocardial

CHAPTER 3

VAGAL NERVE STIMULATION ACTIVATES VAGAL AFFERENT FIBERS THAT INHIBIT EFFERENT CARDIAC PARASYMPATHETIC EFFECTS

INTRODUCTION

The autonomic nervous system plays a central role in the initiation and maintenance of ventricular arrhythmias(41, 47). Parasympathetic withdrawal, as manifested by decreased heart rate variability and baroreflex sensitivity, is pro-arrhythmic, while increasing parasympathetic input to the heart via vagal nerve stimulation (VNS) is thought to be cardio-protective (10, 16, 23, 25, 55). Specifically, VNS has been shown to decrease infarct size (21, 42), reduce ischemia related ventricular arrhythmias (38, 42), and improve survival in animal models of heart failure (35). The electrophysiological effects of stimulation of the intact right and left vagosympathetic trunk appear to be similar in a porcine model, without significant global or regional differences (52). Although the vagosympathetic trunk provides important cardiomotor efferent fibers to the heart, more than 80% of the fibers within the vagal nerve are afferent neural fibers, transducing information from visceral organs, including the heart, to the central nervous system (14, 32, 49). Vagal nerve stimulation likely leads to activation of both afferent and efferent fibers, and may cause reflex autonomic activation through the contralateral trunk and via the sympathetic chain and dorsal root ganglia. However, the role of cardiac afferent fibers on efferent parasympathetic outflow during VNS remains unknown. Furthermore, whether VNS elicits primarily activation of afferent fibers in the stimulated trunk or activation of afferent (and efferent) fibers in the contralateral trunk due to reflex mechanisms remains to be elucidated. This is especially important, as many of the studies that demonstrated an anti-arrhythmic benefit from VNS were performed in the decentralized state, after transection of the vagal trunk, stimulating only the efferent fibers (2, 8, 18, 24, 27, 34, 45, 50, 53, 56).

Other studies have used an isolated innervated preparation, where cardiac afferent fibers no longer play an important role (6, 7, 29). Meanwhile, the majority of the studies showing pro-arrhythmic effects were done in the intact state (17, 22, 36, 37, 46). Furthermore, a large-scale human clinical trial of VNS for the management of heart failure did not reproduce the expected benefit noted in animal studies (54). These conflicting results are likely due to a lack of understanding of the contribution of afferent fibers to efferent control during VNS. The purpose of this study was to evaluate the effect of vagal nerve transection on modulation of cardiac hemodynamic and electrophysiological parameters by VNS, in order to delineate influences of afferent activation."

METHODS

All procedures were performed in accordance with guidelines of University of California, Los Angeles (UCLA) Institutional Animal Care and Use Committee and the National Institutes of Health Guide for the Care and Use of Laboratory Animals.

Anesthesia and Surgical Preparation

Yorkshire pigs (n = 37, weighing 50 ± 3 kg, male or female) were sedated with intramuscular telazol (6-8 mg/kg), followed by endotracheal intubation, mechanical ventilation, and anesthesia with isoflurane (1-1.5%, inhalation). Intermittent intravenous boluses of fentanyl (50-100 mcg) were given for analgesia during surgical preparation. A surface 12 lead electrocardiogram was obtained via Prucka Cardio Lab System (GE Healthcare, Fairfield, CT). Arterial blood pressure monitoring was performed via a 5F sheath in the femoral artery, and sailine and medications were infused via a 5F sheath

in the femoral vein. Bilateral cervical vagal nerves were isolated carefully at the cricoid level, and the heart was exposed via median sternotomy. Arterial blood gas levels were measured hourly. The ventilator settings were adjusted or sodium bicarbonate administered to maintain acid-base homeostasis. After completion of surgical exposure, anesthetics were switched from isoflurane to α-chloralose (50 mg/kg initial bolus, subsequently 20-30 mg/kg/hr, continuous infusion), followed by stabilization period of one hour. Animals were euthanized by an overdose of intravenous anesthesia (sodium pentobarbital) followed by intravenous saturated potassium chloride to arrest the heart

Electrophysiological Recordings and Analysis

Multiple unipolar epicardial electrograms were continuously recorded from a 56-electrode sock placed over the ventricles, connected to a Prucka Cardio Lab System (GE Healthcare, Fairfield, CT). ARI from each electrode was analyzed using iScaldyn (University of Utah, Salt Lake City, UT) (1, 48, 52). Briefly, activation time (AT) was defined from the origin to the minimum dV/dt of the activation wavefront and recovery time (RT) was defined as the time to the maximum dV/dt in repolarization wave. ARI was then calculated by subtracting AT from RT. ARI has been shown to correlate well with local action potential duration (11, 28). For purposes of this manuscript, anterior refers to the ventral aspect and posterior refers to the dorsal aspect of the animal. Mean ARIs in the following regions were quantified: LV anterior, lateral, posterior, and apex, RV anterior, lateral, posterior, and RV outflow tract (RVOT). The median number of electrodes in each region was 4 (range of 3-6). Polar maps were generated from the sock electrode to assess regional ARI's qualitatively, as reported in chapter 1, figure 1.

The PR interval was measured as the interval from the beginning of the P wave to the start of the Q wave on the surface electrocardiogram. Either lead II or AVF was used, whichever provided the clearest P wave. The same lead was used under all conditions in each animal.

Vagal Nerve Stimulation (VNS)

Helical bipolar VNS electrodes (Cyberonics, Houston, TX) were placed around the cervical vagal trunks and connected to a Grass S88 stimulator (Grass Technologies, Warwick, RI) via photoelectric current isolation units for subsequent stimulation. VNS was performed with square pulses (10 Hz, 1 ms). Bradycardia threshold for each vagus nerve was defined as the current required to achieve a 10% decrease in heart rate (HR). VNS was performed for 20 seconds at 1.2 times threshold.

Hemodynamic Assessment

A 12-pole conductance pressure catheter (5 F) was placed in the left ventricle (LV) via the left carotid artery and connected to a MPVS Ultra Pressure Volume Loop System (Millar Instruments, Houston, TX). Appropriate catheter placement was confirmed by cardiac ultrasound (GE Healthcare, Fairfield, CT) and via the pressure – volume loops recorded. Tau was calculated using the method, defined by Weiss et al (51) from the pressure-volume loop as a parameter describing the time course of the exponential decay in LV pressure during isovolumic relaxation. The following equation was used to calculate Tau: $P(t) = A \exp(-t/Tau)$.

Experimental Protocol

The experimental protocol and the number of animals used in each condition are shown in figure 1.

Intact Vagal Nerve Stimulation

Unilateral right and left VNS were performed randomly (10Hz, 1ms, 1.2 times threshold) in 25 animals with both vagal trunks intact.

Ipsilateral Vagal Nerve Transection

Subsequently, the right vagus nerve (n = 11) or the left vagus nerve (n= 14) was transected 2 cm above the stimulation probe. At least 20 minutes of observation was used to allow for hemodynamic and ARI parameters to return to stable values. Then, the threshold test was repeated, and the current required to achieve a 10% decrease in HR was re-measured. After obtaining the new threshold, ipsilateral efferent stimulation (of the distal/caudal end of the vagal trunk) was performed using the same current as the intact condition.

Contralateral Vagal Nerve Transection

Right VNS was performed in the setting of left (contralateral) VNTx in 10 animals, and left VNS was performed in setting of right (contralateral) VNTx in 7 animals. After contralateral VNTx, at least 20 minutes of observation was allowed for stabilization of hemodynamic and ARI parameters. Then, the threshold current required for a 10% decrease in HR was reevaluated in the setting of contralateral VNTx. Right VNS (in the setting of left VNTx) or left VNS (in the setting of right VNTx) was then performed using the same current as the intact condition, and ARI and hemodynamic parameters were analyzed.

Bilateral Vagal Nerve Transection

After right or left ipsilateral VNTx, the remaining intact vagal trunk was transected to study the effect of bilateral VNTx on hemodynamic and ARI parameters. The new

threshold current for either right or left VNS was remeasured after bilateral transection. Subsequently, right or left VNS (stimulation of the distal end of the vagal trunk) was performed in the setting of bilateral VNTx at 1.2 times the intact threshold current.

Atropine infusion

To compare electrophysiological effects of efferent muscarinic blockade with bilateral transection, atropine was administered as an intravenous bolus (0.04 mg/kg) in 12 animals with both vagi intact. The HR, systolic blood pressure, and ARI's were measured prior to and after 5 minutes of infusion. These parameters were compared to changes in ARI pre- and post-bilateral VNTx. Comparison of muscarinic efferent blockade with atropine to bilateral VNTx was performed to provide insight as to whether the hemodynamic and electrophysiological effects observed arter transection were due to sympatho-excitation from vagotomy or parasympathetic efferent tone withdrawal.

Statistical analysis

Data are presented as mean ± standard error (SE). Comparison of the change in ARI with atropine to bilateral VNTx was performed using the Wilcoxon Rank Sum Test. Baseline values and percent changes from baseline after stimulation were compared between various experimental conditions (intact, ipsilateral, contralateral, and bilateral transection) using separate linear mixed effects models, including random animal effects to account for repeated measurements. Comparisons between pairs of conditions were performed using model contrasts. P-values less than 0.05 were considered statistically significant. To account for multiple comparisons within each experiment, we report which differences remained significant after controlling for the false discovery rate at 5%. The Benjamini-Hochberg procedure was used to control the

false discovery rate. All analyses were performed using SAS version 9.4 (SAS Institute Inc., Cary, NC).

RESULTS

Effect of vagal nerve transection on hemodynamic and electrophysiological parameters

Hemodynamic and electrophysiological responses to ipsilateral and bilateral vagal nerve transection are shown in table 1. Right VNTx increased HR, decreased systolic blood pressure (SBP), and decreased Tau, table 1. Left VNTx also affected HR and Tau, but did not significantly affect blood pressure or dP/dt max. There were no statistically significant differences in hemodynamic parameters after bilateral transection compared to ipsilateral transection.

Both right and left VNTx shortened PR interval. Global ventricular ARI was decreased by right or left VNTx (right VNTx: from 338 ± 15 ms to 298 ± 20 ms, $p<0.01$; left VNTx: from 361 ± 14 ms to 330 ± 13 ms, $p<0.01$), figures 2 and 3. Hemodynamic and electrophysiological influences, however, stabilized at approximately 5 min after VNTx and remained stable at 20 min, table 2. Immediately after right VNTx, a rise in systolic blood pressure and dP/dt was noted that returned to baseline after 5 minutes. This rise in blood pressure persisted after left VNTx. After bilateral transection, differences in electrophysiological and hemodynamic parameters remained significant compared to the intact condition, but were not statistically different from ipsilateral transection. The mean global ventricular ARI in all animals (n = 25) decreased from 351 ± 10 ms in the intact condition to 303 ± 13 ms after bilateral VNTx (delta ARI = 47 ± 9

ms, percent change in ARI = 14 ± 3%, p<0.001 compared to intact condition). Activation time was not influenced by right or left VNTx.

Effect of Atropine on ARI

Atropine increased HR (from 75 ± 3 bpm to 91 ± 3 bpm, p<0.05) and systolic blood pressure (SBP) (from 124 ± 5 mmHg to 130 ± 6 mmHg, p<0.05). Atropine shortened ARI from 365 ± 20 ms to 319 ± 15 ms, p<0.05. Furthermore, the change in ARI (delta ARI of 46 ± 12 ms, percent change of 11 ± 2%) with atropine was not statistically different than the change in ARI after bilateral VNTx (delta ARI of 51 ± 10 ms, percent change in ARI of 15 ± 13%, p=0.6 compared to atropine).

Hemodynamic response to right and left VNS in the setting of intact, ipsilateral, contralateral, and bilateral VNTx

Intact Vagal Nerve Stimulation

With both vagi intact, right and left VNS decreased HR, SBP, and dP/dt max, p<0.05, table 3. Diastolic function worsened with VNS with a rise in dP/dt min. Tau was increased with left VNS, table 3.

Ipsilateral and Bilateral Vagal Nerve Transection and VNS

The effects on HR, SBP, dP/dt max, dP/dt min, and Tau in response to right VNS were significantly augmented after ipsilateral VNTx, table 1. Right VNS after bilateral VNTx had no significant additional effects, table 1.

An augmentation of the effects of left VNS on the change in HR and SBP was observed after left VNTx. Left VNS after left VNTx did not significantly affect the change in Tau (intact: 7 ± 2% vs. left VNTx: 12 ± 2%, p=0.051). Furthermore, percentage change in dP/dtmax during left VNS was unchanged after left VNTx. After subsequent

right VNTx, hemodynamic effects of left VNS were further augmented, and the changes in ionotropic parameters and Tau during left VNS reached statistical significance (14 ± 3% in Tau and -7 ± 2% in dP/dt max, $p<0.05$ compared to left VNS in the intact condition).

Contralateral Vagal Nerve Transection and VNS

Right VNS in the setting of left VNTx (contralateral VNTx) did not significantly affect the changes in HR, SBP, dP/dt max, dP/dt min, or Tau as compared to those observed during VNS with both vagal nerves intact, table 3. Also, left VNS in the setting of right VNTx did not demonstrated augmented effects on hemodynamic or electrophysiological parameters.

Impact of ipsilateral, contralateral, and bilateral VNTx on stimulation threshold during right and left VNS

Bradycardia threshold with right VNS was reduced after ipsilateral and bilateral VNTx, figure 2. A significant reduction in threshold was also observed for left VNS after ipsilateral and bilateral VNTX, figure 3. There was no significant difference in the threshold current between ipsilateral VNTx and bilateral VNTx for right or left VNS. The right VNS threshold decreased after contralateral VNTx, whereas, left VNS threshold was unchanged by contralateral right VNTx, figure 4.

Effect of ipsilateral, contralateral, and bilateral VNTx on electrophysiological parameters during right and left VNS

Using the same current as the intact condition, right VNS after ipsilateral (right) transection augmented the percentage change in ARI from 2.2 ± 0.9% to 5.8 ± 1.7% ($p<0.01$), figure 2. Subsequent right VNS after bilateral VNTx did not demonstrate

significant additional effects. Left VNS after left VNTx demonstrated a trend for augmented ARI effects (intact: 1.1 ± 0.5% vs. 3.6 ± 0.7%), but these differences did not reach statistical significance (p=0.07), figure 3. After subsequent right-sided transection (i.e. after bilateral transection), left VNS had a greater effect on ARI as compared to the intact condition (bilateral VNTx: 6.6 ± 1.6% vs. intact: 1.1 ± 0.5%, $p < 0.01$).

In the setting of ipsilateral VNTx, both right and left VNS significantly prolonged PR interval more than the intact condition. During right VNS after right VNTx, the PR interval increased by 23 ± 5% compared to 13 ± 3% prior to transection, p=0.036, table 1. During left VNS after left VNTx, PR interval increased by 23 ± 5% compared to 13 ± 3% prior to transection, $p<0.05$, table 1. After bilateral transection, the increase in PR interval remained significant compared to the intact condition, but was not different from ipsilateral transection.

Right VNS in the setting of contralateral VNTx (ipsilateral side intact and stimulated) lead to a decrease in bradycardia threshold, but effects on ARI during VNS were not significantly augmented (intact: 2.8 ± 1% vs. contralateral VNTx: 3.3 ± 1%, p=0.53). Left VNS after contralateral (right-sided) VNTx didn't alter threshold, figure 4, or effects on ARI (intact: 4 ± 1% vs. contralateral VNTx: 6 ± 2%, p=0.15), figure 4.

Activation time was not affected by VNS prior to transection (24 ± 2 ms vs. 25 ±2 ms for right VNS and 22 ± 1 ms vs. 21 ± 1 ms for left VNS). Furthermore, ipsilateral, contralateral, and bilateral VNTx did not affect activation time.

Impact of vagal nerve transection on regional ARI

After ipsilateral (right) VNTx, regional ARI shortened in all regions, figure 5. Right VNS after right VNTx had an augmented effect on ARI across all regions ($p < 0.05$ for

the perecentage change in all regions, right VNTx vs. intact). Right VNS after bilateral VNTx did not show significant additional prolongation beyond ipsilateral VNTx. Left VNTx also shortened ARI in all regions compared to the intact condition, figure 6. The additional change in ARI after bilateral VNTx was not statistically significant as compared to ipsilateral VNTx. Left VNS after left VNTx showed a trend for greater prolongation in ARI across all regions, but these differences did not reach statistical significance after controlling for the false discovery rate. However, after subsequent right VNTx, left VNS significantly augmented the effects on regional ARI ($p<0.05$ for the percentage change in all regions, bilateral VNTx vs. intact).

DISCUSSION

Major findings

In this study, a comprehensive evaluation of the electrophysiological (global and regional) and hemodynamic effects of VNS before and after vagotomy was undertaken in order to assess the role of vagal afferent fiber activation on cardiac efferent parasympathetic control. The major findings in this porcine model are that activation of afferent fibers with VNS reduces its efferent effects and diminishing parasympathetic drive. Therefore, the effect of VNS on hemodynamic and electrophysiological parameters was augmented after ipsilateral VNTx. This data suggests that activation of afferent fibers in the stimulated trunk directly contributes to withdrawal of parasympathetic tone, and possibly, sympathoexcitation. In addition, the magnitude of the effects of bilateral vagotomy prior to any stimulation was similar to infusion of atropine *at rest*, suggesting that these changes were driven primarily by withdrawal of

efferent parasympathetic tone, rather than sympathetic activation due nerve injury, or decrease in inhibition of sympathetic fibers by parasympathetic afferent fibers in the vagal trunk. Finally, unilateral VNTx (right or left) is sufficient to cause a significant withdrawal in parasympathetic tone in the porcine model.

Impact of vagal nerve transection on global ventricular repolarization

Despite the fact that the vagal trunk is complex nerve, consisting of predominantly afferent fibers,(14, 49) the detailed effects of vagotomy on cardiac function and electrophysiological parameters in the resting state have not been elucidated. The effect of vagotomy on HR, sinus cycle length, and AH interval had been previously reported (13, 19, 26, 31), but no further delineations of the reason for these effects were undertaken. In addition, MacCanon and Horvath in 1957 performed bilateral chronic vagotomy in a canine model, and in the animals that survived, noted an initial increase in heart rate and systolic blood pressure that returned to baseline levels within 15-20 minutes. They further observed a chronic decrease in cardiac output over time (26). In the porcine model, unilateral and bilateral vagotomy caused significant hemodynamic and electrophysiological effects that were maintained at 20 minutes. Unlike in our study showing that unilateral vagotomy causes a significant withdrawal of parasympathetic tone, in canines with normal hearts, unilateral vagotomy did not affect heart rates significantly, and only after bilateral vagotomy was significant tachycardia observed, suggesting significant interspecies differences (19). Brooks and colleagues showed a decrease in repetitive extrasystole threshold, a surrogate of ventricular vulnerability to ventricular fibrillation, after either right or left vagotomy in canines with normal hearts, but the effect on vagal nerve stimulation or other cardiac parameters

after vagotomy were not reported (8). They did note that bilateral vagotomy had minimal additional effects to unilateral vagotomy on repetitive extrasystole threshold. Schwartz and colleagues assessed the effects of vagotomy and atropine on ventricular refractory periods. Unlike our findings, this study demonstrated a modest effect of bilateral vagal nerve transection on refractory period (2-3 ms) after atropine infusion (40). Possible explanations for the differences observed are due the fact that, in the study by Schwartz and colleagues ventricular refractory periods were measured with ventricular pacing/extra-stimulus testing, which is known to causes an enhanced sympathetic tone (12), that could additionally shorten refractory period, diluting the results. Furthermore, spatial heterogeneities across the right and left ventricle have not been previously assessed. In this study, we show that bilateral vagotomy has very significant effects on heart rate, PR interval, ARI, and Tau. Regional ARI effects were similar. Possible explanations for these findings are loss of inhibition of sympathetic tone by vagal afferent fibers, and therefore, occurrence of sympathoexcitation post-transection, *or* withdrawal of efferent parasympathetic tone after transection. The effects of bilateral transection on ARI were similar to atropine infusion, suggesting, from the results of this study, that the majority of the electrophysiological effects of transection in the *resting* state are due withdrawal of efferent parasympathetic tone.

Intact VNS compared to after ipsilateral, contralateral, and bilateral VNTx

Vagal afferent fibers from the heart and baroreceptors travel via pseudo-unipolar neurons through nodose ganglia (inferior vagal ganglia) and synapse in the nucleus tractus solitarus (NTS). Efferent vagal fibers originate in the nucleus ambiguus and dorsal motor nucleus (20, 43), innervating the sinoatrial node, atrioventricular node, and

atrial and ventricular myocardium through the intrinsic cardiac nervous system (3, 4). We had previously shown that stimulation of the intact right or left vagal nerves had similar hemodynamic and electrophysiological effects, (52) as both of these nerves provide preganglionic efferent fibers that synapse in the intrinsic cardiac ganglia. As the vagal trunk consists primarily of afferent fibers, the role of these fibers, particularly during stimulation, need to be clearly assessed. Multiple studies have shown beneficial effects of VNS in preventing arrhythmias, but the large majority of these studies were performed in animal models in the decentralized state, after vagal nerve transection (2, 8, 15, 18, 24, 27, 34, 45, 50, 53, 56) or in isolated innervated hearts (6, 7, 30), where afferent activation was not possible. Other studies that demonstrated some benefit in the intact state often had mixed results, showing a reduction of polymorphic ventricular arrhythmias, but an increase monomorphic ventricular tachycardia (44). Still, other studies have reported pro-arrhythmic effects, or greater burden of ventricular arrhythmias during intact stimulation with or without ischemia (17, 22, 36, 37, 46). Meanwhile, a large randomized prospective clinical trial, NEural Cardiac TherApy foR Heart Failure (NECTAR-HF) failed to demonstrate the benefits of VNS in heart failure patients that had been demonstrated in animal models (54). The mixed results of these studies may be due to the method of stimulation, neglecting the role of afferent fiber activation (15). In our study, afferent vagal fibers did not play a significant role on cardiac electrophysiology and hemodynamic parameters in the resting state, and the primary effects of vagal transection could be explained by the removal of efferent parasympathetic tone. However, during stimulation, afferent fibers were activated and played significant role in reducing the effects of efferent vagal nerve stimulation.

Transection of the ipsilateral and bilateral vagosympathetic trunks followed by stimulation significantly augmented electrophysiological and hemodynamic effects of VNS. Transection of the contralateral vagosympathetic trunk and removal of the contralateral vagal afferents did not have as great of an effect, as this was not the trunk that was being actively stimulated. However, the inhibitory role of even these contralateral afferents at modest stimulation levels, as demonstrated by the decrease in threshold of right VNS after left VNTx, suggests that the autonomic nervous system is an integrated network that senses hemodynamic changes acutely and acts to return these changes to the baseline state. Direct stimulation of afferent fibers as well as hemodynamic changes transduced by contralateral vagal afferent fibers can lead to activation of neurons in the NTS, that subsequently could inhibit parasympathetic outflow from the dorsal motor nucleus or nucleus ambiguous and may even cause sympathoexcitation. It is also possible that activation of these fibers could lead to symapathoexcitation either via reflex activation or by direct activation of these fibers in the vagal trunk. It has been reported that the vagal trunk is a complex nerve that has contains sympathetic fibers, particularly at the level of the thorax.(33) Therefore, the possibility of activating these fibers also exists with electrical stimulation. However, in this study, the role of these sympathetic fibers is likely to be more negligible. If these fibers were responsible for “sympathoexcitation,” then upon transection, similar sympathetic effects would have been observed. Instead, an increase in parasympathetic effects was found.

Previous studies had also suggested an inhibitory role of vagal afferent fibers on reflex sympathetic outflow (5, 39). Based on these studies, we would have expected a

decrease in the magnitude of the effects of VNS after vagal transection, rather than augmentation, as the inhibitory input of vagal afferents on sympathetic efferents would be removed. The results of our study were surprising, but do show that activation of afferent fibers by electrical stimulation of the vagus nerve reduces parasympathetic efferent outflow and may cause reflex sympathoexcitation, counteracting or reducing the beneficial effects of VNS. Therefore, the role of these afferent fibers must be remembered when performing vagal nerve stimulation in the intact state.

Right vs. Left VNTx and Effects of VNS

Compared to right VNS, the effect of left VNS on ARI was more significant after bilateral VNTx compared ipsilateral VNTx. This may suggest that the right vagal trunk may contain greater cardiac afferent mechanoreceptor fibers. These fibers are intact in the setting of ipsilateral (left) VNTx, and may be activated by the drop in SBP and dP/dt max during VNS, causing reflex sympathetic activation or greater withdrawal of parasympathetic tone through this intact nerve, and subsequently inhibiting to some degree, the increase in ventricular ARI observed during left VNS. Our results support those of Hirota et al., who performed vagotomy pre- and post-bilateral IXth nerve stimulation to assess the effect of afferent activation using gustatory stimuli. As in our study, Hirota and colleagues also noted subtle differences in heart rate and blood pressure, depending on the order that the right or left vagal trunk was transected, with less tachycardia after left-sided transection compared to right (13). They also showed that the tachycardia response to gustatory stimuli was reduced more after right vagotomy than left vagotomy, again suggesting that the right vagal trunk may contain more cardiac afferents fibers (13). Chen et al. showed an increase in heart rate, blood

pressure, LV systolic pressure, and dP/dt min after both unilateral left and unilateral right vagotomy (9). However, baroreflex sensitivity was increased only after right vagotomy, also suggesting a greater role for cardiac vagal afferent fibers in the right vagus.

Limitations

General anesthesia can cause suppression of nerve activity. However, we were able to reliably record a cardiomotor response during VNS. To reduce the effect of inhaled anesthetics, α-chloralose infusion was used during ARI and hemodynamic evaluation. For global and regional analysis, ARIs were not corrected for HR, as any HR effects, particularly with regards to assessment of parasympathetic tone are physiologically important. Furthermore, HR would not affect regional differences, as these were assessed at the same HR and percentage changes used to assess regional differences. Atrial and ventricular pacing was not performed to correct for HR, given the effect of pacing on altering autonomic tone.(12) Effects of VNS were evaluated at one frequency and pulse width. This frequency and pulse width was chosen to avoid aggressive stimulation. Higher frequencies that are thought to specifically and only activate afferent fibers in epilepsy studies were avoided. Additionally, narcotics, such as fentanyl, can cause central modulation of parasympathetic tone through interaction with the opioid mu and OLR-1 receptors in the nucleus ambigiuus. However, the use of fentanyl was standardized across all animals and recordings were performed after initiation of α-chloralose during steady state. Finally, the vagal trunk contains afferent fibers from many visceral organs. Therefore, it is not clear from this study activation of

which afferent fibers may have led to a reduction in cardiac parasympathetic efferent outflow or sympathoexcitation.

CONCLUSIONS

Parasympathetic efferent cardiomotor fibers in both the right and left vagal trunks are required for maintaining the resting basal parasympathetic tone. Vagal afferents are activated during VNS and decrease efferent parasympathetic electrophysiological and hemodynamic effects of electrical stimulation. The activation of both ipsilateral afferent fibers as well as reflex activation of the autonomic nervous system must be considered when applying vagal nerve stimulation.

REFERENCES

1. Ajijola OA, Yagishita D, Patel KJ, Vaseghi M, Zhou W, Yamakawa K, So E, Lux RL, Mahajan A, and Shivkumar K. Focal myocardial infarction induces global remodeling of cardiac sympathetic innervation: neural remodeling in a spatial context. *Am J Physiol Heart Circ Physiol*. 2013;305:H1031-1040.

2. Ando M, Katare RG, Kakinuma Y, Zhang D, Yamasaki F, Muramoto K, and Sato T. Efferent vagal nerve stimulation protects heart against ischemia-induced arrhythmias by preserving connexin43 protein. *Circulation*. 2005;112: 164-170.

3. Armour JA. The little brain on the heart. *Cleve Clin J Med* 74 Suppl. 2007;1:S48-51, 2007.

4. Armour JA, Murphy DA, Yuan BX, Macdonald S, and Hopkins DA. Gross and microscopic anatomy of the human intrinsic cardiac nervous system. *Anat Rec*. 1997;247:289-298.

5. Barron KW and Bishop VS. The influence of vagal afferents on the left ventricular contractile response to intracoronary administration of catecholamines in the conscious dog. *Circ Res*. 1981;49:159-169.

6. Brack KE, Coote JH, and Ng GA. Vagus nerve stimulation protects against ventricular fibrillation independent of muscarinic receptor activation. *Cardiovasc Res*. 2011;91:437-446.

7. Brack KE, Patel VH, Coote JH, and Ng GA. Nitric oxide mediates the vagal protective effect on ventricular fibrillation via effects on action potential duration restitution in the rabbit heart. *J Physiol*. 2007;583:695-704.

8. Brooks WW, Verrier RL, and Lown B. Influence of vagal tone on stellectomy-induced changes in ventricular electrical stability. *Am J Physiol*. 1978;234:H503-507.

9. Chen LN, Zang WJ, Yu XJ, Liu J, Li DL, Kong SS, Lu J, and Xu XL. Compensatory recovery of vagal control of hemodynamics after unilateral vagotomy. *Physiol Res*. 2008;57:119-132.

10. Farrell TG, Paul V, Cripps TR, Malik M, Bennett ED, Ward D, and Camm AJ. Baroreflex sensitivity and electrophysiological correlates in patients after acute myocardial infarction. *Circulation*. 1991;83:945-952.

11. Haws CW and Lux RL. Correlation between in vivo transmembrane action potential durations and activation-recovery intervals from electrograms. Effects of interventions that alter repolarization time. *Circulation*. 1990;81:281-288.

12. Herre JM and Thames MD. Responses of sympathetic nerves to programmed ventricular stimulation. *J Am Coll Cardiol*. 1987;9:147-153.

13. Hirota K and Ishiko N. Influences of the sympathetic and parasympathetic nerve transection on cardiovascular reflexes induced by volleys in the IXth nerve fibers of rat. *J Auton Nerv Syst*. 1994;46:237-249.

14. Hoover DB, Shepherd AV, Southerland EM, Armour JA, and Ardell JL. Neurochemical diversity of afferent neurons that transduce sensory signals from dog ventricular myocardium. *Auton Neurosci*. 2008;141:38-45.

15. Huang WA, Shivkumar K, and Vaseghi M. Device-based autonomic modulation in arrhythmia patients: the role of vagal nerve stimulation. *Curr Treat Options Cardiovasc Med*. 2015;17:379.

16. Hull SS, Jr., Evans AR, Vanoli E, Adamson PB, Stramba-Badiale M, Albert DE, Foreman RD, and Schwartz PJ. Heart rate variability before and after myocardial infarction in conscious dogs at high and low risk of sudden death. *J Am Coll Cardiol*. 1990;16:978-985.

17. Imataka K, Yamaoki K, Seki A, Takayama Y, and Fujii J. Peculiar mitral valve and papillary muscle lesions induced by vagus manipulations in rabbits. An experimental model for nonrheumatic mitral regurgitation. *Jpn Heart J*. 1986;27: 377-386.

18. James R, Arnold J, Allen JD, Pantridge JF, and Shanks RG. The effects of heart rate, myocardial ischemia and vagal stimulation on the threshold for ventricular fibrillation. *Circulation*. 1977;55:311-317.

19. Jellinek M, Kaye MP, Kaiser GC, and Cooper T. Effect of cervical vagosympathectomy on myocardial catecholamine concentration. *Am J Physiol*. 1965;209:951-954.

20. Kalia M and Sullivan JM. Brainstem projections of sensory and motor components of the vagus nerve in the rat. *J Comp Neurol*. 1982;211:248-265.

21. Katare RG, Ando M, Kakinuma Y, Arikawa M, Handa T, Yamasaki F, and Sato T. Vagal nerve stimulation prevents reperfusion injury through inhibition of opening of mitochondrial permeability transition pore independent of the bradycardiac effect. *J Thorac Cardiovasc Surg*. 2009;137:223-231.

22. Kerzner J, Wolf M, Kosowsky BD, and Lown B. Ventricular Ectopic Rhythms following Vagal Stimulation in Dogs with Acute Myocardial Infarction. *Circulation*. 1973;47:44-50.

23. Kleiger RE, Miller JP, Bigger JT, Jr., and Moss AJ. Decreased heart rate variability and its association with increased mortality after acute myocardial infarction. *Am J Cardiol*. 1987;59:256-262.

24. Kolman BS, Verrier RL, and Lown B. The effect of vagus nerve stimulation upon vulnerability of the canine ventricle: role of sympathetic-parasympathetic interactions. *Circulation*. 1975;52:578-585.

25. La Rovere MT, Bigger JT, Jr., Marcus FI, Mortara A, and Schwartz PJ. Baroreflex sensitivity and heart-rate variability in prediction of total cardiac mortality after myocardial infarction. ATRAMI (Autonomic Tone and Reflexes After Myocardial Infarction) Investigators. *Lancet*. 1998;351:478-484.

26. Maccanon DM and Horvath SM. Effect of bilateral cervical vagotomy in the dog. *Am J Physiol*. 1957;189:569-572.

27. Matta RJ, Verrier RL, and Lown B. Repetitive extrasystole as an index of vulnerability to ventricular fibrillation. *Am J Physiol*. 1976;230:1469-1473.

28. Millar CK, Kralios FA, and Lux RL. Correlation between refractory periods and activation-recovery intervals from electrograms: effects of rate and adrenergic interventions. *Circulation*. 1985;72:1372-1379.

29. Ng GA, Brack KE, and Coote JH. Effects of direct sympathetic and vagus nerve stimulation on the physiology of the whole heart--a novel model of isolated Langendorff perfused rabbit heart with intact dual autonomic innervation. *Exp Physiol*. 2001;86: 319-329.

30. Ng GA, Brack KE, Patel VH, and Coote JH. Autonomic modulation of electrical restitution, alternans and ventricular fibrillation initiation in the isolated heart. *Cardiovasc Res*. 2007;73:750-760.

31. Olgin JE, Takahashi T, Wilson E, Vereckei A, Steinberg H, and Zipes DP. Effects of thoracic spinal cord stimulation on cardiac autonomic regulation of the sinus and atrioventricular nodes. *J Cardiovasc Electrophysiol*. 2002;13:475-481.

32. Prechtl JC and Powley TL. The fiber composition of the abdominal vagus of the rat. *Anat Embryol (Berl)*. 1990;181:101-115.

33. Randall WC and Armour JA. Complex cardiovascular responses to vagosympathetic stimulation. *Proc Soc Exp Biol Med*. 1974;145:493-499.

34. Rosenshtraukh L, Danilo P, Anyukhovsky EP, Steinberg SF, Rybin V, Brittain-Valenti K, Molina-Viamonte V, and Rosen MR. Mechanisms for vagal modulation

of ventricular repolarization and of coronary occlusion-induced lethal arrhythmias in cats. *Circ Res*. 1994;75:722-732.

35. Sabbah HN, Ilsar I, Zaretsky A, Rastogi S, Wang M, and Gupta RC. Vagus nerve stimulation in experimental heart failure. *Heart Fail Rev*. 2001;16:171-178.

36. Scherf D, Blumenfeld S, and Yildiz M. Experimental study on ventricular extrasystoles provoked by vagal stimulation. *Am Heart J*. 1961;62:670-675.

37. Scherlag BJ, Kabell G, Harrison L, and Lazzara R. Mechanisms of bradycardia-induced ventricular arrhythmias in myocardial ischemia and infarction. *Circulation*. 1982;65:1429-1434.

38. Schwartz PJ, Billman GE, and Stone HL. Autonomic mechanisms in ventricular fibrillation induced by myocardial ischemia during exercise in dogs with healed myocardial infarction. An experimental preparation for sudden cardiac death. *Circulation*. 1984;69:790-800.

39. Schwartz PJ, Pagani M, Lombardi F, Malliani A, and Brown AM. A cardiocardiac sympathovagal reflex in the cat. *Circ Res*. 1973;32:215-220.

40. Schwartz PJ, Verrier RL, and Lown B. Effect of stellectomy and vagotomy on ventricular refractoriness in dogs. *Circ Res*. 1977;40:536-540.

41. Shen MJ and Zipes DP. Role of the autonomic nervous system in modulating cardiac arrhythmias. *Circ Res*. 2014;114:1004-1021.

42. Shinlapawittayatorn K, Chinda K, Palee S, Surinkaew S, Thunsiri K, Weerateerangkul P, Chattipakorn S, KenKnight BH, and Chattipakorn N. Low-

amplitude, left vagus nerve stimulation significantly attenuates ventricular dysfunction and infarct size through prevention of mitochondrial dysfunction during acute ischemia-reperfusion injury. *Heart Rhythm*. 2013;10:1700-1707.

43. Standish A, Enquist LW, and Schwaber JS. Innervation of the heart and its central medullary origin defined by viral tracing. *Science*.1994;263:232-234.

44. Takahashi N, Ito M, Ishida S, Fujino T, Saikawa T, and Arita M. Effects of vagal stimulation on cesium-induced early afterdepolarizations and ventricular arrhythmias in rabbits. *Circulation*. 1992;86:1987-1992.

45. Takahashi N, Ito M, Iwao T, Ohie T, Yonemochi H, Nakagawa M, Saikawa T, and Sakata T. Vagal modulation of ventricular tachyarrhythmias induced by left ansae subclaviae stimulation in rabbits. *Jpn Heart J*. 1998;39:503-511.

46. Takato T, Ashida T, Seko Y, Fujii J, and Kawai S. Ventricular tachyarrhythmia-related basal cardiomyopathy in rabbits with vagal stimulation--a novel experimental model for inverted Takotsubo-like cardiomyopathy. *J Cardiol*. 2010;56:85-90.

47. Vaseghi M and Shivkumar K. The role of the autonomic nervous system in sudden cardiac death. *Prog Cardiovasc Dis*. 2008;50:404-419.

48. Vaseghi M, Yamakawa K, Sinha A, So EL, Zhou W, Ajijola OA, Lux RL, Laks M, Shivkumar K, and Mahajan A. Modulation of regional dispersion of repolarization and T-peak to T-end interval by the right and left stellate ganglia. *Am J Physiol Heart Circ Physiol*. 2013;305:H1020-1030.

49. W J. Functional anatomy of the peripheral sympathetic and parasympathetic system. In: *The Integrative Action of the Autonomic Nervous System: Neurobiology of Homeostasis* edited by W. J. Cambridge: Cambridge University Press, 2006:13-34.

50. Waxman MB, Sharma AD, Asta J, Cameron DA, and Wald RW. The protective effect of vagus nerve stimulation on catecholamine-halothane-induced ventricular fibrillation in dogs. *Can J Physiol Pharmacol*. 1989;67:801-809.

51. Weiss JL, Frederiksen JW, and Weisfeldt ML. Hemodynamic determinants of the time-course of fall in canine left ventricular pressure. *J Clin Invest*. 1976;58:751-760.

52. Yamakawa K, So EL, Rajendran PS, Hoang JD, Makkar N, Mahajan A, Shivkumar K, and Vaseghi M. Electrophysiological effects of right and left vagal nerve stimulation on the ventricular myocardium. *Am J Physiol Heart Circ Physiol*. 2014;307:H722-731.

53. Yoon MS, Han J, Tse WW, and Rogers R. Effects of vagal stimulation, atropine, and propranolol on fibrillation threshold of normal and ischemic ventricles. *Am Heart J*. 1977;93: 60-65.

54. Zannad F, De Ferrari GM, Tuinenburg AE, Wright D, Brugada J, Butter C, Klein H, Stolen C, Meyer S, Stein KM, Ramuzat A, Schubert B, Daum D, Neuzil P, Botman C, Castel MA, D'Onofrio A, Solomon SD, Wold N, and Ruble SB. Chronic vagal stimulation for the treatment of low ejection fraction heart failure:

results of the NEural Cardiac TherApy foR Heart Failure (NECTAR-HF) randomized controlled trial. *Eur Heart J.* 2015; 36:425-433.

55. Zhao M, Sun L, Liu JJ, Wang H, Miao Y, and Zang WJ. Vagal nerve modulation: a promising new therapeutic approach for cardiovascular diseases. *Clin Exp Pharmacol Physiol*. 2012;39:701-705.

56. Zuanetti G, De Ferrari GM, Priori SG, and Schwartz PJ. Protective effect of vagal stimulation on reperfusion arrhythmias in cats. *Circ Res*. 1987;61:429-435.

Figure 1. Flow chart of the experimental protocol. 25 of 37 animals underwent vagal nerve stimulation (VNS) followed by vagal nerve transection (VNTx), and 12 of 37 animals received only intravenous infusion of atropine. Animals with ipsilateral transection also underwent bilateral transection after right or left VNS. RVNS = right vagal nerve stimulation, LVNS = left vagal nerve stimulation.

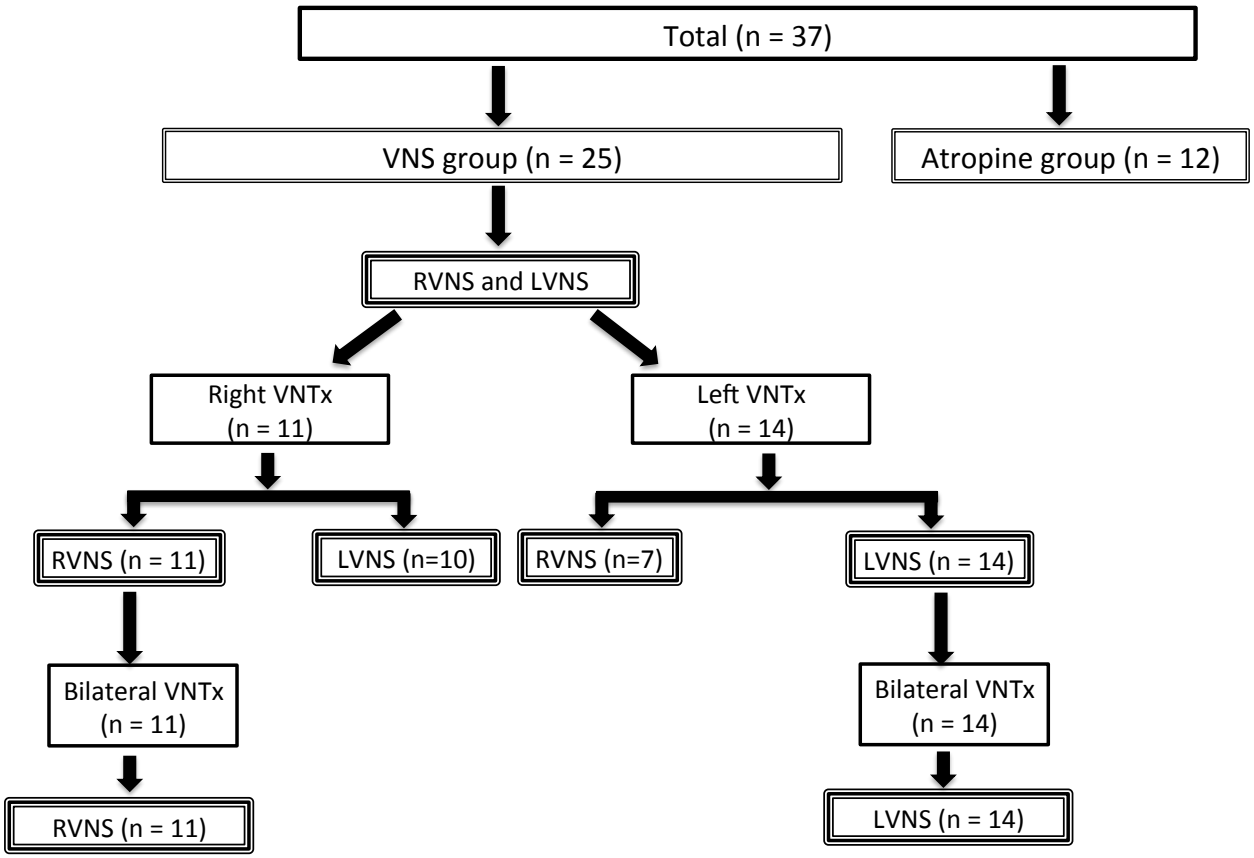

Figure 2. Effect of ipsilateral (right) and bilateral vagal nerve transection on ARI, stimulation threshold, and dP/dt max before and after RVNS. Upper panels: polar maps from the sock electrode of one animal at baseline and during RVNS before and after transection demonstrated that ARIs in all regions increased with stimulation. After transection, the magnitude of increase in ARI was greater in all regions. Lower panels: combined data from all animals that underwent RVNS after right VNTx is shown. Stimulation threshold and global epicardial ARI decreased after ipsilateral and bilateral VNTx. Effects of RVNS on ARI and dP/dt max during RVNS were augmented by ipsilateral and bilateral VNTx. *P<0.05 vs. baseline. #P<0.05 vs. intact condition. BL = baseline, RVNS = right vagal nerve stimulation, VNTx = vagal nerve transection.

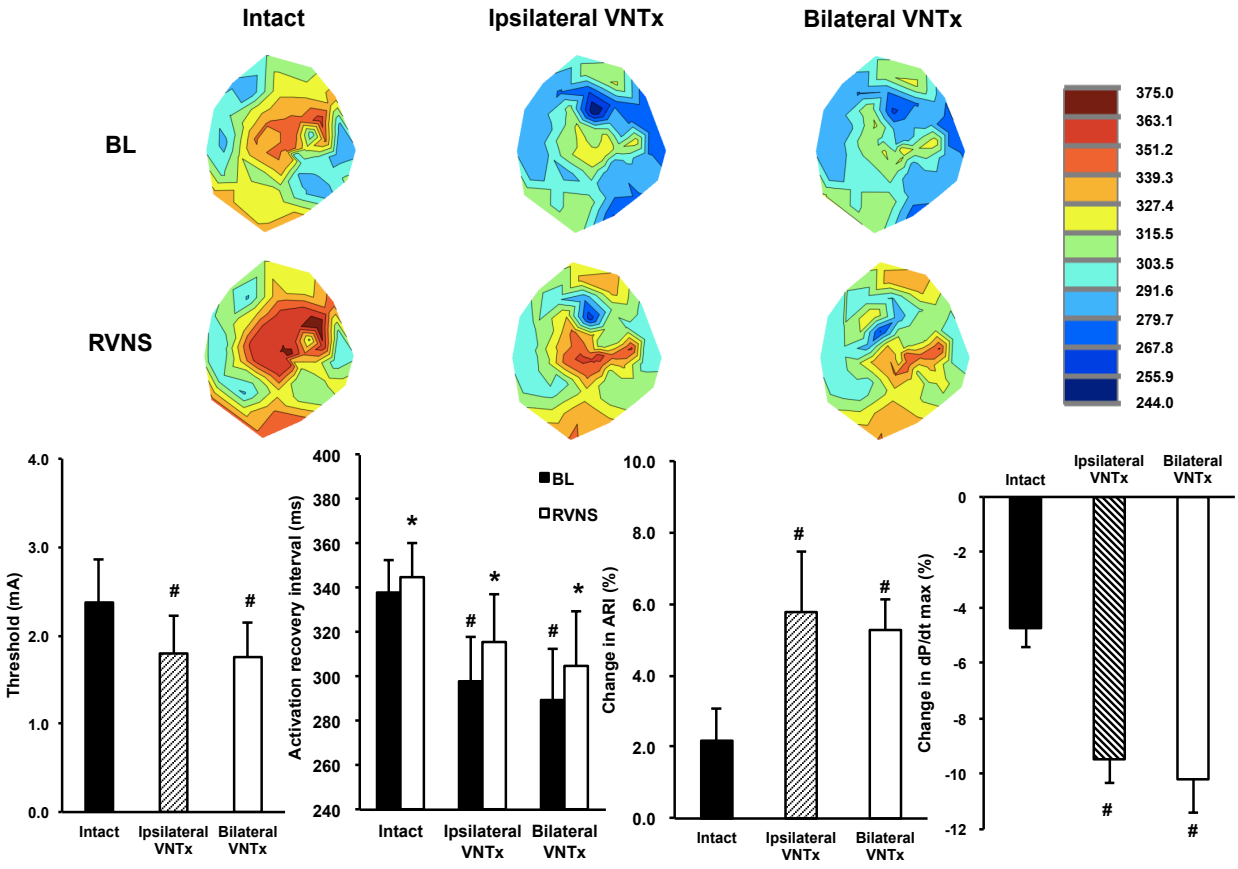

Figure 3. Effect of ipsilateral (left) and bilateral VNTx on ARI, stimulation threshold, and dP/dt max before and after LVNS. Upper panels: polar maps from the sock electrode in one animal at baseline and during left VNS demonstrated a uniform decrease in regional ARIs after VNTx. The increase in ARI from baseline during left VNS appears to be greatest after bilateral VNTx. Lower panels: combined data from all animals that underwent LVNS after left VNTx demonstrated a decrease in stimulation threshold and global epicardial ARIs after ipsilateral and bilateral VNTx. The change in ARI and dP/dt max during LVNS was somewhat augmented by ipsilateral VNTx, but this difference did not reach statistical significance until after bilateral VNTx. *P<0.05 for pre vs. post VNS. #P<0.05 vs. intact condition. BL = baseline, LVNS = left vagal nerve stimulation, VNTx = vagal nerve transection.

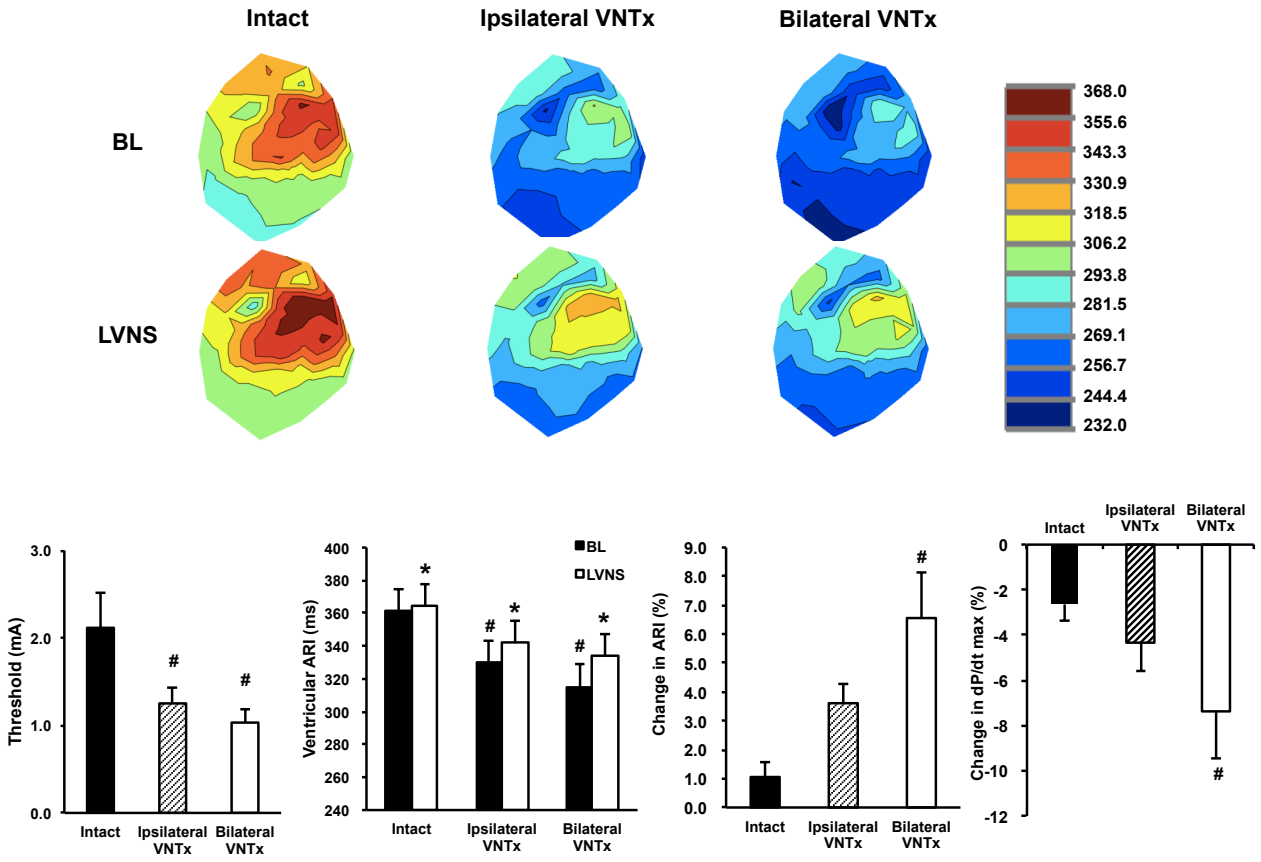

<u>Figure 4.</u> Effects of contralateral vagal nerve transection (VNTx) on stimulation threshold, global ventricular ARI, and LV contractility with VNS. (A) The current required to achieve a 10% decrease in HR, defined as the bradycardia threshold, was decreased with right vagal nerve stimulation (RVNS) after contralateral VNTx. However, no significant additional changes in ARI with VNS were observed. (B) During left vagal nerve stimulation (LVNS) after contralateral (right) VNTx, stimulation threshold, global ventricular ARI, and LV contractility were not altered. *P<0.05 for pre vs. post stimulation. #P<0.05 for transection vs. intact vagal trunk. BL= baseline, RVNS = right vagal nerve stimulation, LVNS = left vagal nerve stimulation.

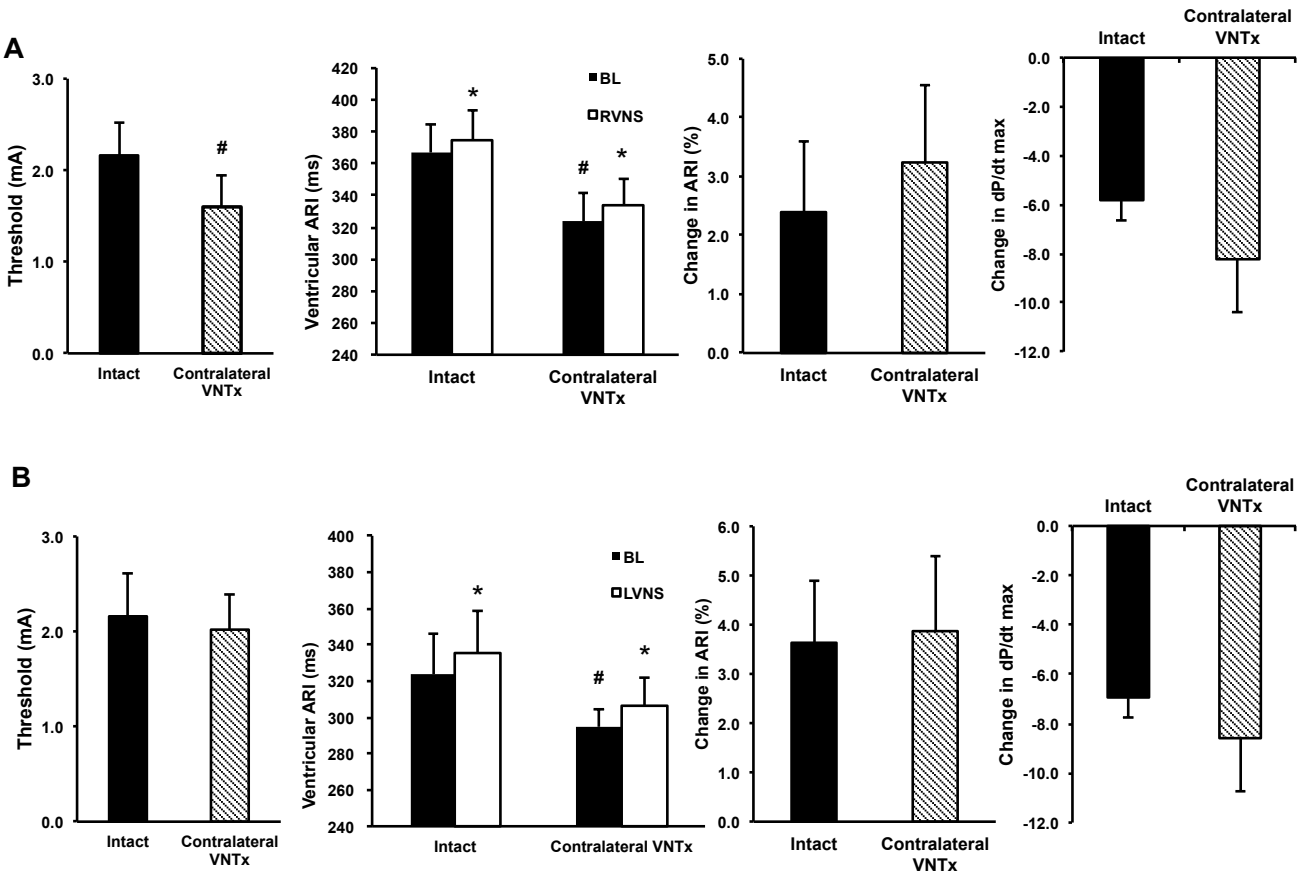

<u>Figure 5.</u> Regional ARIs after ipsilateral and bilateral VNTx. ARIs decreased after ipsilateral VNTx (right), with minimal additional effects after bilateral VNTx. Regional ARIs prolonged similarly during RVNS. *P<0.05 pre vs. post stimulation, #P<0.05 pre vs. post VNTx. RVNS = right vagal nerve stimulation, BL = baseline.

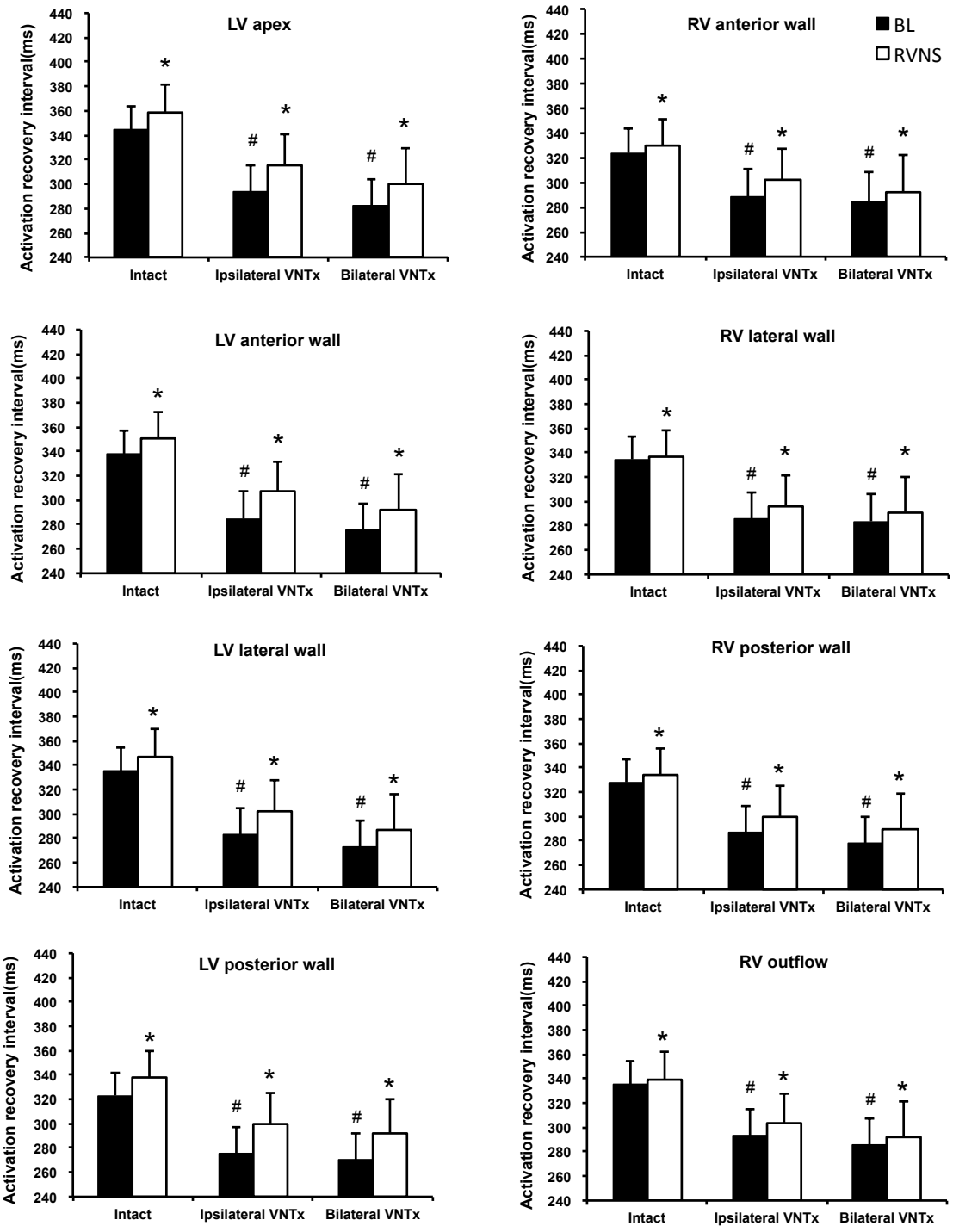

<u>Figure 6.</u> Regional ARIs after ipsilateral and bilateral VNTx. Regional ARIs were somewhat decreased by ipsilateral VNTx (left). This difference became significant after bilateral VNTx. LVNS increased ARI similarly in all regions. *P<0.05 for pre vs. post LVNS. #P<0.05 for baseline after transection vs. both vagal nerves intact. BL = baseline.

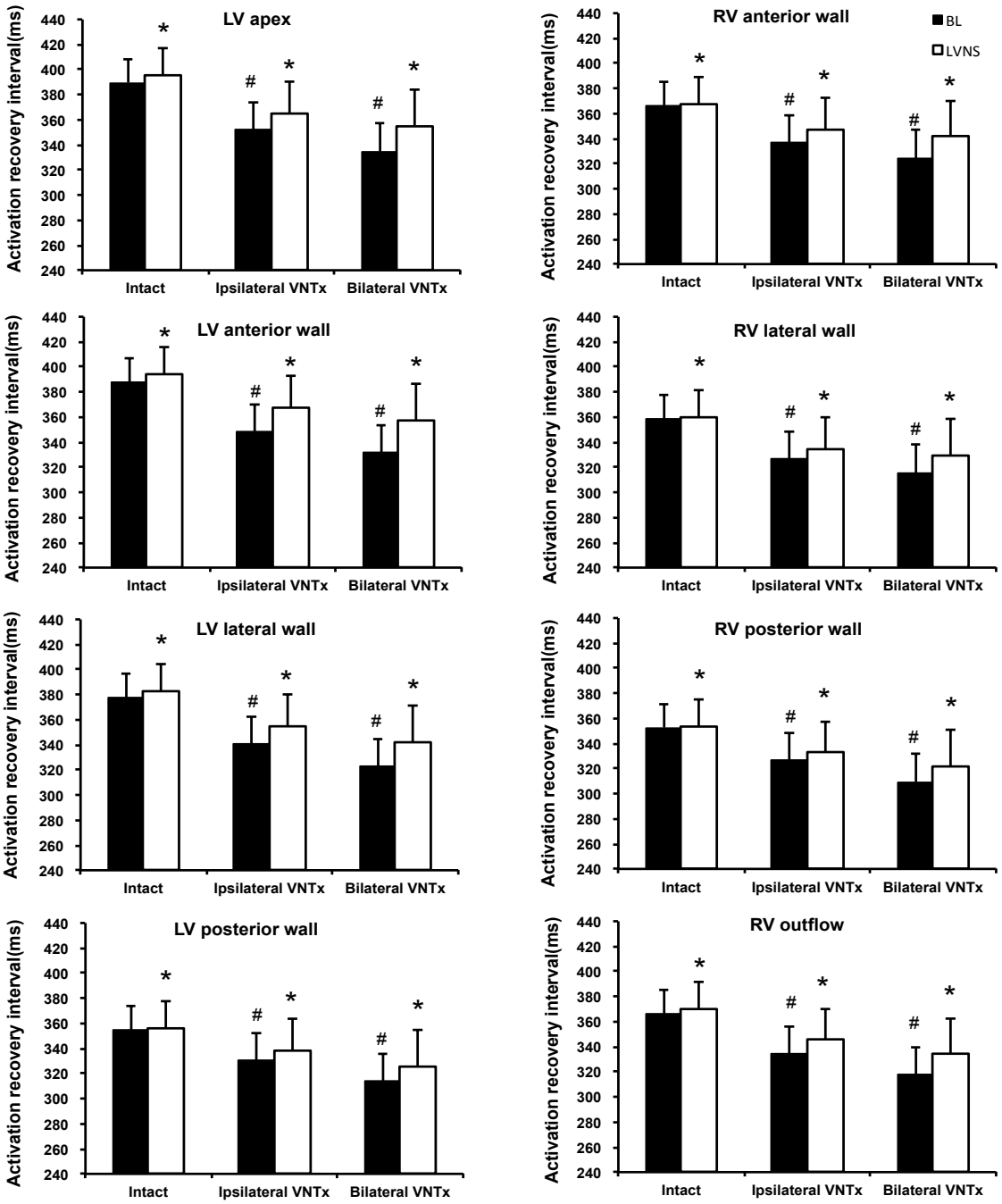

TABLE 1. EFFECT OF VAGAL NERVE STIMULATION ON HEMODYNAMIC PARAMETERS AFTER VAGAL NERVE TRANSECTION

Table 1	Intact			Ipsilateral VNTx			Bilateral VNTx		
	BL	VNS	% Change	BL	VNS	% Change	BL	VNS	% Change
HR (bpm)									
Right (n = 11)	82 ± 4	74 ± 4*	-10 ± 1	96 ± 5$^{\#}$	82 ± 5*	-15 ± 2§	101 ± 5$^{\#}$	87 ± 6*	-14 ± 2§
Left (n = 14)	74 ± 3	67 ± 3*	-10 ± 1	84 ± 2$^{\#}$	72 ± 3*	-15 ± 1	91 ± 4$^{\#}$	74 ± 3*	-18 ± 2§
SBP (mmHg)									
Right (n = 11)	117 ± 6	112 ± 7*	-5 ± 2	104 ± 7$^{\#}$	95 ± 6*	-9 ± 1§	96 ± 7$^{\#}$	86 ± 6*	-11 ± 1§
Left (n = 14)	126 ± 6	120 ± 6*	-5 ± 1	127 ± 6	115 ± 6*	-10 ± 1§	122 ± 8	102 ± 7*	-16 ± 1§
dP/dt max (mmHg/s)									
Right (n = 10)	1830 ± 149	1752 ± 137*	-4 ± 1	1666 ± 111	1518 ± 107*	-9 ± 1§	1560 ± 129	1402 ± 116*	-10 ± 1§
Left (n = 13)	1679 ± 111	1628 ± 104*	-3 ± 1	1799 ± 122	1722 ± 116*	-4 ± 1	1883 ± 249	1731 ± 205*	-7 ± 2§
dP/dt min (mmHg/s)									
Right (n = 10)	-2859 ± 438	-2686 ± 429*	8 ± 2	-2540 ± 380	-2180 ± 362*	17 ± 4§	-2211 ± 491	-1825 ± 456*	20 ± 3§
Left (n = 13)	-2869 ± 248	-2747 ± 253*	5 ± 2	- 3222 ± 262	-2783 ± 259*	14 ± 3§	-3086 ± 367	-2558 ± 336*	17 ± 5§
Tau (ms)									
Right (n = 9)	41 ± 2	42 ± 3	4 ± 2	35 ± 3$^{\#}$	39 ± 4*	10 ± 3§	33 ± 3$^{\#}$	37 ± 4*	10 ± 3§
Left (n = 12)	39 ± 2	41 ± 2*	7 ± 2	35 ± 2$^{\#}$	39 ± 2*	12 ± 2	34 ± 2$^{\#}$	39 ± 2*	14 ± 3§
PR interval (ms)									
Right (n = 10)	118 ± 2	135 ± 3*	13 ± 3	109 ± 3$^{\#}$	133 ± 5*	23 ± 5§	102 ± 3$^{\#}$	128 ± 7*	26 ± 6§
Left (n = 9)	117 ± 5	135 ± 5*	13 ± 3	109 ± 5$^{\#}$	132 ± 6*	23 ± 5§	105 ± 5$^{\#}$	128± 8*	24 ± 5§

HR = Heart rate, SBP = systolic blood pressure, VNTx = vagal nerve transection, VNS = vagal nerve stimulation. $^{\#}$P<0.05 compared to intact baseline. §P<0.05 compared to percentage change during VNS with both vagal nerves intact.

TABLE 2. HEMODYNAMIC AND ELECTROPHYSIOLOGICAL RESPONSES TO RIGHT AND LEFT VAGAL NERVE TRANSECTION

Hemodynamics					
	BL	**post 1 min**	**post 5 min**	**post 10 min**	**post 20 min**
Right VNTx (N = 8)					
HR (bpm)	81 ± 6	91 ± 6*	91 ± 6	92 ± 6	94 ± 6
SBP (mmHg)	108 ± 6	114 ± 7*	109 ± 8*	107 ± 8	104 ± 8
dP/dt max (mmHg/s)	1837 ± 166	1894 ± 145*	1883 ± 135	1875 ± 130	1833 ± 130
dP/dt min (mmHg/s)	-2697 ± 478	-2931 ± 430*	-2927 ± 460	-2832 ± 465	-2744 ± 448
Left VNTx (N = 13)					
HR (bpm)	73 ± 4	81 ± 4*	83 ± 5	85 ± 5	84 ± 5
SBPP (mmHg)	125 ± 6	136 ± 7*	134 ± 7	135 ± 7	133 ± 7
dP/dt max (mmHg/s)	1682 ± 130	1768 ± 131*	1800 ± 137	1812 ± 136	1806 ± 145
dP/dt min (mmHg/s)	-2933 ± 226	-3184 ± 243*	-3219 ± 267	-3236 ± 251	-3249 ± 275

Global ventricular ARI (ms)					
	BL	**post 1 min**	**post 5 min**	**post 10 min**	**post 20 min**
Unilateral Left VNTx (N=14)	354 ± 14	338 ± 14*	333 ± 13	331 ± 13	331 ± 12
Unilateral Right VNTx (N=9)	339 ± 20	321 ± 19*	321 ± 19	318 ± 20	316 ± 20
Bilateral VNTx (N = 23)	322 ± 11	310 ± 12*	309 ± 11	308 ± 11	310 ± 11

HR = Heart rate, SBP = systolic blood pressure, VNTx = vagal nerve transection.*P<0.05 compared to the prior measured time/condition.

TABLE 3. EFFECT OF VAGAL NERVE STIMULATION ON HEMODYNAMIC PARAMETERS AFTER CONTRALATERAL VAGAL NERVE TRANSECTION

Table 3	Intact			Contralateral VNTx		
	Intact	VNS	% Change	BL	VNS	% Change
HR (bpm)						
Right (n = 10)	79 ± 4	69 ± 3*	-11 ± 2	86 ± 4#	73 ± 2*	-15 ± 2
Left (n = 8)	82 ± 5	75 ± 5*	-9 ± 1	94 ± 6#	83 ± 5*	-11 ± 2
SBP (mmHg)						
Right (n = 10)	133 ± 8	123 ± 7*	-7 ± 1	130 ± 8#	118 ± 8*	-10 ± 1
Left (n = 8)	119 ± 7	115 ± 8*	-4 ± 1	101 ± 9#	94 ± 9*	-8 ± 2
dP/dt max (mmHg/s)						
Right (n = 7)	1673 ± 102	1576 ± 96*	-6 ± 1	1613 ± 99	1475 ± 82*	-8 ± 2
Left (n = 7)	2060 ± 191	1904 ± 173*	-7 ± 1	1815 ± 159	1678 ± 161*	-8 ± 2
dP/dt min (mmHg/s)						
Right (n = 7)	-2916 ± 373	-2705 ± 368*	8 ± 1	-3030 ± 334	-2704 ± 321*	11 ± 2
Left (n = 7)	-3281 ± 509	-2981 ± 468*	10 ± 3	-2832 ± 534	-2565 ± 554*	14 ± 4
Tau (ms)						
Right (n = 7)	37 ± 2	41 ± 3*	10 ± 3	35 ± 2#	38 ± 3*	6 ± 2
Left (n = 7)	39 ± 5	43 ± 5*	10 ± 3	31 ± 2#	35 ± 2*	13 ± 3
PR interval (ms)						
Right (n = 10)	115 ± 4	131 ± 5*	14 ± 2	101 ± 4#	127 ± 5*	27 ± 6
Left (n = 8)	115 ± 4	141 ± 11*	22 ± 8	105 ± 3#	132 ± 9*	25 ± 6

HR = Heart rate, SBP = systolic blood pressure, VNTx = vagal nerve transection.*P<0.05 compared to baseline prior to VNS. #P<0.05 compared to intact baseline.

CHAPTER 4

MECHANISMS OF PARASYMPATHETIC DYSFUNCTION AND ANTI-ARRHYTHMIC EFFECT OF VAGAL NERVE STIMULATION FOLLOWING MYOCARDIAL INFARCTION

INTRODUCTION

The autonomic nervous system plays a critical role in the genesis and maintenance of ventricular tachy-arrhythmias (VT/VF) that lead to sudden cardiac death (1, 2). In particular, sympathetic activation and parasympathetic dysfunction, are known to accompany myocardial infarction (MI), and increase risk of sudden cardiac death (1, 2). Parasympathetic dysfunction is manifested as abnormal baro-reflex sensitivity and heart rate variability (3-7). However, the mechanism behind this dysfunction and the level at which it occurs (cardiac vs. extra-cardiac) are poorly characterized. In addition, it has been shown that vagal nerve stimulation (VNS) can reduce inflammation and ischemia driven ventricular arrhythmias, particularly if initiated at the time of or before onset of myocardial infarction (8-16). However, introducing VNS before MI is not clinically feasible in humans. Importantly, it is unknown if VNS can reduce ventricular arrhythmias in the setting of chronic myocardial infarction, when the scar has pathologically remodeled and cardiac neural remodeling has already occurred. The implications of this therapy in the setting of chronic MI are extremely important for the many patients with ischemic cardiomyopathy and ventricular arrhythmias, who receive internal cardiac defibrillator shocks and experience VT/VF despite catheter ablation and medical therapies (17-19).

In this study, we hypothesized that the primary dysfunction in the setting of MI is due to a decrease in central parasympathetic drive from the central nervous system. Therefore, we hypothesized that the primary parasympathetic neurotransmitter, acetylcholine (ACh) should remain intact in the setting of MI, but that parasympathetic neurons in the intrinsic cardiac ganglia (the ganglia on the surface heart) demonstrate

abnormal activity due to the decreased central drive. Furthermore, we hypothesized that increasing this drive with VNS should restore myocardial electrical stability and decrease VT/VF inducibility in the setting of chronic MI. We investigated these questions in a porcine infarct model, utilizing neurotransmitter measurements, direct neuronal recordings and electrophysiological mapping.

METHODS

Study Approval

All animal procedures and surgeries were performed according to the University of California, Los Angeles (UCLA) Institutional Animal Care and Use Committee and the National Institutes of Health Guide for the Care and Use of Laboratory Animals.

Creation of Percutaneous Myocardial Infarction

Myocardial infarcts were created in Yorkshire pigs as previously published.(20) Briefly, animals were sedated with intramuscular telazol (6-8 mg/kg), followed by endotracheal intubation, mechanical ventilation, and anesthesia with isoflurane (1-2%, inhalation). An Amplatzer guide sheath (Boston Scientific, Marlborough, MA) was advanced via the right femoral artery to the aortic root and used to cannulate the left coronary artery. Over a BMW wire (Abbott Medical, Abbott Park, IL), a luminal angioplasty balloon (3 mm in diameter, Abbott Vascular, FoxCross PTA Catheter, Temecula, CA) was advanced into the mid-left anterior descending artery past the first diagonal branch, and 5 to 7 ml of microspheres (Polybead® 90.0μm, Polysciences, Inc. Warrington, PA) was injected through the lumen of the balloon after inflation of the balloon, figure 1. T wave inversions and ST segment elevation and/or depression were

noted on the surface electrocardiogram (ECG). Pigs were observed for 20-30 minutes with continuous ECG monitoring. External shocks (360 J) via paddles were delivered if the animal developed VT/VF. The animals were then extubated and monitored until they could ambulate without assistance.

Anesthesia and Surgical Preparation-Open chest procedures

Yorkshire pigs were sedated with intramuscular telazol (6-8 mg/kg), followed by endotracheal intubation, mechanical ventilation, and anesthesia with isoflurane (1-1.5%, inhalation). A bolus of fentanyl (2-5 mcg/kg) was given for analgesia prior to sternotomy and/or lateral neck cut-down. A surface 12 lead ECG was obtained via Prucka Cardio Lab System (GE Healthcare, Fairfield, CT). Arterial blood pressure was monitored via a 5F sheath in the femoral artery, and saline and medications were infused via a 5F sheath in the femoral vein. Arterial blood gas levels were measured hourly. The ventilator settings were adjusted or sodium bicarbonate administered to maintain acid-base homeostasis. After completion of surgical exposure, anesthetics were switched from isoflurane to α-chloralose (50 mg/kg initial bolus, subsequently 20-30 mg/kg/hr, continuous infusion), followed by stabilization period of one hour. Animals were euthanized by an overdose of intravenous anesthesia (sodium pentobarbital) followed by intravenous saturated potassium chloride to arrest the heart.

Acetylcholine Content Measurements

In 15 sham and 14 MI animals, ACh content was assessed. Bipolar epicardial voltage mapping (Prucka Cardiolab system and NAVX electroanatomic mapping system, St. Jude Medical) was performed in all infarcted hearts *in vivo* after sternotomy. Based on the epicardial voltage map results, areas of scar (voltage < 0.5 mV), border

zone (voltage 0.5-1.5 mV) and viable (voltage > 1.5 mV) were marked. These voltages have been previously validated and also are used in the clinical setting to delineate scar, border zone, and viable regions during catheter ablation of VT procedures in patients (21, 22). Border zone and scar regions are characterized by low voltage electrograms that often have prolonged duration or fractionation, and represent targets of catheter ablation in patients (23). These electrical characteristics were also observed in this porcine infarct model, figure 1a (20). Based on the bipolar voltage map, samples (3 mm in diameter punch biopsies) from scar, border zone, and viable regions were obtained and snap frozen at - 80°C. In addition, ACh content was measured from the LV apex, anterior, and lateral walls on the epicardium of 12 sham hearts (to evaluate regional changes that may be present, and given that in the infarcted hearts, these were the predominant regions affected by scar.) Finally, ACh content from paired epicardial vs. endocardial samples was also assessed in 9 control hearts to evaluate epicardial vs. endocardial differences.

Prior to analysis of ACh, the tissue was pulverized with a mortar and pestle chilled on dry ice, and aliquots of the pulverized tissue (5-20 mg) were homogenized in 300 µL of 0.1 M perchloric acid containing deuterated ACh (acetylcholine-1,1,2,2 d_4 chloride; 0.5 µM, CDN Isotopes, Quebec, Canada). A standard curve for ACh (Sigma-Aldrich, St. Louis, MO) was made up in the above homogenization solution with final ACh concentrations in the range of 0-500 nM. The homogenates were centrifuged and filtered through 0.22 µm filters before analysis by HPLC-MS. Samples were chromatographically separated on a Scherzo SS-C18 column (3 µm, Imtakt, Japan) using a gradient from 0-60% ammonium formate and acetonitrile (100 mM ammonium

formate/acetonitrile; 65/35) in 0.5% formic acid with a flow rate of 0.4 mL/min. The ACh was detected and quantified by a linear ion trap mass spectrometer (Applied Biosystems MDS SCIEX 4000 QTrap mass spectrometer, Carlsbad, CA) as previously described (24).

Neural Recording From Ventral Interventricular (VIV) Ganglionated Plexi

The VIV fat pad containing the VIV ganglia is readily accessed via a sternotomy and is located at the atrio-ventricular junction, beneath the left atrial appendage, figure 1. In 10 infarcted and 10 control hearts, a linear microelectrode array (MicroProbes, Gaithersburg, MD, USA) was placed in the VIV fat pad to record activity of these neurons *in vivo*. The microelectrode array consists of 16 platinum/iridium electrodes (25 μm diameter electrodes, 500 μm spacing; impedance 0.3-0.5 MΩ at 1 kHz), figure 1. The electrode wires, as well as ground and reference electrodes, were connected to a 16-channel microelectrode amplifier with a head-stage pre-amplifier (A-M Systems Inc., Model 3600, Carlsborg, WA, USA). Neuronal waveform (filter 300 Hz-3 KHz), ECG, and right atrial electrogram (obtained from a right atrial electrode) data were recorded continuously via a data acquisition system (Cambridge Electronic Design, Power1401, Cambridge, UK). Data analysis and signal processing was performed offline using the software Spike2 (Cambridge Electronic Design), as previously described (25).

Characterization and Classification of Parasympathetic Neurons

In order to determine which neurons receive parasympathetic efferent input, bipolar spiral cuff electrodes (Cyberonics Inc., PerenniaFlex Model 304, Houston, TX, USA) were placed around the bilateral cervical vagi after lateral neck cut-down. Right and left VNS were performed in a random order to identify parasympathetic neurons that

respond to either right or left VNS by either increasing or decreasing their firing frequency. Any increase or decrease in firing activity during stimulation compared to pre-stimulation was quantified in both infarcted and porcine hearts and used to identify parasympathetic neurons. Vagal nerve stimulation threshold was defined as the current that lead to a 10% decrease in heart rate (1 ms, 20Hz). Right and left VNS were each performed for one minute at 4Hz at this current, to avoid hemodynamic changes that may reflexively alter neuronal activity, and to measure neural activity independent of cardiac function. Basal activity of neurons that responded to right and/or left VNS was recorded for one minute prior to stimulation. The firing frequency (basal activity) of these in the minute prior to VNS was compared in infarcted and sham hearts. Based on this criterion, the basal activity of 58 control neurons and 34 MI neurons that increased their firing frequency with left VNS, and 61 control and 22 MI neurons that increased their firing activity with right VNS was analyzed. In addition, the basal activity of 95 control neurons and 20 MI neurons, whose activity was suppressed by left VNS, as well as 89 control neurons and 29 MI neurons, whose activity was suppressed by right VNS, was evaluated.

Electrophysiological Recordings, Analysis, and Assessment of Arrhythmia Inducibility during VNS

In 21 infarcted and 12 control animals, multiple unipolar epicardial electrograms were continuously obtained using a 56-electrode sock placed over the ventricles, *in vivo* (Prucka Cardio Lab System, GE Healthcare, Fairfield, CT). Location of each electrode was recorded and color coded, figure 1. In addition, in infarcted hearts, voltage and electroanatomic mapping using bipolar recordings was performed as described above,

and the location of each electrode lying over scar, border zone, or viable myocardium was meticulously noted. Activation recovery interval (ARI), a surrogate of action potential duration, was analyzed from unipolar electrograms of each electrode using iScaldyn (University of Utah, Salt Lake City, UT) (26-28). Briefly, activation time (AT) was defined from the origin to the minimum dV/dt of the activation wavefront of the unipolar electrogram and recovery time (RT) was defined as the start of activation to the maximum dV/dt of repolarization wavefront. ARI was then calculated by subtracting AT from RT. ARI has been shown to correlate well with local action potential duration (29, 30). In this manuscript, anterior refers to the ventral aspect and posterior refers to the dorsal aspect of the animal. Regional ARI (scar, viable, border zone) was quantified in 18 of 21 hearts. In 3 infarcted hearts, the epicardial scar was not large enough to allow for a minimum of 3 electrodes to have contact with scar regions for assessment of regional dispersion. Cardiac magnetic resonance imaging with delayed enhancement was obtained in 16 infarcted hearts *ex vivo*. Gadolinium was infused 20 minutes prior to euthanasia and removal of the heart. The images were used to further confirm location and extent of scar.

In control animals, regional ARI from LV apex, anterior, and lateral and right ventricular anterior wall was used for comparison to similar regions in infarcted hearts. The median number of electrodes in each region was 4 (range of 3-6). To qualitatively evaluate regional ARIs, polar maps were created from the sock electrode, figure 1.

Intermittent bilateral VNS (10 Hz, 1 ms, 15 s ON, 15 s OFF) in control and infarcted hearts was performed via lateral neck cut-down and placement of bipolar electrodes around the cervical vagi, as described above. The sympathetic chain was

also dissected in the neck and moved away from the stimulation electrodes. The current required to cause a 10% decrease in heart rate was defined as threshold, and stimulation was performed at 1.2x this current. ARI were continuously recorded before and during stimulation, and global ARI in addition to regional ARI compared in sham and infarcted hearts.

VT/VF inducibility was assessed before and during VNS using programmed ventricular stimulation (Micropace, EPS320, New South Wales, Australia) at two different cycle lengths, up to three extra stimuli (down to 200 ms or effective refractory period), from two different sites (right ventricular endocardium and LV anterior epicardium). If VT or VF was induced from one specific site at baseline, this same site was used to induce VT/VF during VNS.

Statistics

Data are reported as mean±SE. For comparison of regional ACh and ARI, linear mixed effects models, with a fixed region effect and a random animal effect was used and statistical significance assessed after applying the Benjamini-Hochberg procedure to control the false discovery rate at 5%. Dispersion in ARI was defined as the variance in the mean ARIs obtained from the electrodes of a particular region. For the response to VNS, the percent changes from baseline were calculated first, prior to comparing various regions. Paired t-test was use to compare changes from baseline for a specific region to VNS and for hemodynamic response to VNS. Unpaired student t-test was used to assess differences in stimulation threshold and basal neural activity in MI and control animals. Comparison of VT/VF inducibility pre and during VNS was performed using the McNemar's test.

RESULTS

ACh Content in Infarcted and Normal Hearts

Myocardial ACh content from scar, border zone, and viable regions was analyzed based on the bipolar voltage of each of these regions (figure 2). In normal hearts regional variations in Ach content, including LV epicardial and endocardial levels, and LV apex, LV anterior wall, and LV lateral wall were also evaluated. These specific regions were selected as the regional ACh content of the control tissue was then compared to the ACh content of the infarcted heart, where the infarct involved the LV apex, LV anterior wall, and LV lateral wall. There was no statistically significant difference in ACh levels across the LV epicardium in these regions, including the LV apex, anterior, and lateral walls (0.71±0.16 pmol/mg vs. 0.62±0.1 pmol/mg vs. 0.71±0.11 pmol/mg, respectively, P=0.2), figure 2b. Furthermore, there was no statistically significant difference between the ACh content of the epicardium and endocardium (0.73±0.14 pmol/mg vs. 0.73±0.12 pmol/mg, respectively, P=0.5), figure 2. In infarcted hearts, scar had the lowest level of ACh as compared to border zone and viable regions (figure 2d, $P<0.01$). Although the ACh content of scar regions was to some extent reduced compared to normal controls, this difference was not statistically significant (P=0.1). Therefore, the ACh content of the infarcted hearts was unchanged compared to controls.

Direct Neuronal Recordings From Cardiac Ganglia of Control and Infarcted Hearts

Given that the ACh levels in the myocardium of infarcted hearts were maintained, we then evaluated the activity of the efferent parasympathetic neurons in the intrinsic cardiac ganglia to discern differences in parasympathetic function of normal animals vs.

those with MI (n=10 in each group). The ventral interventricular (VIV) fat pad contains multiple ganglia that innervate the ventricular myocardium and can be classified as parasympathetic efferent neurons based on their response to right or left vagal nerve stimulation.(25) An increase or decrease in firing frequency of a recorded neuron in response to VNS is used to classify it as a parasympathetic efferent neuron (figure 3a and b). Basal activity of neurons that *increase* their firing frequency in response left VNS was reduced in infarcted compared to normal hearts (0.29±0.07 Hz vs. 0.14±0.03 Hz, respectively, P=0.03), figure 3c. Furthermore, the basal activity of neurons that *decrease* their firing in response to left VNS was increased in infarcted compared to control hearts (0.56±0.14 Hz vs. 0.29±0.07 Hz, respectively, P=0.04), figure 3d. No significant difference was found in the basal activity of neurons that increase (MI: 0.16±0.04 Hz vs. control: 0.21±0.4 Hz, P=0.4) or decrease their firing frequency to right VNS (MI: 0.47±0.06 Hz vs. control: 0.47±0.1 Hz, P=0.42). Therefore, neurons receiving inputs from the left vagal nerve demonstrated abnormal activity at baseline, with a decrease in activity of neurons that would be activated with parasympathetic stimulation and an increase in basal firing of neurons that would be suppressed with left VNS, suggesting a decrease in central parasympathetic drive, particularly through the left vagal trunk.

Electrophysiological Effects of Bilateral VNS in Control and Infarcted Hearts

Electrophysiological effects of VNS can be determined by simultaneous mapping and measurement of activation recovery intervals (ARI), a surrogate of local action potential duration, from multiple epicardial ventricular unipolar electrodes, without causing myocardial injury. Given that the central parasympathetic drive to the ganglia of

the heart appeared to be reduced in infarcted hearts, we hypothesized that restoring this drive with VNS may improve electrical stability of the infarcted heart, particularly in the absence of significant alterations in ACh levels. There was no difference in the stimulation current used in control and infarcted hearts (right VNS 2.4±0.3 mA vs. 2.2± 0.5 mA, P=0.6; left VNS 2.6±0.5 mA vs. 2.3±0.4 mA, respectively, P=0.6). Intermittent VNS decreased heart rate from 86±3.8 bpm to 71±2.5 bpm, systolic blood pressure from 123±6.5 mmHg to 113±7.1mmHg, and diastolic blood pressure from 92±5 mmHg to 79±6 mmHg in control animals, P<0.001 for all parameters. Global epicardial ARI obtained from unipolar electrograms (figure 4) increased from 336±13 ms to 354±15 ms (figure 4b, 5.4±1%, P=0.035), in control hearts. In infarcted animals, VNS decreased heart rate from 84±3 bpm to 70±3 bpm, systolic blood pressure from 112±6 mmHg to 99±6 mmHg, and diastolic blood pressure from 99±6 mmHg to 65±4 mmHg (P<0.001 for all parameters compare to baseline). Global epicardial ARI, calculated from all unipolar electrograms increased from 361±13 ms to 405±12 ms (13±2%, P<0.001), figure 4. The percentage change in global ARI in infarcted hearts was significantly greater than in normal hearts (P = 0.035), despite similar stimulation currents.

In infarcted hearts the scar had the greatest ARI at baseline (397±14 ms) as compared to border zone (380±14 ms) or viable myocardium (363±14 ms), P<0.01, figure 4d. VNS significantly increased ARI in all regions (scar by 9.7±11%, border zones by 14±3.5%, and viable myocardium by 12±3%, P<0.001 compared to baseline); however, border zone and viable regions showed a greater increase than scar regions, P<0.05, figure 4e. The greater response in border zone and viable regions likely improves the electrical stabilization of the peri-infarct areas, given that the scar had the

greatest ARI at baseline. When specifically comparing the anterior and lateral walls of the ventricles of normal hearts to the viable myocardium from similar regions in infarcted hearts, there was the suggestion of a greater increase in ARI in infarcted compared to control hearts, but this difference did not reach statistical significance (11±1.4% compared to 6.4±1.2%, P=0.1), figure 4e.

Inducibility of VT/VF was tested with programmed ventricular stimulation in infarcted hearts. At baseline, 12 of 21 (57%) of infarcted animals were inducible for VT/VF that required defibrillation. During intermittent VNS, only 5 of 21(23%) of these animals were inducible. There was one animal, however, that was non-inducible at baseline, and inducible with triple extra-stimuli during VNS. Overall, VNS significantly decreased inducibility of ventricular arrhythmias by 40% ($P<0.05$), figure 5.

Given the reduction in VT inducibility, the dispersion in ARI, or heterogeneity in repolarization in various regions of the infarcted myocardium was analyzed. At baseline, border zone regions showed the greatest dispersion in ARI 387±12ms^2 compared to scar (73±23 ms^2) and viable (160±25 ms^2) myocardium. During VNS, there was a significant reduction in ARI dispersion of border zone regions by 52% to 185±62 ms^2 ($P<0.01$), figure 5. Scar regions did not show a significant change in dispersion during VNS (69±26 ms^2, P=0.9), while there was suggestion of a mild increase in dispersion in viable regions from 160±25 ms^2 to 253±188 ms^2 (P=0.05).

DISCUSSION

In this study, we demonstrate that ACh levels in infarcted hearts remain preserved in the first 6 to 8 weeks after MI, while the efferent input, particularly from the left vagal

nerve, to the parasympathetic neurons in the VIV ganglia is reduced. Efferent neurons under left vagal control that should be highly “active” demonstrate low levels of neural firing, and those neurons that would be suppressed by parasympathetic outflow demonstrate a higher activity in infarcted compared to control hearts, suggesting a decrease in parasympathetic central drive. We also show the novel finding that restoring this drive via VNS can reduce VT/VF inducibility in the setting of a chronic MI, a finding that has important implications for patients with cardiomyopathy and recurrent ventricular tachycardia/defibrillator shocks. Finally, a novel mechanism behind the benefit of VNS is suggested by the decrease in dispersion of repolarization of border zone regions, which can potentially reduce risk of reentry.

The mechanism behind parasympathetic dysfunction and increased risk of sudden cardiac death in patients with cardiomyopathy is not clearly understood. In patients with heart failure, abnormal heart rate variability and baroreceptor sensitivity are manifestations of parasympathetic nervous system abnormality and increase risk of sudden cardiac death (3-7). The vago-sympathetic trunk, the primary highway of the parasympathetic nervous system, carries preganglionic efferent neural fibers from the brainstem (primarily the nucleus ambiguus and dorsal motor nucleus of the vagus) that synapse on the neurons of the intrinsic cardiac ganglia. The neurons of the intrinsic cardiac ganglia are an important processing center for the heart, responding to beat-by-beat changes in mechano-electrical function (25, 31, 32). The parasympathetic efferent neurons within these ganglia send post-ganglionic projections to the atrial and ventricular myocardium. The primary neurotransmitter of the parasympathetic nervous system is ACh. It has been shown that the intrinsic cardiac ganglia of the heart remodel

both structurally and functionally in response to myocardial infarction and pressure overload, with abnormal responses to simple interventions, such as a decrease in preload, compared to control hearts (33, 34). In this study, we demonstrate that the basal activity of efferent parasympathetic neurons in the VIV ganglionated plexus is altered by MI, and the change suggests that the vagal input to these neurons from the brainstem is reduced. In particular, we observed an alteration in activity of parasympathetic neurons that receive inputs from the left vagal trunk, and not the right vagal trunk. This may be due to the location of the infarct (the majority of the infarct involved the left ventricle) or the ganglia from which we recorded. Multiple ganglia provide innervation to the ventricular myocardium, and it is possible that if neural activity had been recorded from the dorsal ventricular fat pad of the heart, abnormal responses to right VNS may have also been noted. However, it is currently unknown what factors lead to the decrease in central parasympathetic drive observed in this study, particularly on the left side. Each vagal trunk also carries afferent fibers from the myocardium to the nuclear tractus solitarius (NTS) in the brainstem (35-37). The NTS provides input to both the dorsal motor nucleus and nucleus ambiguous,(38-44) where the efferent preganglionic vagal fibers originate (45, 46). Therefore, it is possible that a primarily left ventricular myocardial infarct would lead to a change in afferent sensory and mechanical neurotransmission through the left vagal trunk to the left NTS, that would then decrease parasympathetic efferent outflow to the heart from the dorsal motor nucleus and nucleus ambiguus on that side. It is known that very few fibers cross from the left NTS to the right NTS or from the ispislateral to the contralateral nucleus ambiguus,(42, 47) and therefore, a lack of change in the right vagal outflow is perhaps

not surprising. It is known, however, that both vagal trunks are needed to maintain a normal baseline parasympathetic tone, and transection of one trunk can have significant electrophysiological and hemodynamic effects in porcine and canine hearts (48, 49). Therefore, decreased parasympathetic outflow through the left vagus can have profound electrophysiological effects on the ventricular myocardium, particularly in the regions of the infarct.

Given that we found that ACh levels in infarcted hearts remained unchanged, and that the primary abnormality of efferent parasympathetic neurons was due to a decreased drive, we hypothesized that VNS would be able to suppress electrophysiological instability, or heterogeneity in ventricular repolarization, that leads to ventricular arrhythmias, reducing inducibility of VT/VF. Low to moderate levels of VNS have been shown to reduce ventricular arrhythmias due to myocardial ischemia (8, 11, 12, 16, 50-52). However, institution of VNS just prior to occurrence of ischemia is not clinically feasible. In this study, we demonstrate that moderate levels of VNS can reduce inducibility of ventricular arrhythmias in a chronically infarcted heart. This has important implications for patients with ischemic cardiomyopathy who have refractory ventricular arrhythmias. Approximately 30% of patients with cardiomyopathy and defibrillator shocks continue to experience arrhythmias and shocks despite medical therapy and catheter ablation procedures (17-19, 53). VNS represents a potential therapy that can now be used far after the occurrence of myocardial infarction, to reduce these arrhythmias.

Ventricular arrhythmias in infarcted hearts are thought to occur due to changes in conduction velocity as well as differences in regional action potential duration, setting up

the substrate for reentry (54-58). In this study, we found that the regions with the greatest heterogeneity in ARI were the border zone regions around the infarct. It is known that these areas can serve as highly arrhythmogenic foci, where complex intertwining of variable amounts of viable myocardium and fibrosis is observed (57, 59). Our study demonstrates that intermittent VNS significantly reduced the dispersion or heterogeneity in ARI of these areas, providing a novel mechanism for the reduction in arrhythmias observed.

Surprisingly, we found that the increase in global ARI of infarcted hearts was greater than in normal hearts. Given the decrease in central drive, this increase in response may be due to up-regulation of muscarinic receptors in the heart. Although an increase in receptor density has not been evaluated in ischemic cardiomyopathy, in a guinea pig model of pacing induced heart failure, M2 receptors have been shown to be up-regulated, and VNS is able to normalize these receptor levels (60).

The decreased electrical response to VNS in scar regions compared to border zone and viable myocardium is not surprising, given that MI is known to damage nerve fibers within the scar, although the neural cell bodies in the ganglia remain primarily intact. The reduction in nerve fibers would explain both the decrease in ACh levels as well as the decreased electrophysiological response to VNS in the scar compared to border zone and viable regions. However, it was surprising that even in the scar, ACh levels and response to VNS, although reduced, were not significantly different from similar normal regions in control hearts. This finding points to the dramatic impact that the change in the activity of parasympathetic efferent neurons of the cardiac ganglia has on the myocardium, and the profound effects VNS can, therefore, have in restoring

electrical stability to the injured heart. Future studies using neural recordings from the NTS are warranted to further understand the mechanisms underlying the decrease in central parasympathetic drive.

REFERENCES

1. Vaseghi M, and Shivkumar K. The role of the autonomic nervous system in sudden cardiac death. *Progress in cardiovascular diseases.* 2008;50:404-19.
2. Zipes DP, and Rubart M. Neural modulation of cardiac arrhythmias and sudden cardiac death. *Heart Rhythm.* 2006;3:108-13.
3. Farrell TG, Bashir Y, Cripps T, Malik M, Poloniecki J, Bennett ED, Ward DE, and Camm AJ. Risk stratification for arrhythmic events in postinfarction patients based on heart rate variability, ambulatory electrocardiographic variables and the signal-averaged electrocardiogram. *J Am Coll Cardiol.* 1991;18:687-97.
4. Farrell TG, Paul V, Cripps TR, Malik M, Bennett ED, Ward D, and Camm AJ. Baroreflex sensitivity and electrophysiological correlates in patients after acute myocardial infarction. *Circulation.* 1991;83:945-52.
5. Hull SS, Jr., Evans AR, Vanoli E, Adamson PB, Stramba-Badiale M, Albert DE, Foreman RD, and Schwartz PJ. Heart rate variability before and after myocardial infarction in conscious dogs at high and low risk of sudden death. *J Am Coll Cardiol.* 1990;16:978-85.
6. Kleiger RE, Miller JP, Bigger JT, Jr., and Moss AJ. Decreased heart rate variability and its association with increased mortality after acute myocardial infarction. *Am J Cardiol.* 1987;59:256-62.
7. La Rovere MT, Bigger JT, Jr., Marcus FI, Mortara A, and Schwartz PJ. Baroreflex sensitivity and heart-rate variability in prediction of total cardiac mortality after myocardial infarction. ATRAMI (Autonomic Tone and Reflexes After Myocardial Infarction) Investigators. *Lancet.* 1998;351:478-84.

8. Ando M, Katare RG, Kakinuma Y, Zhang D, Yamasaki F, Muramoto K, and Sato T. Efferent vagal nerve stimulation protects heart against ischemia-induced arrhythmias by preserving connexin43 protein. *Circulation.* 2005;112:164-70.

9. Kent KM, Smith ER, Redwood DR, and Epstein SE. Electrical Stability of Acutely Ischemic Myocardium: Influences of Heart Rate and Vagal Stimulation. *Circulation.* 1973;47:291-8.

10. Kolman BS, Verrier RL, and Lown B. The effect of vagus nerve stimulation upon vulnerability of the canine ventricle: role of sympathetic-parasympathetic interactions. *Circulation.* 1975;52:578-85.

11. Myers RW, Pearlman AS, Hyman RM, Goldstein RA, Kent KM, Goldstein RE, and Epstein SE. Beneficial Effects of Vagal Stimulation and Bradycardia During Experimental Acute Myocardial Ischemia. *Circulation.* 1974;49:943-7.

12. Rosenshtraukh L, Danilo P, Anyukhovsky EP, Steinberg SF, Rybin V, Brittain-Valenti K, Molina-Viamonte V, and Rosen MR. Mechanisms for vagal modulation of ventricular repolarization and of coronary occlusion-induced lethal arrhythmias in cats. *Circulation Research.* 1994;75:722-32.

13. Scherlag BJ, Helfant RH, Haft JI, and Damato AN. Electrophysiology underlying ventricular arrhythmias due to coronary ligation. *Am J Physiol.* 1970;219:1665-71.

14. Takahashi N, Ito M, Iwao T, Ohie T, Yonemochi H, Nakagawa M, Saikawa T, and Sakata T. Vagal modulation of ventricular tachyarrhythmias induced by left ansae subclaviae stimulation in rabbits. *Jpn Heart J.* 1998;39:503-11.

15. Vanoli E, De Ferrari GM, Stramba-Badiale M, Hull SS, Foreman RD, and Schwartz PJ. Vagal stimulation and prevention of sudden death in conscious dogs with a healed myocardial infarction. *Circulation Research.* 1991;68:1471-81.

16. Yoon MS, Han J, Tse WW, and Rogers R. Effects of vagal stimulation, atropine, and propranolol on fibrillation threshold of normal and ischemic ventricles. *Am Heart J.* 1977;93:60-5.

17. Dukkipati SR, d'Avila A, Soejima K, Bala R, Inada K, Singh S, Stevenson WG, Marchlinski FE, and Reddy VY. Long-term outcomes of combined epicardial and endocardial ablation of monomorphic ventricular tachycardia related to hypertrophic cardiomyopathy. *Circ Arrhythm Electrophysiol.* 2011;4:185-94.

18. Kuck KH, Schaumann A, Eckardt L, Willems S, Ventura R, Delacretaz E, Pitschner HF, Kautzner J, Schumacher B, Hansen PS, et al. Catheter ablation of stable ventricular tachycardia before defibrillator implantation in patients with coronary heart disease (VTACH): a multicentre randomised controlled trial. *Lancet.* 2010;375:31-40.

19. Mathuria N, Tung R, and Shivkumar K. Advances in ablation of ventricular tachycardia in nonischemic cardiomyopathy. *Curr Cardiol Rep.* 2012;14:577-83.

20. Nakahara S, Vaseghi M, Ramirez RJ, Fonseca CG, Lai CK, Finn JP, Mahajan A, Boyle NG, and Shivkumar K. Characterization of myocardial scars: electrophysiological imaging correlates in a porcine infarct model. *Heart Rhythm.* 2011;8:1060-7.

21. Cesario DA, Vaseghi M, Boyle NG, Fishbein MC, Valderrabano M, Narasimhan C, Wiener I, and Shivkumar K. Value of high-density endocardial and epicardial mapping for catheter ablation of hemodynamically unstable ventricular tachycardia. *Heart Rhythm.* 2006;3:1-10.

22. Marchlinski FE, Callans DJ, Gottlieb CD, and Zado E. Linear ablation lesions for control of unmappable ventricular tachycardia in patients with ischemic and nonischemic cardiomyopathy. *Circulation.* 2000;101:1288-96.

23. Harada T, Stevenson WG, Kocovic DZ, and Friedman PL. Catheter ablation of ventricular tachycardia after myocardial infarction: relation of endocardial sinus rhythm late potentials to the reentry circuit. *J Am Coll Cardiol.* 1997;30:1015-23.

24. Hasan W, Woodward WR, and Habecker BA. Altered atrial neurotransmitter release in transgenic p75(-/-) and gp130 KO mice. *Neurosci Lett.* 2012;529:55-9.

25. Beaumont E, Salavatian S, Southerland EM, Vinet A, Jacquemet V, Armour JA, and Ardell JL. Network interactions within the canine intrinsic cardiac nervous system: implications for reflex control of regional cardiac function. *J Physiol.* 2013;591:4515-33.

26. Vaseghi M, Lux RL, Mahajan A, and Shivkumar K. Sympathetic stimulation increases dispersion of repolarization in humans with myocardial infarction. *Am J Physiol Heart Circ Physiol.* 2012;302:H1838-46.

27. Yagishita D, Chui RW, Yamakawa K, Rajendran PS, Ajijola OA, Nakamura K, So EL, Mahajan A, Shivkumar K, and Vaseghi M. Sympathetic nerve stimulation, not circulating norepinephrine, modulates T-peak to T-end interval by increasing

global dispersion of repolarization. *Circulation Arrhythmia and electrophysiology.* 2015;8:174-85.

28. Yamakawa K, So EL, Rajendran PS, Hoang JD, Makkar N, Mahajan A, Shivkumar K, and Vaseghi M. Electrophysiological effects of right and left vagal nerve stimulation on the ventricular myocardium. *Am J Physiol Heart Circ Physiol.* 2014;307:H722-31.
29. Haws CW, and Lux RL. Correlation between in vivo transmembrane action potential durations and activation-recovery intervals from electrograms. Effects of interventions that alter repolarization time. *Circulation.* 1990;81:281-8.
30. Millar CK, Kralios FA, and Lux RL. Correlation between refractory periods and activation-recovery intervals from electrograms: effects of rate and adrenergic interventions. *Circulation.* 1985;72:1372-9.
31. Armour JA. Potential clinical relevance of the 'little brain' on the mammalian heart. *Exp Physiol.* 2008;93:165-76.
32. Huang MH, Sylven C, Pelleg A, Smith FM, and Armour JA. Modulation of in situ canine intrinsic cardiac neuronal activity by locally applied adenosine, ATP, or analogues. *Am J Physiol.* 1993;265:R914-22.
33. Hardwick JC, Ryan SE, Beaumont E, Ardell JL, and Southerland EM. Dynamic remodeling of the guinea pig intrinsic cardiac plexus induced by chronic myocardial infarction. *Auton Neurosci.* 2014;181:4-12.
34. Rajendran PS, Nakamura K, Ajijola OA, Vaseghi M, Armour JA, Ardell JL, and Shivkumar K. Myocardial infarction induces structural and functional remodeling of the intrinsic cardiac nervous system. *J Physiol.* 2016;594:321-41.

35. Janig W. In: W. J ed. *The Integrative Action of the Autonomic Nervous System: Neurobiology of Homeostasis* Cambridge: Cambridge University Press; 2006:13-34.

36. Hoover DB, Shepherd AV, Southerland EM, Armour JA, and Ardell JL. Neurochemical diversity of afferent neurons that transduce sensory signals from dog ventricular myocardium. *Auton Neurosci.* 2008;141:38-45.

37. Prechtl JC, and Powley TL. The fiber composition of the abdominal vagus of the rat. *Anat Embryol (Berl).* 1990;181:101-15.

38. Loewy AD, and Burton H. Nuclei of the solitary tract: efferent projections to the lower brain stem and spinal cord of the cat. *J Comp Neurol.* 1978;181:421-49.

39. Morest DK. Experimental study of the projections of the nucleus of the tractus solitarius and the area postrema in the cat. *J Comp Neurol.* 1967;130:277-300.

40. Norgren R. Projections from the nucleus of the solitary tract in the rat. *Neuroscience.* 1978;3:207-18.

41. Ricardo JA, and Koh ET. Anatomical evidence of direct projections from the nucleus of the solitary tract to the hypothalamus, amygdala, and other forebrain structures in the rat. *Brain Res.* 1978;153:1-26.

42. Stuesse SL, and Fish SE. Projections to the cardioinhibitory region of the nucleus ambiguus of rat. *J Comp Neurol.* 1984;229:271-8.

43. Travers JB, and Norgren R. Afferent projections to the oral motor nuclei in the rat. *J Comp Neurol.* 1983;220:280-98.

44. Warren Cottle MK, and Calaresu FR. Projections from the nucleus and tractus solitarius in the cat. *J Comp Neurol.* 1975;161:143-57.

45. Kalia M, and Sullivan JM. Brainstem projections of sensory and motor components of the vagus nerve in the rat. *J Comp Neurol.* 1982;211:248-65.

46. Standish A, Enquist LW, and Schwaber JS. Innervation of the heart and its central medullary origin defined by viral tracing. *Science.* 1994;263:232-4.

47. Amendt K, Czachurski J, Dembowsky K, and Seller H. Bulbospinal projections to the intermediolateral cell column: a neuroanatomical study. *J Auton Nerv Syst.* 1979;1:103-7.

48. Yamakawa K, Rajendran PS, Takamiya T, Yagishita D, So EL, Mahajan A, Shivkumar K, and Vaseghi M. Vagal nerve stimulation activates vagal afferent fibers that reduce cardiac efferent parasympathetic effects. *Am J Physiol Heart Circ Physiol.* 2015;309:H1579-90.

49. Ardell JL, Rajendran PS, Nier HA, KenKnight BH, and Armour JA. Central-peripheral neural network interactions evoked by vagus nerve stimulation: functional consequences on control of cardiac function. *Am J Physiol Heart Circ Physiol.* 2015;309:H1740-52.

50. Kent KM, Smith ER, Redwood DR, and Epstein SE. Electrical stability of acutely ischemic myocardium. Influences of heart rate and vagal stimulation. *Circulation.* 1973;47:291-8.

51. Zuanetti G, De Ferrari GM, Priori SG, and Schwartz PJ. Protective effect of vagal stimulation on reperfusion arrhythmias in cats. *Circ Res.* 1987;61:429-35.

52. Huang WA, Shivkumar K, and Vaseghi M. Device-based autonomic modulation in arrhythmia patients: the role of vagal nerve stimulation. *Curr Treat Options Cardiovasc Med.* 2015;17:379.

53. Calkins H, Epstein A, Packer D, Arria AM, Hummel J, Gilligan DM, Trusso J, Carlson M, Luceri R, Kopelman H, et al. Catheter ablation of ventricular tachycardia in patients with structural heart disease using cooled radiofrequency energy: results of a prospective multicenter study. Cooled RF Multi Center Investigators Group. *J Am Coll Cardiol.* 2000;35:1905-14.

54. Allessie MA, Bonke FI, and Schopman FJ. Circus movement in rabbit atrial muscle as a mechanism of tachycardia. II. The role of nonuniform recovery of excitability in the occurrence of unidirectional block, as studied with multiple microelectrodes. *Circ Res.* 1976;39:168-77.

55. Baker LC, London B, Choi BR, Koren G, and Salama G. Enhanced dispersion of repolarization and refractoriness in transgenic mouse hearts promotes reentrant ventricular tachycardia. *Circ Res.* 2000;86:396-407.

56. Kuo CS, Munakata K, Reddy CP, and Surawicz B. Characteristics and possible mechanism of ventricular arrhythmia dependent on the dispersion of action potential durations. *Circulation.* 1983;67:1356-67.

57. Wit AL, Allessie MA, Bonke FI, Lammers W, Smeets J, and Fenoglio JJ, Jr. Electrophysiologic mapping to determine the mechanism of experimental ventricular tachycardia initiated by premature impulses. Experimental approach and initial results demonstrating reentrant excitation. *Am J Cardiol.* 1982;49:166-85.

58. de Bakker JM, van Capelle FJ, Janse MJ, Tasseron S, Vermeulen JT, de Jonge N, and Lahpor JR. Slow conduction in the infarcted human heart. 'Zigzag' course of activation. *Circulation.* 1993;88:915-26.

59. Rutherford SL, Trew ML, Sands GB, LeGrice IJ, and Smaill BH. High-resolution 3-dimensional reconstruction of the infarct border zone: impact of structural remodeling on electrical activation. *Circ Res.* 2012;111:301-11.

60. DeMazumder D, Kass DA, O'Rourke B, and Tomaselli GF. Cardiac resynchronization therapy restores sympathovagal balance in the failing heart by differential remodeling of cholinergic signaling. *Circ Res.* 2015;116:1691-9.

Figure 1. Creation of porcine myocardial infarct, neural and electrical recordings. (a) Myocardial infarction in the porcine heart is created percutaneously under fluoroscopic guidance. A percutaneous angioplasty balloon (PTCA) is used to occlude the left anterior descending artery (LAD) prior to injection of microspheres though the lumen of the balloon. (b) 6-8 weeks after MI, when the infarct has matured, the chest is opened and the antertoapical infarct identified. (c) The vagal trunk is dissected from the sympathetic chain via a lateral cutdown and bipolar electrodes are used for stimulation of the trunk. (d) The VIV fat pad sits below the left atrial appendage, at the junction of the atrio-ventricular groove and a 16 electrode LMA is inserted in this fat pad for neural recordings. (e) A 56 electrode sock is placed over the heart for unipolar electrical recordings and location of electordes are noted. (f) At the end of the procedure, the location and extent of scar is confirmed with cardiac magnetic resonance imaging *ex vivo*. (g) A template of the polar map of the sock with the location of the electrode relative to the LAD, used to qualitatively assess regional electrical signals, is shown

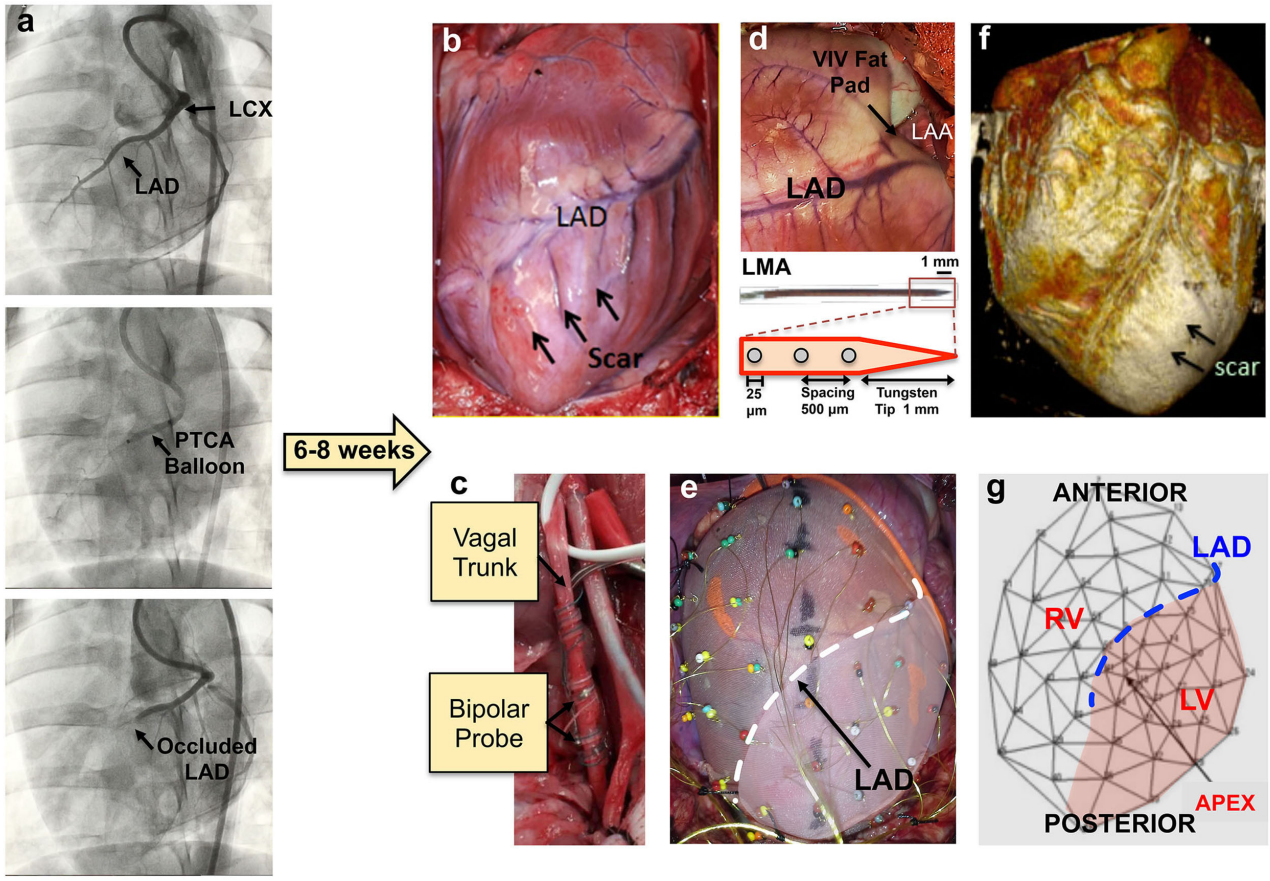
a
LCX
LAD
PTCA Balloon
Occluded LAD
6-8 weeks
b
LAD
Scar
d
VIV Fat Pad
LAA
LAD
LMA
1 mm
25 µm
Spacing 500 µm
Tungsten Tip 1 mm
f
scar
c
Vagal Trunk
Bipolar Probe
e
LAD
g
ANTERIOR
LAD
RV
LV
APEX
POSTERIOR

.

Figure 2. Cardiac voltage mapping and ACh analysis. (a) A bipolar voltage electroanatomic map of infarcted hearts was obtained and used to identify viable, border zone, and scar regions by their electrogram voltage. Examples of bipolar electrical recordings from viable, border zone, and scar regions are shown. Examples of uinpolar electrograms obtained from similar regions are also shown. This map and bipolar voltage measurements were used to obtain samples for ACh analysis from appropriate locations. The scale bar shows the voltage from 0-10 mV (b) In sham hearts (n=12), ACh levels were not significnatly different on the LV apex, anterior, lateral walls using a mixed effect model (c) ACh levels from paired LV epicardium and endocardium samples obtained from 9 different sham animals were also not siginificantly different using Student's paired t-test. (d) In infarcted hearts (n=14), scar regions have the lowest ACh content compared to viable and border zone regions ($P<0.01$, linear mixed effects model). However, the ACh content between viable and border zone regions compared to control regions of sham hearts (n=15) was not statistically significant ($P = 0.4$ linear mixed effects model). There is a suggestion that the scar ACh may be somewhat reduced compared to sham hearts, however, this difference did not reach statistical significance, implying that overall, ACh levels are preserved in the setting of MI.

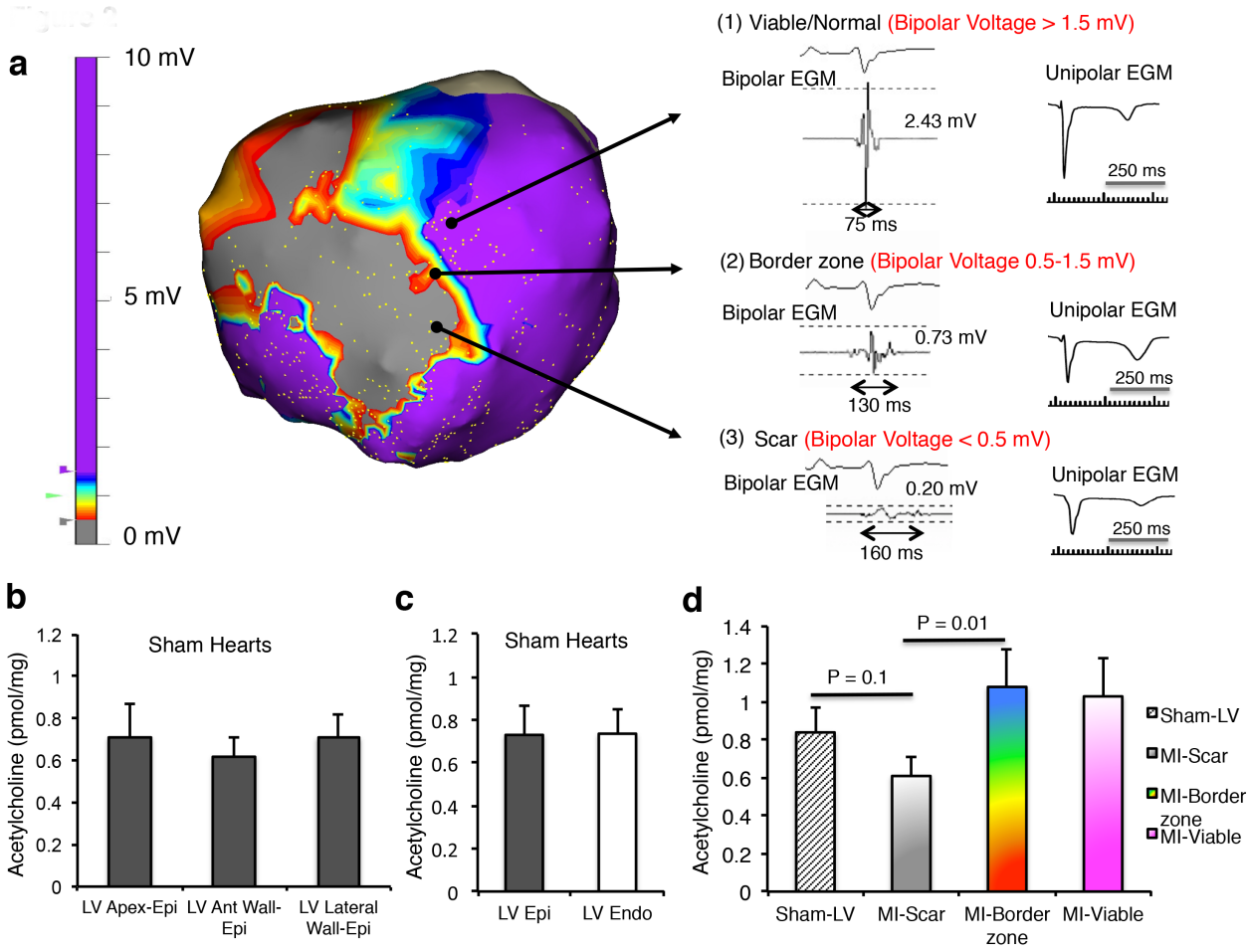
a
10 mV
5 mV
0 mV
(1) Viable/Normal (Bipolar Voltage > 1.5 mV)
Bipolar EGM
2.43 mV
75 ms
Unipolar EGM
250 ms
(2) Border zone (Bipolar Voltage 0.5-1.5 mV)
Bipolar EGM
0.73 mV
130 ms
Unipolar EGM
250 ms
(3) Scar (Bipolar Voltage < 0.5 mV)
Bipolar EGM
0.20 mV
160 ms
Unipolar EGM
250 ms
b
Sham Hearts
Acetylcholine (pmol/mg)
LV Apex-Epi
LV Ant Wall-Epi
LV Lateral Wall-Epi
c
Sham Hearts
Acetylcholine (pmol/mg)
LV Epi
LV Endo
d
P = 0.01
P = 0.1
Acetylcholine (pmol/mg)
Sham-LV
MI-Scar
MI-Border zone
MI-Viable

Figure 3. Direct neural recording from intrinsic cardiac ganglion neurons. (a) Examples of neural recordings obtained from the VIV fat pad ganglia of a control heart showing two neurons that increased their firing activity with VNS, and were therefore, classified as post-ganglionic parasympathetic neurons. Each neuron was also identified and classifed by its neural waveform (inset). (b) Example of neural recordings obtained from the VIV fat pad ganglia of an infarcted heart demonstrating two neurons that also icnreased their firing frequency with VNS. The basal activity in the minute prior to VNS compared to during VNS was used to identify efferent parasympatehtic neurons. (c) The *basal* (pre-stimulation) activity of parasympathetic neurons that were *activated* by VNS, and therefore, increased their firing with right or left VNS is shown. Note that the basal activity of these types of neurons in response to left VNS is reduced in MI compared to control hearts ($P<0.05$, unpaired Students t-test). The basal activity of neurons that respond to right VNS is unchanged in control vs. infarcted hearts (d) The *basal* (pre-stimulation) activity of neurons in the VIV fat pad ganglia that were *suppressed* by VNS, and therefore, decreased their firing with right or left VNS is shown. Note that basal activity of these types of neurons in response to left VNS is increased in infarcted compared to control hearts ($P<0.05$, unpaired Student's t-test). The basal activity of neurons that respond to right VNS is unchanged in control vs. infarcted hearts. * $P<0.05$, n = number of total neurons recorded for each condition. VIV = ventral interventricular, MI = myocardial infarction, RVNS = right vagal nerve stimulation, LVNS = left vagal nerve stimulation.

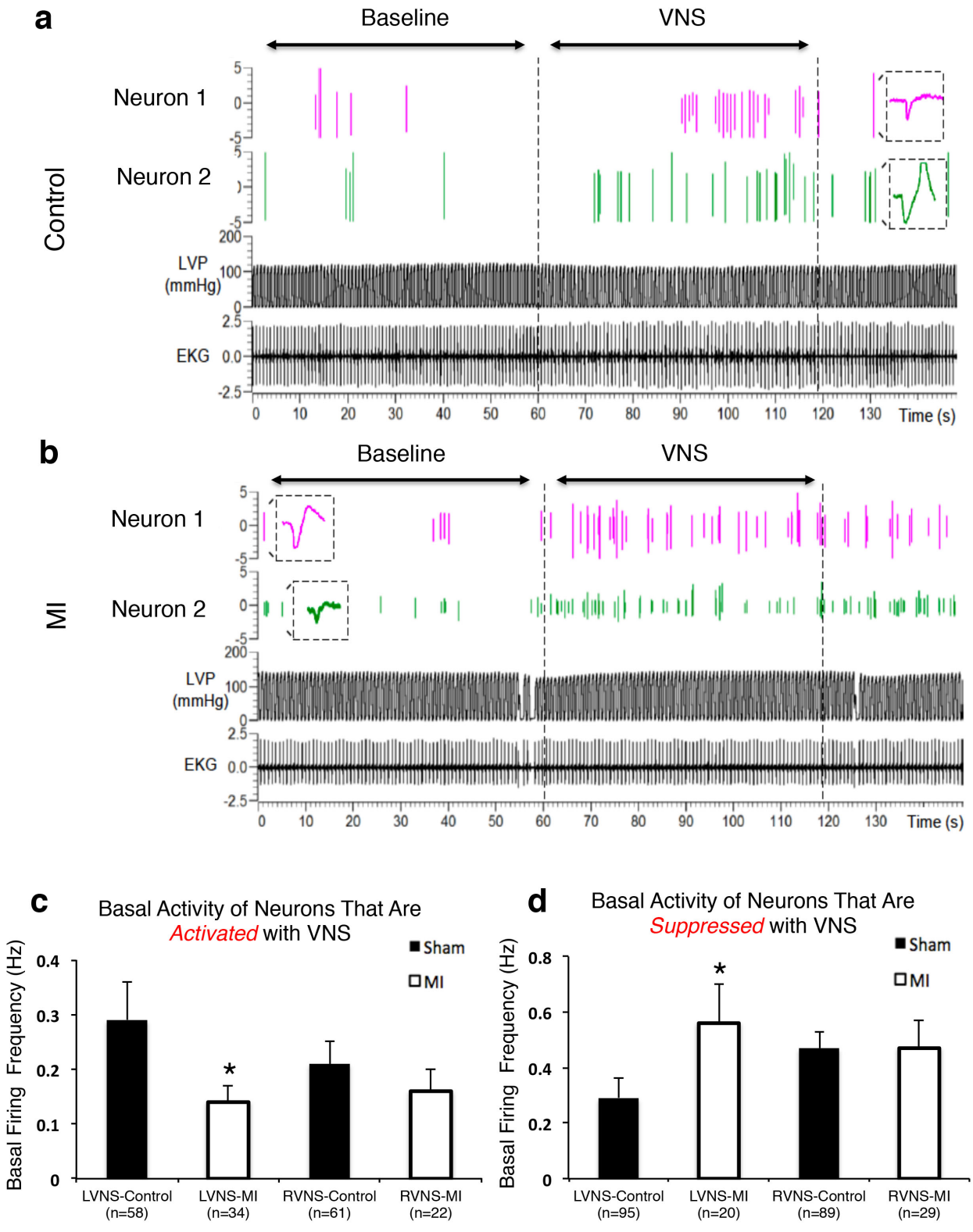
a
Baseline
VNS
Neuron 1
Neuron 2
Control
LVP (mmHg)
EKG
Time (s)
b
Baseline
VNS
Neuron 1
Neuron 2
MI
LVP (mmHg)
EKG
Time (s)
c
Basal Activity of Neurons That Are Activated with VNS
Sham
MI
Basal Firing Frequency (Hz)
LVNS-Control (n=58)
LVNS-MI (n=34)
RVNS-Control (n=61)
RVNS-MI (n=22)
d
Basal Activity of Neurons That Are Suppressed with VNS
Sham
MI
Basal Firing Frequency (Hz)
LVNS-Control (n=95)
LVNS-MI (n=20)
RVNS-Control (n=89)
RVNS-MI (n=29)

Figure 4. ARI analysis in control and infarcted hearts. (a) Examples of unipolar electrograms obtained from the sock electrode and used for ARI analysis from sham hearts and from viable, border zone, and scar regions of infarcted hearts are shown. (b) The global ARI (mean ARI from all 56-sock electrodes) in control animals (n=12) significantly increased with VNS (left panel). An example of regional changes with VNS is shown with polar maps (right panel) from one animal at baseline and during VNS. In the control heart, all regions increase their mean ARI similarly with VNS (* $P<0.05$, Wilcoxon signed rank test was used for analysis of global ARI). (c) The global ARI (mean ARI from all 56-sock electrodes) in infarcted hearts (n=18) significantly increased with VNS (left panel, Wilcoxon signed rank test). An example of a polar maps obtained from one infarcted animal is shown (right panel). In infarcted hearts, VNS has a significant impact on regional ARIs, particularly noticeable along peri-infarct regions (the apex and location of the scar is marked with dashed lines on the cardiac polar maps of this animal with MI) (* $P<0.01$). (d) Scar regions, at baseline, demonstrated the greatest mean ARI (** $P<0.001$) in infarcted hearts (n=18) in the linear mixed effects model. In addition, all regions, even scar, demonstrate a significant increase in mean ARI from baseline (* $P<0.01$, linear mixed effects model). (e) When the percentage increase in ARI with VNS is compared across various regions in infarcted hearts using the linear mixed effects model, consistent with the ACh findings, the scar shows the least response compared to viable and border zone regions (§ $P<0.01$). However, as the with the ACh analysis, there was no statistical difference in the response to VNS of scar compared to control hearts (¥ $P=0.1$).

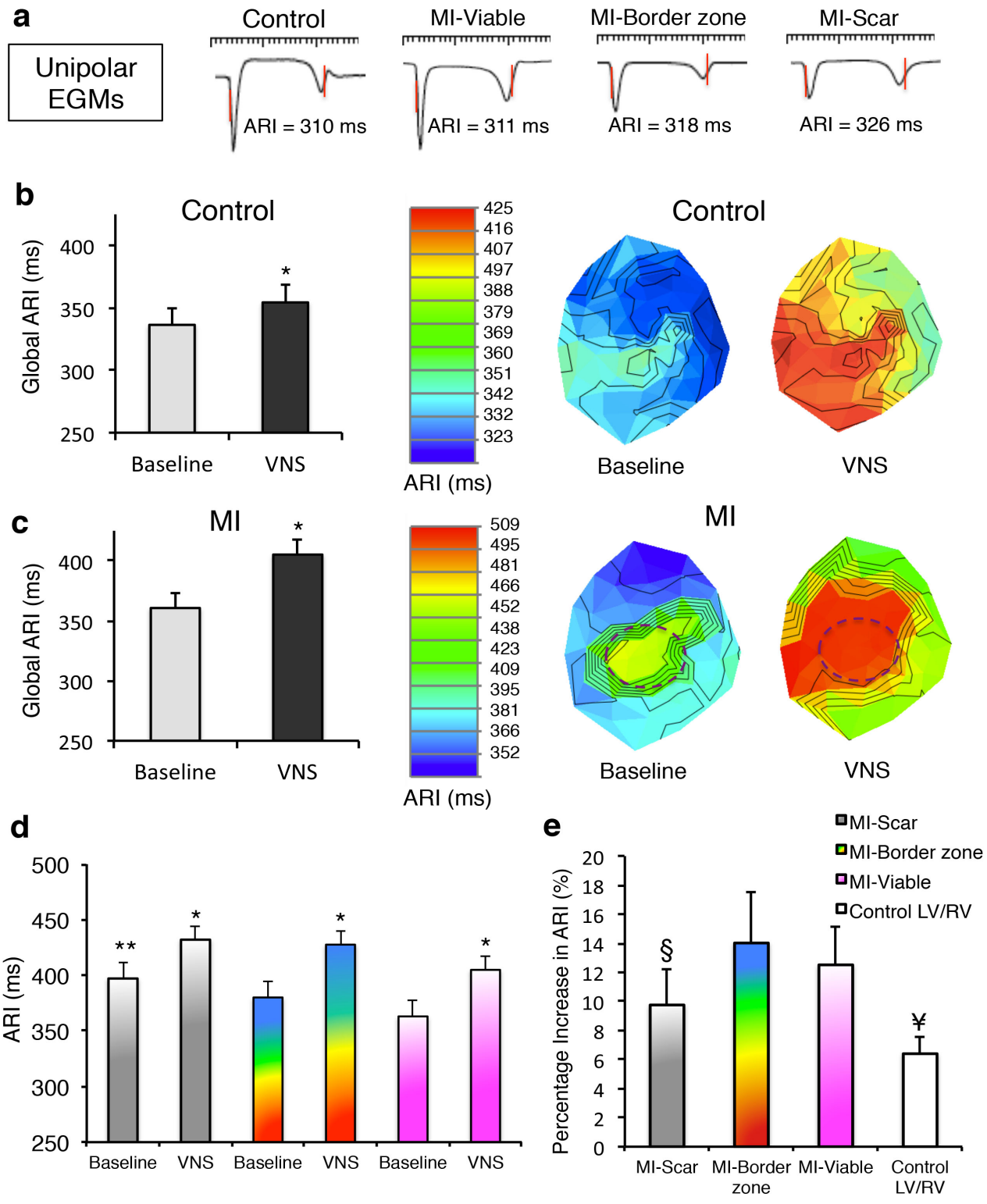
a
Unipolar EGMs
Control
MI-Viable
MI-Border zone
MI-Scar
ARI = 310 ms
ARI = 311 ms
ARI = 318 ms
ARI = 326 ms
b
Control
Global ARI (ms)
400
350
300
250
*
Baseline
VNS
425
416
407
497
388
379
369
360
351
342
332
323
ARI (ms)
Control
Baseline
VNS
c
MI
Global ARI (ms)
400
350
300
250
*
Baseline
VNS
509
495
481
466
452
438
423
409
395
381
366
352
ARI (ms)
MI
Baseline
VNS
d
ARI (ms)
500
450
400
350
300
250
**
*
*
*
Baseline
VNS
Baseline
VNS
Baseline
VNS
e
MI-Scar
MI-Border zone
MI-Viable
Control LV/RV
Percentage Increase in ARI (%)
20
18
16
14
12
10
8
6
4
2
0
§
¥
MI-Scar
MI-Border zone
MI-Viable
Control LV/RV

Figure 5. Arrhythmia inducibility and effects of VNS on dispersion of repolarization. (a) An example of VT/VF induction using extra-stimulus pacing from the RV endocardium is shown. Prior to VNS, this infarcted animal is inducible for VT, which degenerated into VF and required defibrillation. During intermittent VNS, VT/VF is no longer inducible with triple extra-stimuli, and effective refractory period is reached (as demonstrated by the lack of ventricular capture at the pacing stimulus artifact). Four surface leads from the ECG and 3 electrodes from the sock are shown. (b) Intermittent VNS significantly reduced the proportion of animals that were inducible for VT/VF (n=21, $P<0.04$, McNemar's test). (c) The dispersion in ARI at baseline and during VNS is shown across scar, border zone, and viable regions in infarcted hearts (n=18). Regional analysis using the linear mixed effect model showed that the dispersion in ARI in border zone regions was large and greater than scar regions (* $P<0.05$) at baseline. (d) Intermittent VNS significantly reduced the dispersion in ARI of border zone regions compared to scar and viable areas (* $P<0.01$, linear mixed effects model).

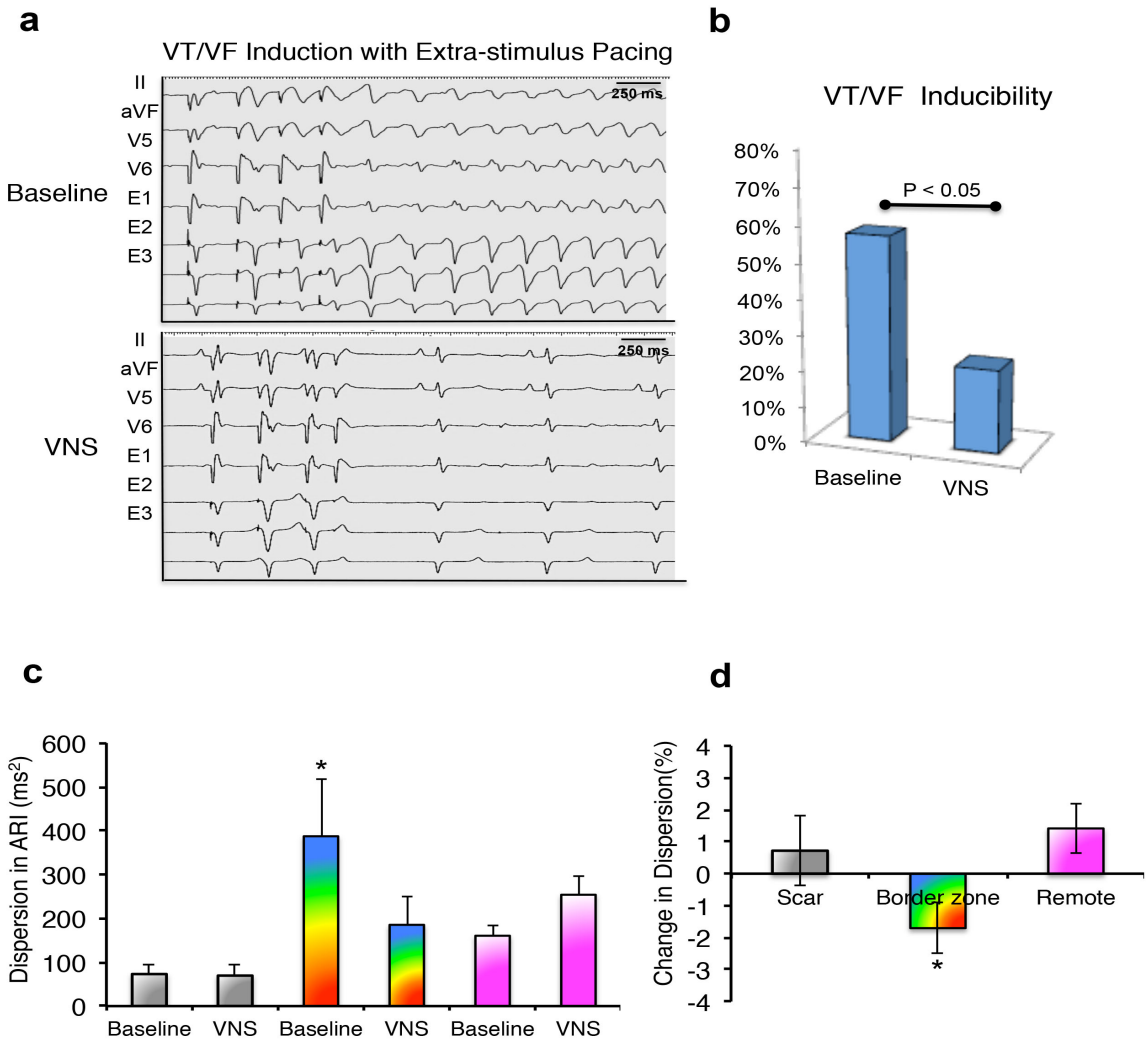
a
VT/VF Induction with Extra-stimulus Pacing
Baseline
VNS
II
aVF
V5
V6
E1
E2
E3
250 ms
b
VT/VF Inducibility
P < 0.05
80%
70%
60%
50%
40%
30%
20%
10%
0%
Baseline
VNS
c
Dispersion in ARI (ms2)
600
500
400
300
200
100
0
Baseline
VNS
Baseline
VNS
Baseline
VNS
d
Change in Dispersion(%)
4
3
2
1
0
-1
-2
-3
-4
Scar
Border zone
Remote

CHAPTER 5

CONCLUSIONS, INTERPRETATIONS, AND FUTURE DIRECTIONS

CONCLUSIONS

The major findings of this dissertation are that both the right and left vagal trunk provide significant parasympathetic pre-ganglionic cardiomotor fibers that affect the electrophysiological and mechanical function of the ventricular myocardium. These effects include increases in regional action potential duration, a decrease in ionotropy, an increase in lusitropy, and a decrease in chronotropy. The effects of right and left vagal nerve stimulation tend to be homogenous across different regions of the ventricle, although small but notable differences between apex and base, as well as endocardium and epicardial action potential durations are observed. Activation of afferent fibers of the stimulated vagal trunk inhibits the cardiomotor efferent effects of vagal nerve stimulation. Finally, significant parasympathetic neural remodeling occurs as a result of myocardial infarction, despite adequate myocardial acetylcholine neurotransmitter levels, suggesting a decrease in central parasympathetic drive. This decrease in drive leads to abnormal activity of parasympathetic neurons of the intrinsic cardiac ganglia. Increasing this drive with vagal nerve stimulation results in reduced inducibility of ventricular arrhythmias in the setting of myocardial infarction by improving the dispersion of repolarization of border zone regions. Border zone areas are known for their pro-arrhythmic potential and electrical stabilization of these regions could have a significant impact on genesis and persistent of ventricular tachy-arrhythmias. This mechanism explains the anti-arrhythmics effects of VNS acutely in an infarcted heart, which up to now, could not have been explained by previously proposed mechanisms such as changes in connexin 43 levels or inflammatory markers, which would require a greater period of time to develop.

INTERPRETATIONS

Efferent and Afferent Parasympathetic Neurotransmission

The histological, electrical, and mechanical evidence of ventricular parasympathetic innervation by the right and left vagal trunk are no longer debatable in normal hearts. Kawano showed histological evidence of parasympathetic nerve fibers in human hearts (1), and these studies have subsequently been confirmed in guinea pigs and porcine hearts (2, 3). In the current studies, regional electrical and mechanical effects of vagal nerve stimulation were observed by both right and left vagal nerve stimulation in porcine hearts, without significant differences between right or left vagal nerve stimulation. However, transection of even one significant vagal trunk had significant electrophysiological effects acutely, suggesting that the parasympathetic tone is maintained by both vagi. These studies also point to the important role of afferent fibers in the vagal trunk, which represent the majority of the fibers in this nerve (4). These fibers continuously transduce the mechanical and chemical milieu of the heart, and send this information directly to the brainstem (5-7), and are also clearly activated by electrical stimulation. Furthermore, the types of fibers in the vagal trunk vary and can be activated at different stimulation parameters. For example, at low stimulation currents, activation of afferent fibers often leads to an increase in heart rate, whereas at higher currents, efferent cardiomotor fibers are engaged (8). Furthermore, it has been shown by Yoo and colleagues that the different types of fibers in the vagal trunk are activated at different thresholds (9). For example, the fast conducting A fibers (conduction velocity of ~40 m/s) are activated at much lower currents, on the order of 1-2 mA, while higher currents are needed for activation of B_f and B_s fibers which have

conduction velocities of (10-20 m/s), even higher currents (10-20 mA) are required to activate the C-fibers, unmyelinated fibers with the slowest conduction velocity (9). Therefore, therapeutic strategies that aim to use vagal nerve stimulation need to bear in mind both the extent of innervation as well as stimulation parameters used for vagal nerve stimulation.

Myocardial Infarction and Parasympathetic Neural Remodeling

Myocardial infarction leads to both pathological cardiac (10-12) and neural remodeling (13-15). Neural remodeling, including sympathetic activation and parasympathetic dysfunction, therefore affects both branches of the autonomic nervous system and contributes to ventricular arrhythmia. For example, neural remodeling of the stellate ganglia has been correlated with occurrence of ventricular arrhythmias in canine models of myocardial infarction (16, 17). In addition, the neurons of the intrinsic cardiac ganglia show both histological and functional changes with myocardial infarction. The size of these neurons increase, while the percentage of choline acetyltransferase (ChAT) positive neurons decrease, and the number of vasoactive intestinal positive (VIP) neurons increase. Furthermore, the percentage of neurons that respond to cardiac hemodynamic alterations, such as inferior vena cava occlusion, is altered (18). The findings of this dissertation showed abnormal basal activity of neurons that respond to left vagal nerve stimulation in the intrinsic cardiac ganglia. Activity of neurons that are normally suppressed by vagal nerve stimulation was increased, while the activity of neurons that are normally activated by vagal nerve stimulation, at baseline, was decreased, demonstrating a decrease in central parasympathetic drive from the left vagal trunk.

Myocardial scars are complex structures, containing live islands myocardium and fibrosis that can serve as the substrate for reentry (12). At the macroscopic level, these viable islands can cause slow conduction, which along with differences in repolarization duration in nearby tissue lead to reentry and arrhythmias (19). Myocardial infarction causes alterations in myocyte metabolism and reduction in connexin-43 levels, interfering with electrical propagation (20, 21). Furthermore, in setting of heart disease, neuronal nitric oxide synthase, which by release of nitric oxide facilitates cholinergic transmission and acetylcholine release and its down stream molecules are down regulated (22-24). In fact, nitric oxide synthase inhibitors can reduce the effects of vagal nerve stimulation on heart rate, action potential duration, and ventricular fibrillation threshold (24, 25).

Given the above findings, VNS protects against ventricular arrhythmias utilizing a variety of mechanisms, including release of nitric oxide, reduction in inflammation via the activation of the cholinergic anti-inflammatory pathway,(26-30) decrease in heart rate which reduces myocardial oxygen demand, and improvement in myocardial metabolism and decrease in myocardial cell death (21), figure 1. The findings of this dissertation demonstrate an additional electrophysiological mechanism for the reduction in ventricular arrhythmias in the setting of myocardial infarction, which includes electrical stabilization of infarct border zones, that explains the acute reduction in VT/VF inducibility observed.

FUTURE DIRECTIONS

Although there is now evidence for a reduction in central parasympathetic drive, which is also manifested as a reduction in heart rate variability (31-34) and baro-reflex sensitivity (35-37) in patients with heart failure, the mechanism behind the reduction in this drive is unknown. It's possible that myocardial infarction causes alteration in afferent signaling that results in decreased efferent parasympathetic outflow from the central nervous system. It is also possible that the inflammation associated with myocardial infarction may affect the same brainstem regions that are also affected in other disease processes associated with inflammation including inflammatory bowel disease (38-40) and rheumatoid arthritis,(41) which may also benefit from vagal nerve stimulation. To prevent the reduction in central drive and to find with better therapeutic targets, these mechanisms need to be better elucidated.

Given the beneficial effects observed in animal models, VNS is undergoing evaluation in clinical trials. However, these clinical studies are employing various stimulation parameters and settings, including a variety of frequencies and stimulation thresholds, without a clear understanding of what parameters may provide the best benefit (42-44). Given the effects of afferent fiber activation and results of studies on threshold of activation of different fibers, it is critical to carefully elucidate the optimal parameters of stimulation to ensure that vagal nerve stimulators achieve the desired therapeutic effect.

Figure 1. Mechanisms behind the anti-arrhythmic effects of vagal nerve stimulation. The anti-arrhythmic effects of vagal nerve stimulation are likely dependent on multiple mechanisms including release of nitric oxide, reduction in heart rate and inflammation, as well as improvement in myocardial metabolism, and electrical stabilization of infarct border zones. ERP = effective refractory period, MVO2 = myocardial oxygen demand, VFT = ventricular fibrillation threshold, eNOS = endothelial nitric oxide synthase, iNOS = inducible nitric oxide synthase, nNOS = neuronal nitric oxide synthase, TNF-α = tumor necrosis factor-α, α-7nAch = αlpha-7-nictonic acetylcholine receptor, HMGB1 = high mobility group box 1 protein.

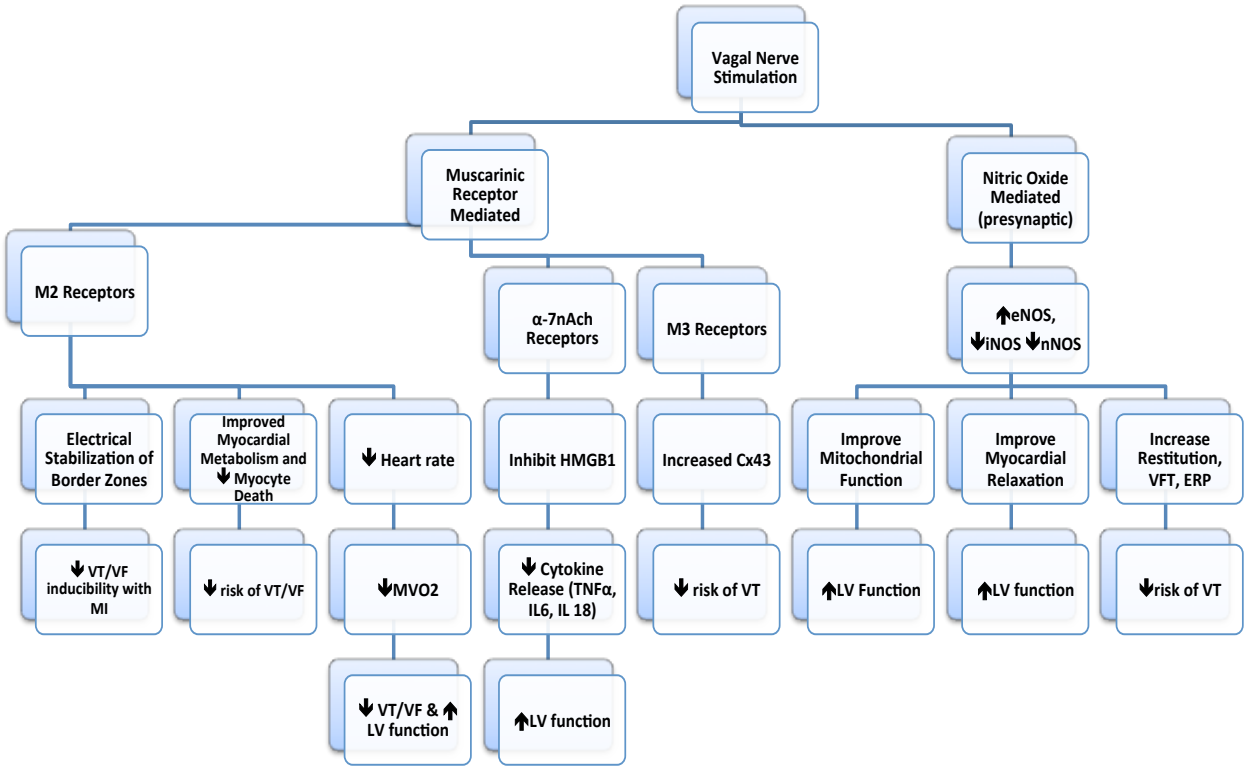

REFERENCES

1. Kawano H, Okada R, and Yano K. Histological study on the distribution of autonomic nerves in the human heart. *Heart Vessels.* 2003;18:32-9.
2. Hoover DB, Ganote CE, Ferguson SM, Blakely RD, and Parsons RL. Localization of cholinergic innervation in guinea pig heart by immunohistochemistry for high-affinity choline transporters. *Cardiovasc Res.* 2004;62:112-21.
3. Ulphani JS, Cain JH, Inderyas F, Gordon D, Gikas PV, Shade G, Mayor D, Arora R, Kadish AH, and Goldberger JJ. Quantitative analysis of parasympathetic innervation of the porcine heart. *Heart Rhythm.* 2010;7:1113-9.
4. Janig W. In: W. J ed. *The Integrative Action of the Autonomic Nervous System: Neurobiology of Homeostasis* Cambridge: Cambridge University Press; 2006:13-34.
5. Armour JA, Huang MH, Pelleg A, and Sylven C. Responsiveness of in situ canine nodose ganglion afferent neurones to epicardial mechanical or chemical stimuli. *Cardiovasc Res.* 1994;28:1218-25.
6. Thompson GW, Horackova M, and Armour JA. Chemotransduction properties of nodose ganglion cardiac afferent neurons in guinea pigs. *Am J Physiol Regul Integr Comp Physiol.* 2000;279:R433-9.
7. Thompson GW, Horackova M, and Armour JA. Role of P(1) purinergic receptors in myocardial ischemia sensory transduction. *Cardiovasc Res.* 2002;53:888-901.
8. Ardell JL, Rajendran PS, Nier HA, KenKnight BH, and Armour JA. Central-peripheral neural network interactions evoked by vagus nerve stimulation:

functional consequences on control of cardiac function. *Am J Physiol Heart Circ Physiol.* 2015;309:H1740-52.

9. Yoo PB, Lubock NB, Hincapie JG, Ruble SB, Hamann JJ, and Grill WM. High-resolution measurement of electrically-evoked vagus nerve activity in the anesthetized dog. *J Neural Eng.* 2013;10:026003.

10. St John Sutton M, Lee D, Rouleau JL, Goldman S, Plappert T, Braunwald E, and Pfeffer MA. Left ventricular remodeling and ventricular arrhythmias after myocardial infarction. *Circulation.* 2003;107:2577-82.

11. de Bakker JM, van Capelle FJ, Janse MJ, Tasseron S, Vermeulen JT, de Jonge N, and Lahpor JR. Slow conduction in the infarcted human heart. 'Zigzag' course of activation. *Circulation.* 1993;88:915-26.

12. Rutherford SL, Trew ML, Sands GB, LeGrice IJ, and Smaill BH. High-resolution 3-dimensional reconstruction of the infarct border zone: impact of structural remodeling on electrical activation. *Circ Res.* 2012;111:301-11.

13. Chen PS, Chen LS, Cao JM, Sharifi B, Karagueuzian HS, and Fishbein MC. Sympathetic nerve sprouting, electrical remodeling and the mechanisms of sudden cardiac death. *Cardiovasc Res.* 2001;50:409-16.

14. Ajijola OA, Wisco JJ, Lambert HW, Mahajan A, Stark E, Fishbein MC, and Shivkumar K. Extracardiac neural remodeling in humans with cardiomyopathy. *Circ Arrhythm Electrophysiol.* 2012;5:1010-116.

15. Vaseghi M, Lux RL, Mahajan A, and Shivkumar K. Sympathetic stimulation increases dispersion of repolarization in humans with myocardial infarction. *Am J Physiol Heart Circ Physiol.* 2012;302:H1838-46.

16. Zhou S, Jung BC, Tan AY, Trang VQ, Gholmieh G, Han SW, Lin SF, Fishbein MC, Chen PS, and Chen LS. Spontaneous stellate ganglion nerve activity and ventricular arrhythmia in a canine model of sudden death. *Heart Rhythm.* 2008;5:131-9.

17. Doytchinova A, Patel J, Zhou S, Chen LS, Lin H, Shen C, Everett THt, Lin SF, and Chen PS. Subcutaneous nerve activity and spontaneous ventricular arrhythmias in ambulatory dogs. *Heart Rhythm.* 2015;12:612-20.

18. Rajendran PS, Nakamura K, Ajijola OA, Vaseghi M, Armour JA, Ardell JL, and Shivkumar K. Myocardial infarction induces structural and functional remodeling of the intrinsic cardiac nervous system. *J Physiol.* 2016;594:321-41.

19. Allessie MA, Bonke FI, and Schopman FJ. Circus movement in rabbit atrial muscle as a mechanism of tachycardia. II. The role of nonuniform recovery of excitability in the occurrence of unidirectional block, as studied with multiple microelectrodes. *Circ Res.* 1976;39:168-77.

20. Ando M, Katare RG, Kakinuma Y, Zhang D, Yamasaki F, Muramoto K, and Sato T. Efferent vagal nerve stimulation protects heart against ischemia-induced arrhythmias by preserving connexin43 protein. *Circulation.* 2005;112:164-70.

21. Beaumont E, Southerland EM, Hardwick JC, Wright GL, Ryan S, Li Y, KenKnight BH, Armour JA, and Ardell JL. Vagus nerve stimulation mitigates intrinsic cardiac neuronal and adverse myocyte remodeling postmyocardial infarction. *Am J Physiol Heart Circ Physiol.* 2015;309:H1198-206.

22. Choate JK, Danson EJ, Morris JF, and Paterson DJ. Peripheral vagal control of heart rate is impaired in neuronal NOS knockout mice. *Am J Physiol Heart Circ Physiol.* 2001;281:H2310-7.

23. Danson EJ, Choate JK, and Paterson DJ. Cardiac nitric oxide: emerging role for nNOS in regulating physiological function. *Pharmacol Ther.* 2005;106(1):57-74.

24. Herring N, Golding S, and Paterson DJ. Pre-synaptic NO-cGMP pathway modulates vagal control of heart rate in isolated adult guinea pig atria. *J Mol Cell Cardiol.* 2000;32:1795-804.

25. Brack KE, Coote JH, and Ng GA. Vagus nerve stimulation protects against ventricular fibrillation independent of muscarinic receptor activation. *Cardiovasc Res.* 2011;91:437-46.

26. Calvillo L, Vanoli E, Andreoli E, Besana A, Omodeo E, Gnecchi M, Zerbi P, Vago G, Busca G, and Schwartz PJ. Vagal stimulation, through its nicotinic action, limits infarct size and the inflammatory response to myocardial ischemia and reperfusion. *J Cardiovasc Pharmacol.* 2011;58:500-7.

27. Hamann JJ, Ruble SB, Stolen C, Wang M, Gupta RC, Rastogi S, and Sabbah HN. Vagus nerve stimulation improves left ventricular function in a canine model of chronic heart failure. *Eur J Heart Fail.* 2013;15:1319-26.

28. Shinlapawittayatorn K, Chinda K, Palee S, Surinkaew S, Thunsiri K, Weerateerangkul P, Chattipakorn S, KenKnight BH, and Chattipakorn N. Low-amplitude, left vagus nerve stimulation significantly attenuates ventricular dysfunction and infarct size through prevention of mitochondrial dysfunction during acute ischemia-reperfusion injury. *Heart Rhythm.* 2013;10:1700-7.

29. Zhang R, Wugeti N, Sun J, Yan H, Guo Y, Zhang L, Ma M, Guo X, Jiao C, Xu W, et al. Effects of vagus nerve stimulation via cholinergic anti-inflammatory pathway activation on myocardial ischemia/reperfusion injury in canine. *Int J Clin Exp Med.* 2014;7:2615-23.

30. Zhang Y, Popovic ZB, Bibevski S, Fakhry I, Sica DA, Van Wagoner DR, and Mazgalev TN. Chronic vagus nerve stimulation improves autonomic control and attenuates systemic inflammation and heart failure progression in a canine high-rate pacing model. *Circ Heart Fail.* 2009;2:692-9.

31. Kleiger RE, Miller JP, Bigger JT, Jr., and Moss AJ. Decreased heart rate variability and its association with increased mortality after acute myocardial infarction. *Am J Cardiol.* 1987;59:256-62.

32. Lammers A, Kaemmerer H, Hollweck R, Schneider R, Barthel P, Braun S, Wacker A, Brodherr-Heberlein S, Hauser M, Eicken A, et al. Impaired cardiac autonomic nervous activity predicts sudden cardiac death in patients with operated and unoperated congenital cardiac disease. *J Thorac Cardiovasc Surg.* 2006;132:647-55.

33. Hull SS, Jr., Evans AR, Vanoli E, Adamson PB, Stramba-Badiale M, Albert DE, Foreman RD, and Schwartz PJ. Heart rate variability before and after myocardial infarction in conscious dogs at high and low risk of sudden death. *J Am Coll Cardiol.* 1990;16:978-85.

34. Farrell TG, Bashir Y, Cripps T, Malik M, Poloniecki J, Bennett ED, Ward DE, and Camm AJ. Risk stratification for arrhythmic events in postinfarction patients

based on heart rate variability, ambulatory electrocardiographic variables and the signal-averaged electrocardiogram. *J Am Coll Cardiol.* 1991;18:687-97.

35. Farrell TG, Paul V, Cripps TR, Malik M, Bennett ED, Ward D, and Camm AJ. Baroreflex sensitivity and electrophysiological correlates in patients after acute myocardial infarction. *Circulation.* 1991;83:945-52.

36. La Rovere MT, Bigger JT, Jr., Marcus FI, Mortara A, and Schwartz PJ. Baroreflex sensitivity and heart-rate variability in prediction of total cardiac mortality after myocardial infarction. ATRAMI (Autonomic Tone and Reflexes After Myocardial Infarction) Investigators. *Lancet.* 1998;351:478-84.

37. La Rovere MT, Specchia G, Mortara A, and Schwartz PJ. Baroreflex sensitivity, clinical correlates, and cardiovascular mortality among patients with a first myocardial infarction. A prospective study. *Circulation.* 1988;78:816-24.

38. Ji H, Rabbi MF, Labis B, Pavlov VA, Tracey KJ, and Ghia JE. Central cholinergic activation of a vagus nerve-to-spleen circuit alleviates experimental colitis. *Mucosal Immunol.* 2014;7:335-47.

39. Munyaka P, Rabbi MF, Pavlov VA, Tracey KJ, Khafipour E, and Ghia JE. Central muscarinic cholinergic activation alters interaction between splenic dendritic cell and CD4+CD25- T cells in experimental colitis. *PLoS One.* 2014;9:e109272.

40. Pellissier S, Dantzer C, Mondillon L, Trocme C, Gauchez AS, Ducros V, Mathieu N, Toussaint B, Fournier A, Canini F, et al. Relationship between vagal tone, cortisol, TNF-alpha, epinephrine and negative affects in Crohn's disease and irritable bowel syndrome. *PLoS One.* 2014;9:e105328.

41. Das UN. Can vagus nerve stimulation halt or ameliorate rheumatoid arthritis and lupus? *Lipids Health Dis.* 2011;10:19.

42. Hauptman PJ, Schwartz PJ, Gold MR, Borggrefe M, Van Veldhuisen DJ, Starling RC, and Mann DL. Rationale and study design of the increase of vagal tone in heart failure study: INOVATE-HF. *Am Heart J.* 2012;163:954-62 e1.

43. Premchand RK, Sharma K, Mittal S, Monteiro R, Dixit S, Libbus I, DiCarlo LA, Ardell JL, Rector TS, Amurthur B, et al. Autonomic Regulation Therapy via Left or Right Cervical Vagus Nerve Stimulation in Patients with Chronic Heart Failure: Results of the ANTHEM-HF Trial. *J Card Fail.* 2014;20:808-16.

44. Zannad F, De Ferrari GM, Tuinenburg AE, Wright D, Brugada J, Butter C, Klein H, Stolen C, Meyer S, Stein KM, et al. Chronic vagal stimulation for the treatment of low ejection fraction heart failure: results of the neural cardiac therapy for heart failure (NECTAR-HF) randomized controlled trial. *Eur Heart J.* 2015;36:452-33.